QUASI TWO-DIMENSIONAL FLOWS THROUGH CASCADES

Thesis by

Ramani Mani

In Partial Fulfillment of the Requirements

For the Degree of

Doctor of Philosophy

California Institute of Technology

Pasadena, California

1967

(Submitted December 16, 1966)

ACKNOWLEDGMENTS

The author wishes to acknowledge, first and foremost, a very deep sense of gratitude to Dr. A. J. Acosta for suggesting the problem and his constant encouragement, guidance and counsel during the years of graduate study.

Many useful conversations were had, during the course of the research, with Dr. R. B. Wade, to whom the author is highly indebted. The author is extremely grateful to Mrs. Phyllis Henderson for her generous and untiring assistance in the typing and editing of the thesis; to Miss Cecelia Lin for drawing the figures; and to Mrs. Z. L. Harrison for assistance in setting up the computing program.

Finally the author acknowledges gratefully the award of various forms of financial assistance by the following institutions: the Institute for tuition scholarships and Teaching Assistantships; the Cole Trust and the Woodrow Wilson Foundation for Fellowship awards; the Office of Naval Research for the award of Research Assistantships and other forms of assistance such as providing computing time.

ABSTRACT

The present thesis is an attempt to develop a thin airfoil theory for an airfoil which spans the gap between a pair of stream surfaces which are slowly diverging or converging, the motivation being to predict, theoretically, the effect of varying axial velocity on cascade performance of axial flow compressor rows.

The procedure involves, firstly, derivation of approximate equations satisfied by suitably defined average potentials and stream functions in such quasi two-dimensional flows. The flow is assumed to be inviscid, irrotational, and incompressible, but as will be argued later, the quasi two-dimensional type equations also result from less restrictive assumptions. Next, fundamental solutions to these equations, corresponding to bound, line sources and vortices, are found. A distribution of such solutions is used to formulate the airfoil problem, using the condition that the flow be tangential to the airfoil contour. The vorticity distribution appears as the solution to a singular integral equation, which is solved by an approximate method. Simple yet physically realistic assumptions are made concerning the gap width as a function of the streamwise length, to obtain numerical results for the effect of contraction of the stream surfaces. Varying degrees of approximation, later discussed, are used in the calculation procedures. A wide variety of the location and the extent of the

contraction, with respect to the airfoil, is investigated.

In all cascade calculations the contraction of the stream surfaces was assumed to be in the same direction as the cascade axis. The main conclusions of the thesis can be summarized as below:

1. The theory predicts a lesser circulation round an airfoil in a contracting flow as compared to the circulation round the same airfoil in a plane flow. There is a similar reduction of circulation for a cascade of airfoils. The percentage reduction of circulation is greater for the cascade case as compared to the isolated case, assuming the contractions to be geometrically similar in both cases. The effect on the circulation of contractions, considered physically reasonable in extent and magnitude, either fully upstream or fully downstream of the airfoil, is quite small.

2. As a very rough rule of thumb, it may be stated that the reduction of circulation as compared to the two-dimensional theory, in the range of parameters applicable to compressors, has about the same magnitude as the reduction of gap between the stream surfaces taking place across the airfoil chords.

3. In a comparison with fixed mean angle of attack, the change in flow turning and deviation angles of the flow are much smaller than changes of circulation and may be stated to be of the order of one degree or less for contraction extents and magnitudes considered realistic for compressor cascades.

TABLE OF CONTENTS

QUASI-TWO-DIMENSIONAL FLOWS THROUGH CASCADES

INTRODUCTION

One of the most profitable approaches to the solution of complex problems in fluid mechanics is to try and effect a conceptual separation of the whole problem into several simpler, relatively independent sub-problems. Such a breakdown of the complicated problem of the flow through an axial flow turbomachine has been indicated by several authors, e.g., in Ref. 1. The axial flow turbomachine is a device consisting of coaxial surfaces of revolution, as inner and outer boundaries, with consecutive rows of either rotating or stationary airfoil-shaped blades, the blades in any row being identical. In a compressor, the blades impart energy to the fluid and in a turbine they extract energy from it. Turbine blades are characteristically thick, sharply curved and closely spaced. Compressor blades are thin, less curved and more widely spaced. The method of thin airfoil theory used in this thesis is therefore much more suitable for application to flow through a compressor cascade than a turbine one. In common with other wing theory problems there are two problems to be solved in axial flow turbomachine aerodynamics. The first is the direct problem when given full geometrical details of the solid boundaries and the flow far upstream of the blade rows, one is asked to predict the details of the flow through the blade passages. The second, the inverse problem, asks for the design of the blades to produce a preassigned force distribution. In both problems, as indicated in Ref. 1, one concentrates separately first on the gross features of the flow, and next, on the details of the flow through the blades. To achieve any simplification several assumptions are necessary. It is customary to assume the fluid to be perfect and often also incompressible. However, the assumptions that are peculiar to the turbomachine problem are the ones that enable the conceptual separation. In studying the gross features of the flow, i.e., the so-called "through flow", one usually assumes axisymmetry, corresponding physically to having an infinite number of blades. To study the details it is usual to ignore the radial velocities and after developing the annular cascade into a plane one, to regard the flow in that plane as a two-dimensional potential flow. The latter study is called cascade theory. These assumptions effect the uncoupling of the problem, because in the former calculation one need not worry regarding the blade shape whilst in the latter the flow in each stream surface is unaffected by the flow in the adjacent surfaces. The inverse problem is definitely less difficult than the direct one because in the latter total uncoupling is not possible. The shape of the blades determines the axi-symmetric stream surfaces and yet these stream surfaces provide the basic mean flows used to predict the forces on the blades by the methods of cascade theory.

We will not outline the details of the axisymmetric three-dimensional through flow theory (we again refer to Ref. 1 for a treatment of this problem) since the present thesis is not directly concerned with it. We just note that even in its most simplified form, this problem involves the study of the motion of a fluid with continuously distributed vorticity, i.e., a rotational fluid motion. The equations of vorticity transport are nonlinear and this constitutes the main obstacle to the solution to the problem. By Helmhotz's theorem for an ideal fluid the vortex lines are material lines and hence the vorticity is transported along material surfaces. But the stream surfaces are influenced by the velocities induced by the vortex lines and this is the source of the non-linearity.

The direct cascade problem consists of predicting the forces on the blades given in advance the axisymmetric flow through them. By developing the annular cascade one arrives at a plane problem for an infinite number of airfoils subject to a known freestream velocity upstream. If one assumes the known axisymmetric stream surfaces to be completely parallel to one another with the gap between them constant, then by suitable mapping the cascade problem can be reduced to a fully two-dimensional one in the plane. Assuming no vorticity normal to this plane and an incompressible fluid leads to a boundary value problem with the two-dimensional potential equation as the governing equation. Some mention will be made of the methods used in two-dimensional cascade theory.

There are two important features of the cascade problem: (a) the periodicity of the flow and (b) the fact that the cascade problem is essentially an interference problem of wing theory. The first is true because with an infinite number of airfoils subject to uniform flow far ahead, there is no difference between any two airfoils so the flow is fully periodic with period equal to the spacing between successive blades. The second feature implies that one has to take account in solving the problem of the influence of all other blades in reckoning the flow about any single airfoil of the cascade. The first feature is strongly made use of in the methods of conformal transformation. A mapping with the periodicity of the flow is used to collapse the infinite number of blades into one contour and the problem for this single contour is solved. The second method, called the method of distribution of singularities, involves using a distribution of source and vortex type solutions to the two-dimensional potential equation on the blades. These source and vortex type solutions are the most elementary singular solutions to the two-dimensional potential equation. The distribution of singularities is unknown but from the symmetry we know the distributions on all blades are identical. The influence of the adjacent blades, the freestream and the blade itself is reckoned on the flow about the chosen single airfoil. The condition that the flow be tangent to the airfoil contour is then used to solve the problem. Thus the singularity methods are more direct and solve the problem in the physical plane itself. In other words, in such methods, the "interference" nature of the problem is fully brought out.

In the earlier use of singularity methods (cf., Refs. 2 and 3) it was customary to lay out the singularities on the blade chord and to separate the effects of camber and thickness. To account for the thickness a source distribution was used and to account for the camber a distribution of vortices was used. A recent and theoretically more satisfying use of singularity methods is due to Martensen (Ref. 4). In this method, the boundary is covered by vortices. We emphasize the two major differences between this procedure and those due to Schlichting and Mellor (Refs. 2 and 3). Firstly no sources are used in the Martensen method and secondly the distribution of vortices is not on the chord but on the boundary. The flow tangency condition yields an integral equation for the vorticity distribution and this integral equation constitutes an exact formulation of the problem. In solving the integral equation one has to resort to collocation of points or iterative methods but quite a high degree of accuracy can be achieved. This method is now widely used, particularly for thick airfoils.

We recall at this point that the principal reason for our arriving at the two-dimensional potential equation in the developed plane is the assumption that the stream surfaces are perfectly parallel to one another. This permits us to achieve the uncoupling of the flow in one stream surface from the flow in the neighboring stream surface. The main objective of this thesis is to try and reduce the degree of approximation involved in this uncoupling. The strip theory of flow through a cascade of airfoils is modified to take some account of the lack of two-dimensionality in this flow. The lack of two-dimensionality arises from the nonparallelism of the stream surfaces. The nonparallelism arises both from deliberate design and the growth of boundary layers on the bounding walls.

The interest in this problem, of the consequences of lack of two-dimensionality, has been considerable. In recent years, the subject has usually been studied under the heading of "Cascade Performance With Varying Axial Velocity." Practically all attention has been focussed on trying to explain the disturbing results of experiments with solid wall cascades.

The experiments reported in Ref. 5 showed a marked difference between calculated lift coefficients, based on two-dimensional cascade aerodynamics, and those actually measured. The most telling evidence for lack of two-dimensionality was the discrepancy between lift forces calculated (a) from the measured turning angles and (b) from the measured pressure distributions. The lack of two-dimensionality was due to the boundary layer displacement effects on the walls enclosing the blades of finite aspect ratio. Later, an experiment with boundary layer suction was tried (the walls were made of carefully selected porous material) and much better agreement with the two-dimensional theory was then obtained (Ref. 6).

The earliest theoretical treatments of the question of lack of two-dimensionality (Refs. 7 and 8) did not attempt to study any effects on the details of the strip theory at all. Hawthorne (Ref. 7) concluded by a Trefftz plane type analysis that if the axial velocity varied, the mean flow, to be used to solve for the circulation, should have an axial component of velocity one-half of the sum of the inlet and outlet axial velocity components. He next pointed out that a change in outlet angle would be produced by acceleration of the mean flow. Scholz's analysis (Ref. 8) indicated how the continuity considerations were affected by the lack of two-dimensionality. Both Hawthorne and Scholz surmised that the centerspan circulation would be unaffected from its two-dimensional value or equivalently that the contraction would not affect the tangential velocities. The fact that the circulation decays to zero at the wall due to boundary layer effects, leading to shed vorticity and secondary flows, was well known. The topic of secondary flows had been the subject of an earlier calculation of induced velocities due to this effect (with some simple assumptions) discussed in Ref. 9. As mentioned earlier none of these papers took any account of having to recast the two-dimensional strip theory in the absence of two-dimensionality.

Two recent attempts have been made to modify the strip theory to take account of the nonparallelism of adjacent stream surfaces, spanned by a cascade of airfoils (Refs. 10 and 11). Both of these use a surface distribution of sources in the centerspan plane of the cascade to represent the effect of increasing axial velocity. For convenience, the source strength per unit area is taken as constant, giving a linear variation of axial component of free stream velocity. The main effect is to alter the freestream velocity normal to the blades and retaining the Kutta-Joukowski condition, one computes the altered distribution of bound vorticity. Both papers compute the velocity fields of bound sources and vortices on a two-dimensional basis. In general the increase in axial velocity, for positive (compressor type) stagger, leads to a decrease of total circulation and lift.

The essential difference between this thesis and the work of Refs. 10 and 11 will now be mentioned. We take explicit account of the fact that the velocity fields of the bound sources and vortices should be reckoned on the basis that these singularities are also subject to lack of two-dimensionality. We mentioned earlier that if one allows for the speeding of the freestream one is led to a decrease in total circulation for positive staggers, as compared to a two-dimensional calculation with constant axial velocity. Allowing for lack of two-dimensionality in computation of the flow fields of the sources and vortices leads to further reduction of circulation. The reduction of circulation due to this latter consideration is at least as great as that due to variation of free stream velocity. Hence the incorporation of such an additional detail is not merely of academic interest. The formulation itself is in more general terms and in fact it was not sought a priori to attempt a modification of two-dimensional theory to produce corrections. Of course, the departure from two-dimensionality or alternatively the deviation from non-parallelism of stream surfaces, was assumed small and fairly crude models were used to obtain numerical estimates. But the general formulation enables a wider class of problems to be solved than merely that of cascade performance with varying axial velocity. It should be pointed out that at least two previous papers (Refs. 12 and 13) have obtained the same equations as in this thesis as the basic equations governing the flow, but in solving the boundary value problem of the cascade the deviation of these equations from the two-dimensional potential equation seems to have been ignored.

A brief outline of the technique of solution will be given now. We assume the axisymmetric stream surfaces to be given. The annular stream surfaces are developed as usual to obtain the infinite cascade. To formulate the problem in two instead of three independent variables, an averaging process is applied to the flow between two adjacent stream surfaces spanned by the infinite cascade. This gives governing equations for the "quasi two-dimensional flow", a terminology used in this thesis to indicate the small departure from two-dimensionality of the class of flows considered. Since this equation is not the two-dimensional potential equation, the methods of conformal transformation are not useful in solving the cascade problem. The method of singularities was therefore used. First, singular solutions to the governing partial differential equations corresponding to source and vortex type solutions were found. From here on, the procedure used to find the right distribution of singularities to satisfy the kinematic condition of flow tangency to the airfoil contour was quite similar to the singularity methods of two-dimensional cascade theory (cf., Ref. 2). We add here that our use of singularity methods involves use of both source and vortex type solutions on the chord. Hence it is an extension to quasi-two-dimensional flows of the methods of Schlichting and Mellor (Refs. 3 and 2) and is not comparable to Martensen's work (Ref. 4).

It was most convenient to consider stream surfaces that were partly straight (i.e., with the gap between two surfaces constant) and partly exponentially converging. In relation to the airfoil location, three types of contractions were considered: (1) those fully upstream of airfoil, (2) those fully covering the airfoil, and (3) those fully downstream of it. Extents of these contractions were varied in numerical calculations.

Since an averaging procedure was used the details of the spanwise variation are apparently lost. This would be true if one considered a high aspect ratio blade spanning a pair of parallel surfaces and directly applied the present theory to it. However, it is conceivable that by considering strips bounded by stream surfaces where the strips are small in spanwise extent a better picture of the spanwise details would be obtained. In each of these strips appropriate quasi-two-dimensional equations would govern the flow. Of course, such a calculation is bound to be arduous. The direct application of the theory given herein to high aspect ratio blades is sure to yield a good estimate of the gross effects on circulation, flow turning, deviation, etc. Designers are often more interested in such gross effects rather than in the spanwise details of the flow. To really understand the latter, a fully three-dimensional lifting surface theory seems inescapable.

CHAPTER I

EQUATIONS SATISFIED BY QUASI TWO-DIMENSIONAL FLOWS AND FUNDAMENTAL SOLUTIONS TO THESE EQUATIONS

Section 1: Class of Flows To Be Considered in This Thesis.

The flow of the fluid is assumed to be inviscid, irrotational and incompressible. Thus the flow is describable in terms of a velocity potential ϕ which is a solution to:

$$\nabla^2\phi = \frac{\partial^2\phi}{\partial x^2} + \frac{\partial^2\phi}{\partial y^2} + \frac{\partial^2\phi}{\partial z^2} = 0 \qquad (1.1)$$

It is assumed to be taking place inside a channel as in Fig. 1, assumed symmetric with respect to the x-axis, whose height is only a function of x. The assumption that the height is a function of x is justifiable for the following reason: Ultimately our objective is to apply the theory to the cascade problem of turbomachine aerodynamics. The full channel (both halves of the symmetric channel) then represents the developed form of the annular portion between two adjacent stream surfaces. The assumed independence of h of y then corresponds to assuming axisymmetry of the stream surfaces. This assumption of axisymmetry is quite commonly employed, and corresponds, physically, to assuming an infinite number of blades. The assumption of symmetry with respect to the x-axis plays no essential part in the equations to be derived below. It only has the effect of increasing the accuracy of the approximation involved in neglecting certain terms of the equations. The symmetry assumption was brought in mainly because this thesis, like all previous papers on such flows, has as an important objective the calculation of flows in the testing of two-dimensional cascades. In such wind tunnel tests one could legitimately expect the symmetry with respect to the x-axis, where now the x-y plane would represent the mid-span plane of the cascade.

A key assumption to be made is that $h(x)$ is a slowly varying function of x. It is clear that if $h(x)$ were constant the flow in the channel would be two-dimensional. The assumption that $h(x)$ be a slowly varying function of x means the deviation of the flow in the channel from two-dimensionality is small - hence the use in this thesis of the phrase "quasi-two-dimensional" flow to describe such a flow.

Section 2: The Averaging Technique and the Equation Satisfied by $\bar{\Phi}$.

As was pointed out in the Introduction, we would like to formulate the problem in two independent variables. Since the wall height is a slowly varying function of x, a natural thought is to try and eliminate z as an independent variable of the problem. To this end, we introduce average quantities as below:

$$\bar{\phi} = \frac{1}{h} \int_0^h \phi \, dz \quad \text{and} \quad \bar{u} = \frac{1}{h} \int_0^h u \, dz, \quad \text{etc.} \tag{1.2}$$

u, v and w denote the x-, y- and z- components of velocity. They are given by φ_x, ϕ_y and ϕ_z.

Now ϕ satisfies $\nabla^2 \varphi = 0$. We integrate this equation from $z = 0$ to $z = h(x)$ using the kinematic boundary condition that $\phi_z = h' \varphi_x$, at $z = h(x)$. This yields:

$$\bar{\phi}_{xx} + \bar{\phi}_{yy} + \left(\frac{h'}{h}\right) \bar{\phi}_x + \left(\frac{h'}{h}\right)' \left[\bar{\phi} - \phi(x, y, h)\right] +$$

$$\frac{h'}{h} \left[\bar{u} - u(x, y, h)\,(1 + h'^2)\right] = 0 \tag{1.3}$$

(DA 1)

The notation "DA 1" indicates the detailed derivation of the indicated equation is in Appendix 1. We propose to replace Eq. (1.3) by the approximate relation:

$$\bar{\phi}_{xx} + \bar{\phi}_{yy} = - \left(\frac{h'}{h}\right) \bar{\varphi}_x \tag{1.4}$$

Section 3: Justification of the Approximation.

The terms we intend to neglect are:

(i) $\left(\frac{h'}{h}\right)' \left[\bar{\phi} - \phi(x, y, h)\right]$ and

(ii) $\left(\frac{h'}{h}\right) \left[\bar{u} - u(x, y, h)\,(1 + h'^2)\right]$.

To study these terms we use the following series for ϕ:

$$\phi = f_o + \sum_1^{\infty} \frac{z^{2n} f_n}{2n(2n-1)} \tag{1.5}$$

where the f_o and f_n are functions only of x, y and only even powers of z are involved from the symmetry of the channel with respect to the x-axis. The use of $\nabla^2\phi = 0$ and equating all powers of z to zero separately yields:

$$\phi = \sum_{n=0}^{\infty} \frac{(-)^n z^{2n} \Delta^n f_o}{(2n)!} \tag{1.6}$$

<u>(DA 2)</u>

where Δ^n stands for the operator $\left[\frac{\partial^2}{\partial x^2} + \frac{\partial^2}{\partial y^2}\right]$ applied n times.

Thus provided the derivatives of f_o are bounded the convergence of the series for ϕ is quite rapid. We restrict ourselves, for example, to a two term series for ϕ:

$$\phi = f_o + \frac{z^2}{2} f_1 \quad . \tag{1.7}$$

The boundary condition at the top is, using the infinite series of Eq. (1.6) :

$$\sum_{1}^{\infty} \frac{h^{2n-1} (\Delta^n f_o) (-)^n}{(2n-1)!} = h' \sum_{0}^{\infty} \frac{\Delta^n f_{ox} (-)^n}{(2n)!} \tag{1.8}$$

The two term series will give:

$$f_1 = \frac{h'}{h} \left[f_{ox} + \frac{h^2}{2} f_{1x} \right] \quad : \tag{1.9}$$

Take as a first approximation:

$$f_1^{(1)} = \left(\frac{h'}{h}\right) f_{ox} = \left(\frac{h'}{h}\right) u_o \tag{1.10}$$

where u_o denotes the component of velocity in the x - y plane (where $z = 0$).

Therefore the term neglected in Eq. (1.9) (using $f_1^{(1)}$) is:

$$\left[\frac{h}{2}\right] \cdot h' \left[\left(\frac{h'}{h}\right)' f_{ox} + \left(\frac{h'}{h}\right) \left(\frac{\partial u_o}{\partial x}\right) \right] \quad . \tag{1.11}$$

We now assign (by assumption) orders of smallness, as follows: The wall slope and hence $\left(\frac{h'}{h}\right)$ has one order of smallness; the wall curvature $\left(\frac{h'}{h}\right)$ has two orders of smallness. Now $\frac{\partial u_o}{\partial x}$ will arise out of non-parallelism of stream surfaces or in the solution of airfoil problems from airfoil camber, thickness or angle of attack. Hence we assign to it also one order of smallness. So the term neglected in Eq. (1.9) by taking $f_1^{(1)}$ as in Eq. (1.10) is of third order of smallness.

We take approximately then:

$$\phi = f_o + \frac{z^2}{2}\left(\frac{h'}{h}\right) f_{ox} \tag{1.12}$$

We note that to this approximation f_o also satisfies the same equation as $\bar{\Phi}$, i.e.:

$$\Delta f_o + \left(\frac{h'}{h}\right) f_{ox} = 0 \tag{1.13}$$

We recall that f_o has the significance of ϕ for $z = 0$, i.e., it is the velocity potential in the centerplane. Using Eq. (1.12) the first term mentioned at the beginning of Section 3 becomes:

$$\left(\frac{h'}{h}\right)'\left(\frac{h'}{h}\right)\left(\frac{-h^2}{3}\right) u_o$$

which is a term of third order of smallness. Thus in case of symmetric channels, in accordance with the above assignment of orders of smallness, one arrives at:

$$\Delta\bar{\Phi} + \left(\frac{h'}{h}\right)\bar{\Phi}_x = 0$$

by neglecting terms of third order of smallness.

Section 4: The Difference Between Average Quantities and Quantities in the Centerplane ($z = 0$), and Further Discussion of Eq. (1.4).

We recall we denote the average quantities by $\bar{u}$ and $\bar{v}$ and the mid-plane quantities by u_o and v_o. Using the approximation of Eq. (1.12):

$$\bar{u} - u_o = \frac{h^2}{6}\left[\left(\frac{h'}{h}\right)' f_{ox} + \left(\frac{h'}{h}\right)\left(\frac{\partial u_o}{\partial x}\right)\right] \tag{1.14}$$

i.e., a quantity of second order of smallness, and

$$\bar{v} - v_o = \frac{h^2}{6} \cdot \left(\frac{h'}{h}\right) \frac{\partial u_o}{\partial y} \tag{1.15}$$

Now $\left(\frac{\partial u_o}{\partial y}\right)$ just as $\left(\frac{\partial u_o}{\partial x}\right)$ may be also argued as having one order of smallness and hence $(\bar{v} - v_o)$ also. Thus both the differences $(\bar{u} - u_o)$ and $(\bar{v} - v_o)$ are of second order of smallness.

We would like, at this point, to clarify the validity of Eq. (1.4). There are two situations to which the equation may be applied. Firstly it could be applied to study the problem of a finite span airfoil, spanning a channel of the type in Fig. 1. Then the equation applies to averaged quantities as defined above in an approximate sense in that certain terms have been neglected. These terms, for the airfoil problem, in accordance with the previously discussed assignment of orders of smallness, can be argued to be of third order of smallness. On the other hand, Eq. (1.4) could be applied to an infinitesimal spanwise strip of the airfoil. Such would be the developed form of the annular stream tube of width Δb shown in Fig. 6. (Fig. 6 is a meridional section of the flow through an axial flow turbomachine.) Let us now let $h(x)$ and $h'(x)$ approach zero such that $h'(x)/h(x)$ tends to some function of x. Now there is no difference between $\bar{\Phi}$ and $\phi(x, y, h)$ or between $\bar{u}$ and $u(x, y, h)$. Then we may say that the flow in this infinitesimal strip is exactly described by Eq. (1.4) in the limit as the height of this tube shrinks to zero. This is true because the terms present in Eq. (1.3) but not in Eq. (1.4) are easily seen to tend to zero in the abovementioned limit.

Section 5: Fundamental Source Type Solutions.

By a fundamental source type solution we mean the most elementary singular solution to Eq. (1.4). This solution should have the attributes of a two-dimensional source type solution; i.e., $\bar{\Phi}$ should become logarithmically singular with $r = \sqrt{x^2 + y^2}$ as r approaches zero and

$$\int_0^{2\pi} r\,\bar{\Phi}_r\, d\theta = \text{unity},$$

for a small circle around the location of the source.

As an illustration consider the case of $\left(\frac{h'}{h}\right) = -\alpha$ which implies $h = h_o \exp(-\alpha x)$. This would be true for an exponentially converging channel of height h_o at the origin.

With this value of $\left(\frac{h'}{h}\right)$:

$$\Delta\phi = a\,\bar{\varphi}_x \tag{1.16}$$

The general solution to Eq. (1.16) using boundary conditions of single valuedness and boundedness at infinity is:

$$\bar{\phi} = \exp\left(\frac{ax}{2}\right) K_n \left(\frac{ar}{2}\right) \begin{cases} \sin(n\theta) \\ \cos(n\theta) \end{cases} \tag{1.17}$$

(DA 3)

The source type solution is found to correspond to $n = 0$ and one has

$$\bar{\varphi}_s = -\frac{1}{2\pi}\exp\left(\frac{ax}{2}\right) K_o \left(\frac{ar}{2}\right) \tag{1.18}$$

The radial and tangential velocities for this source solution are:

$$\overline{V}_{rs} = \frac{a}{4\pi}\left[-\cos(\theta)\exp\left(\frac{ax}{2}\right) K_o\left(\frac{ar}{2}\right) + \exp\left(\frac{ax}{2}\right) K_1\left(\frac{ar}{2}\right)\right]$$

$$\overline{V}_{\theta s} = \frac{a}{4\pi}\exp\left(\frac{ax}{2}\right)\sin(\theta) K_o\left(\frac{ar}{2}\right) . \tag{1.19}$$

A check on the above value of $\overline{V}_{rs}$ is that the flux out of an infinitely large circle centered at the source be "ℓ_o" where "ℓ_o" is the height of the channel where the source is located. This check is carried out in Appendix 4.

The outward flux from any of these sources is "ℓ_o" where "ℓ_o" is the height of the channel where the source is located. The above normalization is convenient because if sources of density $m(x)$ are distributed on a straight line segment L of the x-axis, the velocity component perpendicular to L undergoes a jump of $m(x)$

when one considers points just below L and just above L.

<u>Section 6</u>: Stream Function and Vortex Type Solutions.

The continuity equation is:

$$\frac{\partial u}{\partial x} + \frac{\partial v}{\partial y} + \frac{\partial w}{\partial z} = 0 \tag{1.20}$$

Integrate Eq. (1.20) from $z = 0$ to $z = h(x)$, recalling that:

$$\bar{u} = \frac{1}{h(x)} \int_0^h u dz \quad \text{and} \quad \bar{v} = \frac{1}{h} \int_0^h v dz ,$$

and $w(x, y, 0) = 0$ and $w(x, y, h) = h' u(x, y, h)$. We see that:

$$\frac{\partial}{\partial x}(h \bar{u}) + \frac{\partial}{\partial y}(h \bar{v}) = 0 .$$

Now let

$$h \bar{u} = h_o \frac{\partial \bar{\psi}}{\partial y} \quad \text{and} \quad h \bar{v} = - h_o \frac{\partial \bar{\psi}}{\partial x} \tag{1.21}$$

The condition of irrotationality normal to the x-y plane, i.e., in the z-direction, is:

$$\frac{\partial u}{\partial y} = \frac{\partial v}{\partial x} \tag{1.22}$$

Integration of Eq. (1.22) yields

$$\frac{\partial}{\partial y}(h \bar{u}) = \frac{\partial}{\partial x}(h \bar{v}) - v(x, y, h) h' \tag{1.23}$$

Rewrite

$$v(x, y, h) h' = h \left(\frac{h'}{h} \right) v(x, y, h) \tag{1.24}$$

From the approximation

$$\phi = f_o + \frac{z^2}{2}\left(\frac{h'}{h}\right) f_{ox}. \qquad (1.12)$$

We note $v(x, y, h) - \bar{v}(x, y) = \frac{h^2}{3}\left(\frac{h'}{h}\right)\left(\frac{\partial u_o}{\partial y}\right)$ and hence replacing in Eq. (1.24), $v(x, y, h)$ by $\bar{v}(x, y)$ will introduce errors of third order of smallness. Using this replacement and Eq. (1.23) we find $\bar{\psi}$ satisfies:

$$\Delta\bar{\psi} = \left(\frac{h'}{h}\right)\bar{\psi}_x \quad . \qquad (1.25)$$

Once again for the special case of an exponentially converging channel with $\left(\frac{h'}{h}\right) = -a$, we find

$$\bar{\psi} \sim \exp\left(\frac{-ax}{2}\right) K_n\left(\frac{ar}{2}\right)\begin{cases}\sin(n\theta)\\ \cos(n\theta)\end{cases} .$$

Choosing $n = 0$ gives the solution corresponding to a vortex. We normalize $\bar{\psi}$ such that the circulation about the z-axis is ℓ_o where ℓ_o is the height of the channel where the vortex is located. The expressions for $\bar{u}_{rv}$ and $\bar{u}_{\theta v}$ are as below:

$$\bar{u}_{rv} = \exp\left(\frac{ax}{2}\right)\cdot\frac{a}{4\pi}\cdot\sin(\theta)\, K_o\left(\frac{ar}{2}\right) .$$

$$\bar{u}_{\theta v} = \frac{a}{4\pi}\cdot\exp\left(\frac{ax}{2}\right)\left[\cos(\theta)\, K_o\left(\frac{ar}{2}\right) + K_1\left(\frac{ar}{2}\right)\right] \qquad (1.26)$$

(Recall $\bar{u}$ and $\bar{v}$ are not $\frac{\partial \bar{\psi}}{\partial y}$ and $-\frac{\partial \bar{\psi}}{\partial x}$ but $\frac{\ell_o}{\ell} \frac{\partial \bar{\psi}}{\partial y}$ and $-\frac{\ell_o}{\ell} \frac{\partial \bar{\psi}}{\partial x}$.)

Once again the normalization is such that if vortices of density $\gamma(x)$ are distributed on a line segment L of the x-axis the velocity parallel to this line undergoes a jump of $-\gamma(x)$ on passing from a point just below the line to one just above.

Section 7: Spanwise Variation of Vorticity and Shed Vorticity: Implicit Nature of These Effects and Weinig's Results.

The question we consider in this section is the following: If indeed an airfoil spanned a channel of the type sketched in Fig. 1, would not the vorticity vary spanwise and thus lead to shed vorticity?

Weinig in his article on cascade methods in a recent book (Ref. 12) has derived quasi-two-dimensional type equations very similar to ours for the flow in blade passages. He describes first the procedure of cutting along rotational stream surfaces (from the axisymmetric through flow theory) to obtain the cascade problem. He considers the vane flow (the flow generated by the vanes) to be described by stream and potential functions, ψ_{vane} and ϕ_{vane}.

For these he obtains the following equations (his equations 2 - (10)):

$$\Delta\psi_{vane} = \frac{\partial\psi}{\partial x^*} \quad \frac{d}{dx^*}\left(\ell n \left(\rho\,(x^*) \right)\right) \quad : \text{ and}$$

$$\Delta\phi_{vane} = - \frac{\partial\phi}{\partial x^*} \quad \frac{d}{dx^*}\left(\ell n \left(\rho\,(x^*) \right)\right) \quad .$$

The ρ is a dimensionless term:

$$\rho\,(x^*) = \frac{\Delta b}{\Delta b_m}\left(\frac{\rho}{\rho_m}\right) \quad \text{where} \quad \Delta b$$

is the spacing between two stream surfaces (corresponding to our $h(x)$). Δb_m and ρ_m are respectively a reference width and a reference density. ρ on the right hand side is a density. His $x^* - y^*$ plane is the developed cascade plane. Except for the fact that he allows for compressibility effects, it is seen his equations are identical to ours. Though he remarks at the beginning of his derivation of these equations that the vane flow is an irrotational flow in the absence of viscosity, the only two conditions he really employs in these derivations are (1) the validity of the continuity equation and (2) a condition that the free vorticity normal to the stream surfaces be zero. The latter assumption is quite valid in the study of the motion of a perfect fluid with shed vorticity (as in Prandtl's three-dimensional wing theory). The fluid is unable to support any body forces due to the cross product of free vorticity and flow velocity, and the vorticity is hence to be streamwise. This is a mere restatement of Helmhotz's theorem that the vortex lines associated with the free vorticity are material lines.

The gist of all the above will now be summarized. The shed vorticity enters only implicitly in the determination of axisymmetric stream surfaces. That is to say, it will influence the h(x). But quasi-two-dimensional equations (1.4) and (1.25) result merely from the physically reasonable assumptions that continuity be satisfied and there be no vorticity normal to the stream surfaces. We did arrive at the equation for $\bar{\Phi}$ (Eq. 1.4) by averaging the three-dimensional potential equation. But we could have obtained the same equation just by assuming continuity and the z-component of vorticity to be zero. These are the only two conditions we used to get the equation for $\bar{\psi}$ (Eq. 1.25).

Section 8: A Note on Eq. (1.26).

These bound vortex velocity fields have the property that the line integral of the spanwise average of the tangential velocity (v_θ) taken round a circle centered at the location of the vortex is equal to unity, i.e.,

$$\bar{\Gamma} = R \int_0^{2\pi} \frac{1}{h(\theta)} \int_0^{h(\theta)} v_\theta dz(\theta) \quad d\theta = \text{unity}$$

for all R, where R is the radius of circle used.

CHAPTER II

ISOLATED AIRFOIL PROBLEM:
SETTING UP OF THE INTEGRAL EQUATION

Section 1: Explanation of the Method of Singularities to Solve the Airfoil Problem.

The isolated airfoil problem is as follows (refer to Fig. 2): One has in the channel an airfoil whose spanwise direction is the z-axis. If the section of the airfoil varies along the span, the section indicated as "mean section of the airfoil" is an average section in the same sense as other average quantities. The airfoil is subject to a flow whose magnitude at the center of the airfoil chord is U_o. This flow is inclined at this centerpoint at an angle δ to the airfoil chord. It is necessary to refer to the centerpoint of the chord for the specification of the free stream because the free-stream itself is varying due to the convergence of the channel. We remark at this point that whenever we speak of the convergence we really refer to the fact that the height of the channel is not constant. The term "convergence" is used because in axial flow machines the stream surfaces are usually contracting. In our numerical calculations also all the work is carried out only for contracting channels. By axis of convergence, we mean the direction along which the height is varying, i.e., the x-axis of Figs. 1 and 2. The angle between the airfoil chord and the axis of convergence is denoted by λ . In the cascade problem to be considered later, the axis of convergence will be assumed, in all cases, to be the same as the cascade axis. In this case, λ has also then the meaning of the stagger angle of the cascade.

The problem then is to predict the average flow round the mean section subject to the freestream. We have formulated the problem in two independent variables. The lack of two-dimensionality is disguised in the fact that the stream and potential functions to be used to represent the flow obey Eqs. (1.4) and (1.25). In mathematical terms we seek a solution of a flow governed by Eqs. (1.4) and (1.25) such that when we add to this flow the freestream velocity the average velocity of the combined flow is tangent to the mean airfoil contour.

The method of singularities involves the superposition of the fundamental source and vortex type solutions to solve the problem. Let the distance of a point on the chord from the centerpoint of the chord (the origin in Fig. 2) be denoted by ξ. We use a distribution of sources of density $m(\xi)$ and a distribution of vortices $\gamma(\xi)$ on this chord. The chord extent will be scaled such that ξ runs from -1 to +1 (at the trailing edge). By the use of the phrase "source density" we simply mean that the source solution located at ξ is actually spread over $(\xi - \frac{d\xi}{2})$ to $(\xi + \frac{d\xi}{2})$ such that if $S(\xi)$ is the strength of this source, then the

$$\lim_{d\xi \to 0} \frac{S(\xi)}{d\xi} = m(\xi) \quad .$$

Since each of the little sources $m(\xi)\,d\xi$ and each of the little vortices $\gamma(\xi)\,d\xi$ is a solution to Eq. (1.4) the superposition of them on the chord is a solution to Eq. (1.4). The velocities due to this source vortex distribution are now evaluated on the airfoil. A major approximation in the calculation of these velocities is to calculate them not on the airfoil contour but on the airfoil chord. Suppose we take an $x' - y'$ coordinate system with the x'-axis along the chord and the origin at the mid-chord point. Let ξ' denote the running coordinate on the chord along which there is a source density $m(\xi')$. Then if $\left[x', \epsilon(x')\right]$ denotes the coordinates of a point on the airfoil contour, the approximation mentioned above means that we take the velocity at this point to be that due to the source distribution at the point $\left[x', 0\pm\right]$ with the plus sign for points on the upper surface of the airfoil contour. Thus the approximation constitutes a first order perturbation calculation since $\epsilon(x')$ is small for thin airfoils.

It is true that one cannot have a singular solution in the flow field (i.e., there should be no singular solutions on or outside the airfoil contour). This is because of the physical requirement that the flow velocities should not be infinite anywhere. But there is nothing wrong in using a distribution of singular solutions even if this line of distribution has points on or outside the airfoil contour (as at the leading and trailing edges). The only requirement is that the density of the distribution shall everywhere be finite. Then if $S(\xi)$ denotes the strength of a singular solution in $\left[\xi - \frac{d\xi}{2}, \ \xi + \frac{d\xi}{2}\right]$, since $m(\xi) = \lim_{d\xi \to 0} \frac{S(\xi)}{d\xi}$, if $m(\xi)$ is finite, then $\lim_{d\xi \to 0} S(\xi) = 0$. But it is true that if as a result of our calculation we come up with infinite values for $m(x)$ or $\gamma(x)$ at certain points, our use of singularity distributions is not valid at those points.

Unfortunately, thin airfoil theory (the singularity method) does predict an infinite value for $\gamma(x)$ near the leading edge and also for $m(x)$ at the leading edge for roundnosed airfoils. The reason for the lack of validity of the singularity method near the leading edge is, of course, now well known. The reason is that near the leading edge the flow problem is a singular perturbation problem, thus invalidating a regular perturbation calculation such as the linearized thin airfoil theory. Methods of getting around this difficulty are given in Chapter IV of Ref. 14.

The infinities of $m(x)$ and $\gamma(x)$ mentioned above, however, are integrable in that if the chord extends from "a" to "b" on the x-axis, then

$$\int_a^b \gamma(x)\, dx \quad \text{and} \quad \int_a^b m(x)\, dx$$

exist. It is also true that the integrated lift on the airfoil is predicted correctly to first order in camber, thickness and angle of attack by the thin airfoil theory. In this thesis since the interest is mainly on the integrated lift only the thin airfoil theory will be developed. No attempt will be made to get round the infinities at the leading edge by the use of singular perturbation methods.

There is another limitation of thin airfoil theory which needs to be mentioned here. A consistent restriction to a first order calculation leads to complete separation of the effects of camber and thickness so that thin airfoil theory fails to reveal the interaction of thickness and angle of attack, e.g., the effect of thickness on $\frac{dC_L}{d\alpha}$ i.e., the slope of the lift coefficient versus angle of attack curve.

With the above limitations in mind, we give below the mathematical details of the method of singularities. The coordinate systems, etc., are indicated in Fig. 3. The airfoil chord is along the x-axis extending from -1 to +1.

We first recall that we normalized the expressions for Φ for a source such that if a distribution of sources of density $m(x)$ was laid out on a line segment L of the x-axis the velocity normal to this line underwent a jump of $m(x)$ as we crossed over from below the line L to above it. A similar result applies to the vorticity distribution $\gamma(x)$; there is a jump in velocity parallel to L of $-\gamma(x)$. The procedure is now to write down the velocity normal to the chord, on the upper and lower surfaces and equate it to the product of the slopes (on the upper and lower surfaces) of the airfoil contour and the freestream velocity parallel to the chord. In a first order calculation the velocity parallel to the chord on the right hand side of Eq. (2.1) is taken as just that due to the freestream. The velocity normal to the chord has contributions from the freestream, the source and vortex distributions.

Denote by $\left[K_s(x, \xi)/2\pi\right]$ the continuous portion of the velocity normal to the chord due to a unit source at ξ at a point x. The phrase "continuous" portion is used because the velocity normal to the chord is actually discontinuous with a jump of $m(x)$ where $m(x)$ is the density at x. Let $\left[K_v(x, \xi)/2\pi\right]$ denote the normal component of velocity due to a vortex at ξ, at the point x. Then the flow tangency conditions on the upper and lower surfaces may be written (to first order):

$$\int_{-1}^{1} \frac{m(\xi) K_s(x, \xi)\, d\xi}{2\pi} + \int_{-1}^{1} \frac{\gamma(\xi) K_v(x, \xi)\, d\xi}{2\pi}$$

$$+ V_{fn} + \frac{m(x)}{2} = V_{ft} \frac{dy_u}{dx} \qquad (2.1)$$

$$\int_{-1}^{1} \frac{m(\xi) K_s(x, \xi)\, d\xi}{2\pi} + \int_{-1}^{1} \frac{\gamma(\xi) K_v(x, \xi)\, d\xi}{2\pi}$$

$$+ V_{fn} - \frac{1}{2} m(x) = V_{ft} \frac{dy_\ell}{dx} \qquad (2.2)$$

V_{fn} denotes the component of velocity normal to chord due to free-stream and V_{ft} the component tangential to the chord.

Subtracting Eq. (2.2) from Eq. (2.1) and introducing camber and thickness ordinates of y_c and y_t where:

$$y_c = \frac{1}{2}\left(y_u + y_\ell\right) \tag{2.3}$$

and

$$y_t = \frac{1}{2}\left(y_u - y_\ell\right) \tag{2.4}$$

$$m(x) = 2V_{ft}\frac{dy_t}{dx} \tag{2.5}$$

Adding Eqs. (2.1) and (2.2)

$$\int_{-1}^{1}\frac{\gamma(\xi)K_v(x,\xi)\,d\xi}{2\pi} + \int_{-1}^{1}\frac{m(\xi)K_s(x,\xi)\,d\xi}{2\pi}$$

$$+ V_{fn} = V_{ft}\frac{dy_c}{dx} \quad . \tag{2.6}$$

Equation (2.5) is typical of first order thin airfoil theory. The source strength is fully known and since V_{ft}'s dependence on δ is only as $\cos(\delta)$ (i.e., it is independent of δ to first order of δ for small δ), the source strength is independent of angle of attack. This is the reason for the failure of first order thin airfoil theory to reveal the interaction of thickness and angle of attack.

We recall, in passing, that such an interaction does indeed exist and in case of two-dimensional wing theory, e.g., for a symmetrical Joukowski airfoil, the value of $\left(dC_L/d\alpha\right)$ is not 2π but $2\pi\left(1 + 0.77\,(t/c)\right)$ where (t/c) is the thickness ratio of the airfoil.

Now that the source strength is known we observe that Eq. (2.6) is an integral equation for $\gamma(\xi)$. Now $K_v(x, \xi)$ has (for any $h(x)$) as its most singular term the factor $1/(x - \xi)$. Hence Eq. (2.6) is a singular integral equation for $\gamma(\xi)$. For the case of the exponentially converging channel, $K_v(x, \xi)$ is

$$K_v(x, \xi) = \frac{a}{2} \exp\left(\frac{a}{2}(x - \xi)\cos\lambda\right)\left[\cos(\lambda) K_0\left(\frac{a}{2}\left|x - \xi\right|\right)\right.$$

$$\left.\pm K_1\left(\left(\frac{a}{2}\left|x - \xi\right|\right)\right)\right] \qquad (2.7)$$

where the plus sign goes with $x > \xi$ and the minus sign with $x < \xi$. The limit of $K_v(x, \xi)$ as $a \rightarrow 0$ is $\frac{1}{(x - \xi)}$ as it should be. ($1/(x - \xi)$ is the two-dimensional value.)

A notable feature of the velocity normal to the chord is that the source distribution contributes a continuous component to it. This contribution is for an exponentially converging channel:

$$K_s(x, \xi) = \frac{a}{2} \exp\left(\frac{a}{2}(x - \xi)\cos(\lambda)\right)\left[\sin(\lambda) K_0\left(\frac{a}{2}\left|x - \xi\right|\right)\right] \qquad (2.8)$$

It is seen that this contribution vanishes if $\lambda = 0$ or in the limit as $a \rightarrow 0$. The origin of this term lies in the fact that unlike a completely two-dimensional flow the velocity at a point due to a source at the origin is truly radial only in the special case that the radius vector is parallel to the axis of convergence. The deviation from truly radial flow is greatest when the radius vector is normal to the axis of convergence ($\lambda = \pi/2$).

Section 2: Further Consideration of the Special Case of the Exponentially Converging Channel.

In this section, mainly to fix ideas, we assume the axis of convergence to lie along the freestream direction at the origin, i.e., $\lambda = -\delta$. Also we restrict ourselves to the flat plate for which both y_c and y_t are zero. No source distribution is necessary and the integral equation (in case of the exponentially converging channel) is

$$\frac{a}{4\pi} \int_{-1}^{1} \exp\left[\left(\frac{a}{2}(x-\xi)\right)\cos(\delta)\right]\left[\quad K_o\left[\frac{a}{2}\left|x-\xi\right|\right]\cos(\delta)\right.$$

$$\left.\pm K_1\left[\frac{a}{2}\left|x-\xi\right|\right]\right]\gamma(\xi)\,d\xi + V_{fn} = 0 \qquad (2.9)$$

The plus sign in front of $K_1\left[\frac{a}{2}\left|x-\xi\right|\right]$ goes with $x > \xi$ and the negative sign with $x < \xi$.

Section 3: Some Remarks On the Difference Between This Approach and Some Previous Papers.

Two recent papers (Refs. 10 and 11) have used a surface distribution of sources in the mean plane ($z = 0$) to achieve the effect of varying axial component of freestream velocity. This undoubtedly alters the V_{fn} from the two-dimensional value in Eq. (2.9). The velocity field of the vorticity distribution is calculated on a two-dimensional basis, i.e., it is taken simply as $\frac{1}{2\pi(x-\xi)}$. Thus the singular integral equation to be solved is simply

$$\frac{1}{2\pi} \int_{-1}^{1} \frac{\gamma(\xi)\, d\xi}{(x - \xi)} + V_{fn}(x) = 0 \qquad (2.10)$$

where the dependence of V_{fn} on x is clearly indicated. The present approach takes note of the fact that the flow fields of the singularities themselves are subject to the same limitation as the freestream velocity, i.e., they take place in a channel of varying height. That this difference can lead to substantial differences in the analysis can be seen from the following consideration of the fundamental flow fields in an exponentially converging channel.

Consider the special case of $\lambda = 0$, i.e., the x-axis is taken in the same sense as the axis of convergence. The $\overline{V}_{\theta v}$ due to a unit vortex is

$$\frac{a}{4\pi} \exp\left(\frac{ax}{2}\right)\left[K_o\left(\frac{ar}{2}\right) \cdot \cos(\theta) + K_1\left(\frac{ar}{2}\right)\right] \qquad (2.11)$$

The sinusoidal term $\left[\frac{a}{4\pi} \cdot \exp\left(\frac{ax}{2}\right) \cos(\theta)\, K_o\left(\frac{ar}{2}\right)\right]$ for (ar) sufficiently small does not affect the total circulation since

$$\int_{0}^{2\pi} \cos(\theta)\, d\theta = 0$$

but it alters the distribution of $\overline{V}_{\theta v}$ in that it is no longer cylindrically symmetric (as for the two-dimensional vortices). At the points where $\theta = 0$ and $\theta = \pi$, the $\overline{V}_{\theta v}$ is

$$\frac{\alpha}{4\pi}\ \exp\left(\frac{\alpha x}{2}\right)\left[K_1\left(\frac{\alpha r}{2}\right)+K_o\left(\frac{\alpha r}{2}\right)\right] \quad \text{and}$$

$$\frac{\alpha}{4\pi}\ \exp\left(\frac{\alpha x}{2}\right)\left[K_1\left(\frac{\alpha r}{2}\right)-K_o\left(\frac{\alpha r}{2}\right)\right] \tag{2.12}$$

The effect on the vortices of the lack of two-dimensionality is to increase, as compared to the two-dimensional value, the $\overline{V}_{\theta v}$ downstream and to increase it upstream. If the chord were along the x-axis the $\overline{V}_{\theta v}$ would be V_n for $\theta = 0$ and $-V_n$ for $\theta = \pi$. This fact by itself tends to decrease the circulation for the following reason: Most of the vorticity is near the leading edge (recall the infinity of $\gamma(x)$ near $x = -1$). For the vorticity near the leading edge, most of the rest of the airfoil is downstream. The V_n of most of the vorticity is therefore mostly enhanced. Since the objective of the vorticity is to cancel the V_n due the freestream, there is a reduction of vorticity needed to do this due to the enhancement. It can be easily seen that the above argument applies even for λ non-zero so long as $|\lambda| < \pi/2$. For λ positive, on the other hand, the effect of convergence is to decrease the $V_{fn}(x)$ (for positive angle of attack). This tends to decrease the circulation. Thus there is an interplay of two factors: The enhancement of the vorticity fields downstream tends to decrease the circulation provided $|\lambda| < \pi/2$. The speeding of the freestream tends to decrease the circulation for $\lambda > 0$ and increase it for $\lambda < 0$; all for positive angle of attack. The second of these factors alone is picked up by the approach of Refs. 10 and 11. Thus for $\lambda = -\delta$, the case of the flat plate in an exponentially converging channel, the second of the above factors predicts an increase in circulation. In this case this factor is proportional to α. The factor tending to decrease the circulation due to the altered behavior of the fundamental flow fields, in this special case, turns out to be proportional to $\alpha \ln \alpha$. For small α, therefore, it is the tendency to decrease the circulation that prevails. All this will be made quantitative in the next chapter which discusses the solution of the integral equation (2.6).

CHAPTER III

SOLUTION OF THE INTEGRAL EQUATION

Section 1: Reduction of the Integral Equation.

In all instances arising in this thesis, the integral equation to be solved will be of type

$$\frac{1}{2\pi} \int_{-1}^{1} \frac{\gamma(\xi)\, d\xi}{(x - \xi)} + \int_{-1}^{1} \frac{\gamma(\xi) K_{vr}(x, \xi)}{2\pi} d\xi$$

$$= f(x) \quad \text{for} \quad x \in \left[-1, 1\right] \tag{3.1}$$

where $\gamma(\xi)$ is the unknown function and $K_{vr}(x, \xi)$ and $f(x)$ are both known.

The restriction on $\gamma(\xi)$ is that it be zero at $\xi = +1$ (the trailing edge) due to the Kutta Joukowski condition.

A purely formal way of solving Eq. (3.1) is as follows:

1. Multiply Eq. (3.1) by 2, to get the equation as

$$\frac{1}{\pi} \int_{-1}^{1} \gamma(\xi) \left[\frac{1}{(x - \xi)} + K_{vr}(x, \xi)\right] d\xi = 2f(x) \tag{3.2}$$

2. Now let $\xi = \cos(\phi)$, $x = \cos\theta$, so that as ξ, x run from 1 to -1, ϕ and θ run from 0 to π. Eq. (3.2) can now be written as

$$\frac{1}{\pi} \int_{-1}^{1} \gamma(\phi) \sin\phi \left[\frac{1}{\cos(\theta) - \cos(\phi)} + K_{vr}(\theta, \phi)\right] d\phi$$

$$= 2f(\theta) \qquad (3.3)$$

where for convenience instead of writing $\gamma(\cos\phi)$, $K_{vr}\left[\cos\theta, \cos\phi\right]$ and $f(\cos\theta)$, we write $\gamma(\phi)$, $K_{vr}(\theta\ \phi)$ and $f(\theta)$.

3. Assume for $\gamma(\phi)$ the usual airfoil type series, where all the terms of the series vanish at $\theta = 0$ (at $x = 1$: the trailing edge).

$$\gamma(\theta) = a_o \tan\left(\frac{\theta}{2}\right) + \sum_{1}^{\infty} a_n \sin(n\theta) \qquad (3.4)$$

The above distribution of vorticity as a function of x has the typical square root singularity at the leading edge, i.e., at $x = -1$ or at $\theta = \pi$. That is $\gamma(x) \longrightarrow \infty$ as $x \rightarrow -1$, as $(1 + x)^{-1/2}$.

4. Assume a double Fourier Series expansion of $K_{vr}(x, \xi)$ in form:

$$K_{vr}(x, \xi) = \sum_{0}^{\infty} \sum_{0}^{\infty} b_{\ell m} \cos(\ell\theta) \cos(m\phi) \qquad (3.5)$$

where

$$b_{00} = \frac{1}{\pi^2} \int_0^{\pi} \int_0^{\pi} K_{vr}(\theta, \phi)\, d\theta\, d\phi$$

$$b_{m0} (\text{for } m \neq 0) = \frac{2}{\pi^2} \int_0^{\pi} \int_0^{\pi} K_{vr}(\theta, \phi) \cos(m\theta)\, d\theta\, d\phi \qquad (3.6)$$

$$b_{0\ell}\,(\text{for } \ell \neq 0) = \frac{2}{\pi^2} \int_0^{\pi} \int_0^{\pi} K_{vr}(\theta, \phi) \cos(\ell\,\phi)\, d\theta\, d\phi$$

$$b_{mn}\,(\text{for } m \text{ and } n \neq 0) = \frac{4}{\pi^2} \int_0^{\pi} \int_0^{\pi} K_{vr}(\theta, \phi) \cos(m\theta)$$

$$\cos(\ell\phi)\, d\theta\, d\phi \; .$$

5. Calculation of the integrals in Eq. (3.3) yields on the left hand side:

$$a_o + \sum_{n=1}^{\infty} a_n \cos(n\theta) + a_o \sum_{\ell=0}^{\infty} \cos(\ell\,\theta) \left[b_{\ell o} - \frac{b_{\ell 1}}{2}\right]$$

$$+ \frac{a_1}{2} \sum_{\ell=0}^{\infty} \cos(\ell\,\theta) \left[b_{\ell o} - \frac{b_{\ell 2}}{2}\right]$$

$$+ \sum_{n=2}^{\infty} \frac{a_n}{4} \sum_{\ell=0}^{\infty} \cos(\ell\,\theta) \left[b_{\ell,\,n-1} - b_{\ell,\,n+1}\right] \; . \qquad (3.7)$$

6. Let $2f(x) = d_o + \sum_{1}^{\infty} d_n \cos(n\theta)$ (3.8)

Then equating coefficients of $\cos(\ell\,\theta)$ on both sides with $\ell = 0, 1, 2 \ldots \infty$ one has for the unknown a's the set of infinite simultaneous equations:

$$a_o \left(\delta_{ro} + b_{ro} - b_{r1}\right) + a_1 \left(\frac{b_{ro}}{2} - \frac{b_{r2}}{4} + \delta_{r1}\right)$$

$$+ \sum_{n=2}^{\infty} a_n \left(\delta_{nr} + \frac{1}{4}\left[b_{r,n-1} - b_{r,n+1}\right]\right) = d_r \tag{3.8b}$$

with $r = 0, 1, 2 \ldots \infty$, where δ_{mn} stands for the Kronecker delta and is equal to zero if $m \neq n$ and equal to unity if $m = n$.

In this calculation we make use of two well known results (cf., pp. 92-93 of Ref. 17).

$$\text{(a)} \quad \int_0^{\pi} \frac{\cos (n\theta)\, d\theta}{\cos (\theta) - \cos (\phi)} = \frac{\pi \sin (n\phi)}{\sin (\phi)}$$

and

$$\text{(b)} \quad \int_0^{\pi} \frac{\sin (n\theta) \sin (\theta)\, d\theta}{\cos (\phi) - \cos (\theta)} = \pi \cos (n\phi)$$

The second result is derivable from (a) by writing $\sin (n\theta) \sin (\theta)$ as:

$$\frac{1}{2}\left[\cos \left[(n-1)\,\theta\right] - \cos \left[(n+1)\,\theta\right]\right] .$$

An alternative procedure of arriving at the same set of simultaneous equations is to follow the treatment given in pp. 324-355 of Ref. 15. There is a lot of use of imaginary numbers in the treatment referred to but in essence what is involved is as follows:

The solution to the singular integral equation for $\phi(x)$:

$$f(x) = \frac{1}{\pi} \int_{-1}^{1} \frac{\phi(\xi)\, d\xi}{(x - \xi)} \tag{3.9}$$

for $x, \xi \in \left[-1, 1\right]$ with $\phi(x)$ bounded at $x = 1$ is:

$$\phi(x) = -\frac{1}{\pi}\sqrt{\frac{1 - x}{1 + x}} \int_{-1}^{1} \sqrt{\frac{1 + \xi}{1 - \xi}}\, \frac{f(\xi)\, d\xi}{(x - \xi)} \tag{3.10}$$

We remark at this juncture that in all of the above whenever there are improper integrals involving $(x - \xi)$ in the denominator the sense of the integral is to be understood as that of a Cauchy principal value.

The above inversion (3.10) is the now well-known inversion of the airfoil equation which is the phrase used to describe Eq. (3.9). The inversion is also called the finite Hilbert transform (cf., pp. 173 - 180 of Ref. 16). Rewrite Eq. (3.2) as

$$\frac{1}{\pi} \int_{-1}^{1} \frac{\gamma(\xi)\, d\xi}{(x - \xi)} = 2\, f(x) - \frac{1}{\pi} \int_{-1}^{1} \gamma(\xi)\, K_{vr}(x, \xi)\, d\xi \tag{3.11}$$

Treating the right hand side as known we apply the finite Hilbert transform to Eq. (3.11) thus obtaining (using the requirement that $\gamma(x)$ be bounded at $x = 1$):

$$\gamma(x) = -\frac{1}{\pi}\sqrt{\left[\frac{1 - x}{1 + x}\right]} \int_{-1}^{1} \sqrt{\frac{1 + \xi}{1 - \xi}}\, \frac{2f(\xi)\, d\xi}{(x - \xi)}$$

$$+ \frac{1}{\pi^2}\sqrt{\frac{1-x}{1+x}} \int_{-1}^{1} \sqrt{\frac{1+\xi}{1-\xi}} \frac{1}{(x-\xi)} \left[\int_{-1}^{1} \gamma(\eta) K_{vr}(\xi, \eta) \, d\eta \right] d\xi \, . \tag{3.12}$$

Interchanging the order of integration on the right hand side (the justification for all these steps may be found in Ref. 15) and setting

$$N(x, \eta) = \frac{1}{\pi}\sqrt{\frac{1-x}{1+x}} \int_{-1}^{1} \sqrt{\frac{1+\xi}{1-\xi}} \frac{K_{vr}(\xi, \eta)}{(x-\xi)} \, d\xi \tag{3.13}$$

one has

$$\gamma(x) - \frac{1}{\pi} \int_{-1}^{1} N(x, \eta)\gamma(\eta) \, d\eta = -\frac{2}{\pi}\sqrt{\frac{1-x}{1+x}} \int_{-1}^{1} \sqrt{\frac{1+\xi}{1-\xi}} \frac{f(\xi) \, d\xi}{(x-\xi)} \tag{3.14}$$

Now it is shown in Appendix 5 that if

$$K_{vr}(\xi, \eta) = \sum_{0}^{\infty} C_n(\eta) \cos(n\phi) \tag{3.15}$$

where clearly

$$C_n(\eta) = \sum_{\ell=0}^{\infty} b_{n\ell} \cos(n\psi)$$

with $\eta = \cos(\psi)$: then

$$N(x,\eta) = C_o(\eta)\tan\left(\frac{\theta}{2}\right) + \sum_{1}^{\infty} C_n(\eta)\sin(n\theta) \quad .$$

Now if we again assume for the vorticity distribution

$$\gamma(x) = a_o\tan\left(\frac{\theta}{2}\right) + \sum_{1}^{\infty} a_n\sin(n\theta) \qquad 0 \leqslant \theta \leqslant \pi .$$

Thus we obtain the same set of equations as (3.8b) with the following remark: As a result of Eq. (3.13) what we really obtain is a series equation:

$$f_o\tan\left(\frac{\theta}{2}\right) + \sum_{1}^{\infty} f_n\sin(n\theta) = g_o\tan\left(\frac{\theta}{2}\right) + \sum_{1}^{\infty} g_n\sin(n\theta) . \tag{3.16}$$

Now equating the coefficients in the above in the sense of $f_o = g_o$ and $f_n = g_n$ (with n = 1, 2, 3 . . . .) will be justified if there are only a finite number of non zero f_n and g_n. This is true because consider

$$(f_o - g_o)\tan\left(\frac{\theta}{2}\right) + \sum_{1}^{N} (f_n - g_n)\sin(n\theta) = 0 \tag{3.17}$$

Let $n_1 > N$ and multiply both sides of Eq. (3.15) by $\sin(n_1\theta)$ and integrate from 0 to π . Now

$$\int_0^{\pi} \tan\left(\frac{\theta}{2}\right) \sin(n_1\theta)\, d\theta = \int_0^{\pi} \left(\frac{1 - \cos\theta}{\sin\theta}\right) \sin(n_1\theta)\, d\theta =$$

$$\int_0^{\pi} \frac{1}{\sin(\theta)} \left[\sin(n_1\theta) - \frac{1}{2}\left[\sin\left[(n_1+1)\theta\right] + \sin\left[(n_1-1)\theta\right]\right]\right] d\theta$$

$= \pi$ if n_1 is odd and $= -\pi$ if n_1 is even.

(Recall

$$\int_0^{\pi} \frac{\sin(m\theta)}{\sin(\theta)}\, d\theta \quad \begin{aligned} &= 0 \text{ if } m \text{ is even} \\ &= \pi \text{ if } m \text{ is odd}. \end{aligned}$$)

All other integrals vanish by orthogonality of $\sin(n\theta)$ and $\sin(n_1\theta)$ (since $n \leqslant N < n_1$). Therefore $(-)^{n_1+1}\pi(f_o - g_o) = 0$ or $f_o = g_o$, and $f_n = g_n$ for $n = 1, 2 \ldots$ by orthogonality of the $\sin(n\theta)$ for $\theta \epsilon \left[0, \pi\right]$.

In other words assuming a finite series for the vorticity, the equation of like powers in Eq. (3.14) is justified because for $\theta \epsilon \left[0, \pi\right]$ $\tan\left(\frac{\theta}{2}\right)$ and the set of functions $\sin\theta$, $\sin(2\theta)$, . . . $\sin(N\theta)$ (for finite N) are linearly independent. Such a restriction does not appear explicitly (the restriction of the need to assume a finite vorticity series) in the earlier derivation of Eq. (3.8) where all that was used was to equate like powers in the series equation

$$f_o + \sum_1^{\infty} f_n \cos(n\theta) = g_o + \sum_1^{\infty} g_n \cos(n\theta) \quad .$$

In the above $f_o = g_o$ and $f_n = g_n$ even for an infinite number of terms owing to the orthogonality of $\cos(n\theta)$ for $\theta \epsilon \left[0, \pi\right]$. However in solving the infinite system (3.8) one has to restrict oneself to a finite number of terms in

$$\gamma(x) = a_o \tan\left(\frac{\theta}{2}\right) + \sum_{1}^{\infty} a_n \sin(n\theta) \quad .$$

Section 2: Solution of the Integral Equation.

Enough has already been said to indicate how we solve the integral equation. We now fully detail the calculations involved in solving Eq. (3.1).

1. Assume for $\gamma(x)$ a finite series

$$\gamma(x) = a_o \tan\left(\frac{\theta}{2}\right) + \sum_{1}^{N} a_n \sin(n\theta) \quad . \tag{3.17a}$$

2. Perform a single Fourier analysis of

$$2f(x) = d_o + \sum_{1}^{\infty} d_n \cos(n\theta)$$

(only the first (N + 1) coefficients need be found in the harmonic analysis).

3. Perform a double Fourier analysis of

$$K_{vr}(x, \xi) = \sum_{0}^{\infty} \sum_{0}^{\infty} b_{\ell m} \cos(\ell\theta) \cos(m\phi) ,$$

where (N + 1) (N + 2) coefficients have to be calculated, i.e.,

$$b_{00}, b_{01} \cdots b_{N, N+1} .$$

4. For the (N + 1) unknown a's, i.e., a_o, $a_1 \ldots a_N$, we have the (N + 1) equations (3.8b) taking r from 0 to N. This set of simultaneous equations may be solved, e.g., by matrix inversion.

No ready prescription can be given as to how many a's will be needed to define the vorticity distribution accurately. The only rational procedure is to select arbitrarily some N, carry out the solution of the set of simultaneous equations, and then check whether the decay of the a_n's is rapid enough for the chosen N. We remark however that even for complicated cascade geometries the use of N = 4, i.e., using a 5-term description of the vorticity, seems satisfactory (i.e., quite rapid decay of the last few a_n's is observable). Two more points may be noted: (a) The integrated total vorticity equals $\pi(a_o + \frac{a_1}{2})$ and hence depends only on the first two terms of the vorticity series, and (b) for a chosen N, one has to compute (N + 1) coefficients in the d-series and (N + 1) (N + 2) coefficients in the $b_{\ell m}$-series and so the labor of computation increases rather steeply with increase of N.

Section 3: Remarks on the Nature of $K_{vr}(x, \xi)$.

So far we have made no comment on what restrictions are required to be placed on $K_{vr}(x, \xi)$ insofar as the reduction to a Fredholm equation is concerned. The theory in pp. 324-355 of Ref. 15 assumes that $K_{vr}(x, \xi)$ satisfy the Holder condition with respect to x, ξ for $x, \xi \in [-1, 1]$, which requires, among other things, that $K_{vr}(x, \xi)$ be continuous in the square in the $x - \xi$ plane such that $x, \xi \in [-1, 1]$. Unfortunately for most of the cases to be considered in this thesis, $K_{vr}(x, \xi)$ does not satisfy the requirement of continuity. In many cases it has a weak logarithmic singularity along the line (in the $x - \xi$ plane) $x = \xi$. In other words the singular part of $K_{vr}(x, \xi) \sim \ell n \left[| x - \xi | \right]$. However, the crucial detail (in the treatment of Ref. 15) seems to be the existence of

$$I = \int_{-1}^{1} \sqrt{\frac{1 + x}{1 - x}} \; \frac{K_{vr}(x, \xi) \, dx}{(x - \xi)}$$

as a Cauchy principal value. This, in turn, for the logarithmic singularity, boils down to whether

$$I_1 = \int_{-1}^{1} \frac{\ell n \left[|x - \xi| \right]}{(x - \xi)} \, d\xi$$

exists as a Cauchy principal value.

Let

$$I_1' = \int_{x+\epsilon}^{1} \frac{\ln(\xi - x)}{(x - \xi)} \, d\xi$$

$$I_1'' = \int_{-1}^{x-\epsilon} \frac{\ln(x - \xi)}{(x - \xi)} \, d\xi$$

$$I_1' = -\frac{1}{2}\ln^2(\xi - x) \Big|_{x+\epsilon}^{1} = -\frac{1}{2}\ln^2(1 - x) + \frac{1}{2}\ln^2(\epsilon)$$

$$I_1'' = -\frac{1}{2}\ln^2(x - \xi) \Big|_{-1}^{x-\epsilon} = \frac{1}{2}\ln^2(1 + x) - \frac{1}{2}\ln^2(\epsilon)$$

Therefore

$$\underset{\epsilon \longrightarrow 0}{\ell t} \; (I_1' + I_2'') = \frac{1}{2}\left[\ln^2(1 + x) - \ln^2(1 - x)\right] \quad .$$

does indeed exist, hence proving the existence of I_1 as a Cauchy principal value. To summarize, in this thesis the theory of Ref. 15 has been used despite the lack of continuity of $K_{vr}(x, \xi)$ since the lack of continuity was not strong enough to disallow the existence of the relevant integrals as Cauchy principal values.

One more remark is pertinent here. We have observed earlier that we need the double Fourier series expansion of $K_{vr}(x, \xi)$. So far as the logarithmic singularity is concerned, the double Fourier series expansion was got by using Cauchy principal values again. Undoubtedly the double Fourier series expansion is not convergent along the line of singularity in the $x - \xi$ plane, i.e., for $x = \xi$. But since this expansion is only used for the evaluation of Cauchy principal values, the values in an ϵ-neighborhood of $x = \xi$ should not matter. The series expansion is derived in Appendix 6, and turns out to be

$$\ln\left[\,|x - \xi|\,\right] = -\ln(2) - 2\sum_{1}^{\infty} \frac{\cos(n\theta)\cos(n\phi)}{n} \tag{3.18}$$

for $x \neq \xi$ or $\theta \neq \phi$.

Section 4: An Illustration: The Flat Plate in an Exponentially Converging Channel.

We revert now to the special case of the flat plate in an exponentially converging channel $\left[h(x) = h_o \exp(-\alpha x)\right]$ with $\lambda = -\delta$ subject to a mean flow of unit magnitude at the mid-chord point and inclined (at the mid-chord point) to the chord at δ. Clearly this amounts to using in Eq. (3.1) a $K_{vr}(x, \xi)$ given by:

$$K_{vr}(x, \xi) = \frac{\alpha}{2}\exp\left[\frac{\alpha}{2}\cos(\delta)(x - \xi)\right]\left[\cos(\delta)K_o\left[\frac{\alpha}{2}\left|x - \xi\right|\right]\right.$$

$$\left. \pm K_1\left[\frac{\alpha}{2}\left|x - \xi\right|\right]\right] - \frac{1}{(x - \xi)} \tag{3.19}$$

where the plus sign goes with $x > \xi$ and the negative sign with $x < \xi$. Notice the most singular portion $\left(\frac{1}{(x - \xi)}\right)$ arising from the small value expansion of $\pm K_1\left[\frac{a}{2}\left|x - \xi\right|\right]$, has been subtracted out to get $K_{vr}(x, \xi)$. The f(x) is, in this instance

$$- \sin(\delta) \exp(ax \cos \delta) \tag{3.20}$$

It is quite hard to deal with the whole kernel of Eq. (3.17) and it was decided to expand all terms in there for small a restricting oneself to an $0(a^2 \log a)$ calculation. The expansion of Eq. (3.17) yields powers $\sim a \log a,\ a^2 \log^2 a,\ a^2 \log a$, etc. To the same order, $d_o = -\sin(\delta)$, $d_1 = -\frac{a}{2}\sin(2\delta)$; and all other d's of $0(a^2)$.

$$b_{00} = \frac{a}{2}\left[\ell n \frac{4}{a} + 1.1159\right] \cos(\delta) = C_o \tag{3.21}$$

$$b_{mm} = \frac{a \cos(\delta)}{m} = C_m \quad \text{with all other } b_{\ell m} \ (\text{for } \ell \neq m)$$

$= 0$ (to this order of a). These details will not be considered here and simply involve use of small value expansions of the K_o and K_1 functions available in any table of special functions, as for instance Ref. 19.

Assuming a two term series for the vorticity one obtains as a result of solving a (2 x 2) set of simultaneous equations (a two term series was used because to the order of a considered, $d_n = 0$ for $n > 1$).

$$\gamma(x) = -\left[\frac{2 \tan \frac{\theta}{2}}{(1 + C_o)} + \frac{3a}{2} \sin(2\delta) \sin \theta\right] \tag{3.22}$$

where C_o is defined in Eq. (3.19). The total circulation is

$$\Gamma_t = -2 \sin(\delta)\pi \left[\frac{1}{1 + C_o} + \frac{3a}{4} \cos(\delta)\right] \qquad (3.23)$$

The two-dimensional value is

$$\Gamma_{t\ T.D} = -2 \sin(\delta)\pi \quad .$$

Section 5: Discussion of Eq. (3.21).

Eq. (3.21) indicates the two influences on the circulation discussed in Section 3 of Chapter II. The $\left(\frac{1}{1 + C_o}\right)$ factor is the one diminishing the circulation due to the enhancement of V_n of the vortices downstream and the $\left(\frac{3a}{4}\cos(\delta)\right)$ factor is the one tending to increase the total circulation due to effect of freestream speeding. An expansion of $\left(\frac{1}{1 + C_o}\right)$ as $\left[1 - C_o + C_o^2 \ldots\right]$ etc., is enough to show that the tendency to decrease the circulation is as $(a \ln a)$ whereas the one tending to increase it is as a. For $a = 0.075$, giving an increase in freestream from leading to trailing edge by a factor of Eq. (1.16), there is a dimunition of total circulation by a factor of 0.892.

It should be pointed out that the same results for $\gamma(x)$ (for the flat plate in an exponentially converging channel with $\lambda = -\delta$) are obtained by assuming for $\gamma(x)$ a series of type

$$\gamma_o(x) + a \ln(a) \gamma_1(x) + \ldots .$$

This series is substituted into the left hand side of Eq. (3.1) and like powers of $\alpha \ln \alpha$, etc., equated on both sides of Eq. (3.1). Thus $\gamma_1(x)$, etc., are evaluated. A table of improper airfoil integrals given in Ref. 20 is found quite useful in this procedure. It will be noted this alternative procedure is more intuitive since one has to know in advance the nature of powers of α involved in the solution as function of α. It is also not very amenable to adaptation to numerical methods intended to be used on the computer. This latter consideration of the possibility of writing a computer program to solve Eq. (3.1) is rather important in solving the cascade problem where the kernels are too complicated to permit hand calculation.

CHAPTER IV

THE CASCADE PROBLEM

Section 1: Formulation and Description of the Problem.

The cascade problem involves an infinite set of identical airfoils spaced equally apart (see Fig. 4). Figure 5 shows the difference between a turbine and a compressor cascade. These airfoils are subject to a flow known in magnitude and direction far upstream. The reason for studying this problem is as follows: Figure 6 indicates a sketch of an axial flow turbomachine. The direction of the flow is indicated by the arrows on the streamline in Fig. 6 (which shows a meridional section). The conceptual separation of the flow problem along with the idealizations employed to simplify the problem, have been well described in Ref. 10 (pp. 13-14):

> As a final result, the aerodynamics of turbomachines should integrate all the factors that contribute to the flow and the energy transfer inside them. This means that for given inlet conditions, which are not necessarily uniform and stationary across the inlet, it is desirable to compute this truly three-dimensional and nonstationary flow taking into consideration compressibility, viscosity, and clearance effects, as well as the mutual interference between the stationary and rotating blade rows. This task is so complex that certain short cuts are essential.
>
> First of all, no consideration is normally given to non-uniform inlet conditions due to varied angles of attack of

the airplane or to unsymmetric inlet scoops. Also, the influence of the inlet struts and other features of a secondary nature are normally neglected. The remaining problem can then be broken down into three problems:

1. In the first the average flow viewed in a meridional plane is considered, which brings about the so-called axially symmetric flow pattern used later as the "basic flow" of the cascades.

2. The next problem considers the flow as if it occurred between adjacent rotational stream surfaces, as found by the axially symmetric treatment, but which now contains a finite number of blades. By cutting along these rotational surfaces the two-dimensional problem of cascade flow is established.

3. The third problem considers the flow as if it could be observed in cross sections normal to the rotational stream surfaces, that is, in axial turbomachines, practically normal to the axis of rotation. This brings about the problems of the so-called "secondary flow," which compensates for the simplifications inherent in the concepts of axially symmetric and two-dimensional flow. In the first instance, such a correction must extend the axially symmetric treatment to allow for some exchange of matter and therewith of energy across the axially symmetric surfaces. Furthermore, the assumption of two-dimensional cascade flow must be corrected in a manner similar to that which adjusts the result of the lifting line theory to small aspect ratios in the theory of the airfoil of finite span.

As mentioned in Ref. 10, the cascade problem arises out of the second mentioned flow problem. The "cutting along the rotational surfaces" by a suitable mapping, unwraps the annular cascade and gives the problem of the infinite cascade of identical airfoils. The details of the transformation are given in Ref. 10.

We have said earlier that the flow far upstream is given, in magnitude and direction. The effect of all the bound vortices associated with each of the airfoils is to turn the flow to a different direction and magnitude downstream. Unfortunately the flow upstream is not a convenient reference velocity to use in solving the problem. In treatments of plane, incompressible, inviscid flow through the cascade (cf., Ref. 2) it is shown that a good reference velocity to use is the vector mean velocity of the inlet and outlet velocity. By "good" reference velocity, is meant that it can be shown that the lift per unit span on any one airfoil of the cascade is given in magnitude by $\rho U_m \Gamma_t$ where U_m is the mean velocity, Γ_t the total circulation about one airfoil, ρ the density of the fluid. It can also be shown, still within the framework of an inviscid, incompressible fluid theory, that this lift will be perpendicular to the vector mean velocity. The analogy with the Kutta Joukowski law for a single airfoil subject to a known freestream velocity is the basis for regarding the vector mean velocity as an appropriate reference velocity. Most of the proofs given in standard references (again cf., Ref. 2) of the considerations leading to the choice of vector mean velocity as the appropriate reference velocity, assume a constant axial velocity. A constant axial velocity would indeed result for a plane flow from continuity considerations. As was mentioned earlier in the Introduction, Hawthorne, by a Trefftz plane type analysis (Ref. 7), showed that in case of variation of axial velocity due to lack of two-dimensionality, the appropriate reference velocity to be used was still the vector mean velocity.

The conventional two-dimensional plane problem is then formulated, in the singularity methods, as follows: One asks for the source vortex distribution on the chords of all the airfoils such that the induced velocity due to this singularity distribution, added vectorially to the mean velocity, produces a flow tangent to the airfoil contour.

A great aid in the solution is the symmetry of the problem due both to the identical nature of all the blades and because there is an infinite number of blades. There is no difference between any two airfoils and the source vortex distribution on all blades is identical. The flow is completely periodic with period equal to the spacing between the blades. So if the problem is correctly solved for one blade it is also solved for all the blades. This enables one to concentrate on one blade only usually referred to as the zeroth blade. An unknown source vortex distribution is placed on all the chords and the induced velocity for the zeroth blade is calculated. The flow tangency condition once again yields the expression for the source strength and an integral equation for the vorticity distribution.

The calculation of the induced velocities due to the singularity distributions is again done on the chord (and not on the airfoil contour). The sketch in Fig. 5 shows turbine blades to be much thicker and more highly cambered than compressor blades. Hence the method of thin airfoil theory used in this thesis is inherently far more suitable for a compressor cascade than a turbine cascade.

As before, due to the formulation of the quasi-two-dimensional problem in two independent variables, there are only two modifications involved in the setting up of the problem for the quasi-two-dimensional flow as compared to the plane flow. Firstly, the flow fields of all the singularities (sources and vortices) are taken from the singular solutions to the quasi-two-dimensional equations. Secondly, the variation of the mean velocity due to lack of two-dimensionality, has to be included. In other words all the flows are to be derived subject to Eqs. (1.4) and (1.25).

Regarding the airfoil section to be used in the tangency condition, for airfoils of finite span, the section may be regarded as a spanwise average in the same sense as other average quantities. Alternatively if the theory is applied to the developed form of the infinitesimal annual stream tube of radial extent (Δb), as shown in Fig. 6, since the variation of airfoil section in such a small tube is likely to be quite negligible, there should be no trouble in deciding the section to be used in the flow tangency condition. We repeat at this point that Weinig on p. 20 of Ref. 12 obtains the quasi-two-dimensional Eqs. (1.4) and (1.25) for the flow in the infinitesimal stream tube of extent Δb in Fig. 6.

The mathematics in the solution to the cascade problem introduces essentially no new ideas. Let V_n denote the velocity normal to the chord and V_t the velocity parallel to it. Then if ξ denotes the running coordinate of a point on the chord where one has a source density $m(\xi)$ and a vortex density $\gamma(\xi)$ then

$$V_n = \frac{1}{2\pi} \int_{-1}^{1} m(\xi) K_{snc}(x, \xi)\, d\xi + \frac{1}{2\pi} \int_{-1}^{1} \gamma(\xi) K_{vnc}(x, \xi)\, d\xi$$

$$+ \; V_{fn}(x) \; \pm \; \frac{1}{2} m(x) \tag{4.1}$$

where the plus sign is for the upper surface and the negative sign for the lower surface. $V_{fn}(x)$ denotes, as before, the component of velocity normal to the chord arising from the vector mean velocity. The $K_{snc}(x, \xi)$ needs a little explanation. Referring to Fig. 7, $\frac{K_{snc}(x, \xi)}{2\pi}$ is the velocity normal to the chord of the zeroth blade at the point P (whose coordinate is x) due to an infinite array of sources of strength unity placed at ξ on the zeroth blade and at the corresponding points on all other blades: i.e., at $S_{-\infty}, \ldots S_{-2}, S_{-1}, S_0, S_1, S_2 \ldots S_{\infty}$ in Fig. 7. $K_{vnc}(x, \xi)/2\pi$ has a similar interpretation being the velocity normal to the chord at P, due to an infinite array of vortices of strength unity at $S_{-\infty}, \ldots S_{-2}, S_{-1}, S_0, S_1, S_2 \ldots S_{\infty}$. The most singular part of $K_{vnc}(x, \xi)$ will again be $(1/(x - \xi))$. Similarly:

$$V_t = \frac{1}{2\pi} \int_{-1}^{1} m(\xi) K_{stc}(x, \xi) \, d\xi + \frac{1}{2\pi} \int_{-1}^{1} \gamma(\xi) K_{vtc}(x, \xi) \, d\xi$$

$$+ \; V_{ft}(x) \; \pm \; \frac{1}{2} \gamma(x) \quad . \tag{4.2}$$

$K_{stc}(x, \xi)$ and K_{vtc} have a significance similar to K_{snc} and K_{vnc} except we now refer to velocity components tangential to the chord.

$V_{ft}(x)$ is the contribution from the vector mean velocity. For the upper and lower surfaces, with y_u and y_ℓ as the upper and lower coordinates, we write the flow tangency conditions:

$$V_{nu} = V_{tu} \frac{dy_u}{dx} \tag{4.3a}$$

$$V_{n\ell} = V_{t\ell} \frac{dy_\ell}{dx} \tag{4.3b}$$

Subtracting Eq. (4.3b) from Eq. (4.3a) and ignoring the products other than $V_{ft} \cdot \frac{d}{dx}(y_{u,\ell})$ on the right hand side of Eq. (4.3) (again a first order calculation) one has, as before

$$m(x) = 2V_{ft}(x) \frac{dy_t}{dx} \tag{4.4}$$

where $y_t = \frac{1}{2}(y_u - y_\ell)$.

Adding Eqs. (4.3a) and (4.3b) and ignoring the product of $\pm \frac{1}{2}\gamma(x)$ with $\frac{dy_{u,\ell}}{dx}$ and letting $y_c = \frac{1}{2}(y_u + y_\ell)$, one has

$$V_{fn}(x) + \frac{1}{2\pi} \int_{-1}^{1} m(\xi)\, K_{snc}(x,\xi)\, d\xi$$

$$+ \frac{1}{2\pi} \int_{-1}^{1} \gamma(\xi)\, K_{vnc}(x,\xi)\, d\xi = \left[V_{ft}(x) + \frac{1}{2\pi} \int_{-1}^{1} m(\xi) K_{stc}\, d\xi \right.$$

$$+ \frac{1}{2\pi} \int_{-1}^{1} \gamma(\xi) K_{vtc}(x, \xi)\, d\xi \Bigg] \cdot \frac{dy_c}{dx} \qquad (4.5)$$

It is indeed not very consistent if thickness and camber effects are assigned equal orders of smallness to take the source strength as known (a first order calculation) and yet put in the contributions from source and vorticity distributions on the R.H.S. of Eq. (4.5). But the principal reason for doing so was that this mixed order of smallness calculation is what is carried out for plane flows in Ref. 2 and it was decided to develop in this thesis a calculation procedure for quasi-two-dimensional flows that would be completely analogous to that in Ref. 2 for plane flows. Such a mixed order calculation has the advantage that it would be a little more accurate than a fully first order calculation (which involves leaving out all the source and vorticity terms on the R.H.S. of Eq. (4.5)) for a highly cambered but thin airfoil.

One other simplification used was that in reckoning the thickness effects of the blades the thickness distribution was assumed to be that of a symmetrical Joukowski airfoil. This assumption is simply a matter of convenience in performing the numerical calculations.

Section 2: Procedure of Solution.

It is easily observed there is nothing essentially different so far as the solution of Eq. (4.5) goes as compared to Eq. (3.1). Since the source strength is fully known from Eq. (4.4), the equivalence between Eqs. (4.5) and (3.1) is clearly as indicated below:

(a) $K_{vr}(x, \xi)$ of Eq. (3.1) corresponds to:

$$\left[K_{vnc}(x, \xi) - \frac{1}{(x - \xi)} - \frac{dy_c}{dx} \cdot K_{vtc}(x, \xi)\right]$$

of Eq. (4.5). Note again the subtraction off from $K_{vnc}(x, \xi)$ of the most singular term $1/(x - \xi)$, and

(b) $f(x)$ of Eq. (3.1) corresponds to:

$$V_{ft} \frac{dy_c}{dx} - V_{fn} + \frac{1}{2\pi} \frac{dy_c}{dx}\left[\int_{-1}^{1} m(\xi) K_{stc}(x, \xi)\, d\xi - \int_{-1}^{1} m(\xi) K_{snc}(x, \xi)\, d\xi\right]$$

of Eq. (4.5).

The first combination of terms above, corresponding to $K_{vr}(x, \xi)$ of Eq. (3.1) will be referred to as $K_{vrc}(x, \xi)$. The second group of terms will be referred to as $f_c(x)$.

Since the Fourier analysis involves integrals of the type in Eq. (3.6), a computing program can easily be set up to calculate the $b_{\ell m}$ and the d's. $K_{vrc}(x, \xi)$ is too complicated a function of x, ξ for integrals of type (3.6) to be calculable by reference to tables of integrals. An integration subroutine based on Simpson's rule was used to calculate the $b_{\ell m}$'s. An important comment with respect to the calculation of the b-matrix is as follows. As in the case of the isolated airfoil $K_{vrc}(x, \xi)$ has a weak logarithmic singularity $\sim \ln \left[|x - \xi| \right]$. The computer cannot handle any singularities and hence this weakly singular portion of $K_{vrc}(x, \xi)$ is subtracted off from $K_{vrc}(x, \xi)$ before feeding into the computer. From Eq. (3.18) we know the b-matrix associated with $\ln \left[|x - \xi| \right]$ and hence there is no problem in adding on the result of Eq. (3.18) to the double Fourier analysis of the rest of $K_{vrc}(x, \xi)$ supplied by the computer.

All that remains is then to use a suitable N to define the vorticity series as in Eq. (3.17a) and then solve the set of simultaneous equations (3.8) with $r = 0, 1, 2 \ldots N$. As remarked in Chapter III, $N = 4$ (i.e., with the vorticity defined by a 5-term series) seems quite satisfactory in that the last a's are then found to be quite small. The solution of the set of simultaneous equations by matrix inversion can again be conveniently programmed to be done by a computer.

Section 3: Remarks on the Special Case of an Exponentially Converging Channel.

In this case, for the velocity fields of the sources and vortices, we have to use expressions involving the K_o and K_1 functions. As an example, $K_{vnc}(x, \xi)$ will be written down:

Let $r_m^2 = \left[m^2 s^2 - 2ms\,(x - \xi) + (x - \xi)^2 \right]$ and $r_m > 0$,

where m is an integer ranging from $-\infty$ to $+\infty$, s is the spacing between the blades $(2/s =$ solidity of the cascade, since the chord is taken 2 units long). Then with λ as the stagger angle (recall for all cascade calculations, the axis of convergence is taken to be along the axis of the cascade), for a cascade of flat plates with $\frac{dy_c}{dx} = 0$:

$$K_{vrc}(x, \xi) = \frac{a}{2} \exp\left[\frac{a}{2}(x - \xi)\cos(\lambda)\right] \sum_{m=-\infty}^{\infty} \left[K_o\left(\frac{a r_m}{2}\right) \cos(\lambda) + \left(\frac{(x - \xi) - ms \sin(\lambda)}{r_m}\right) K_1 \left(\frac{a r_m}{2}\right)\right] - \frac{1}{(x - \xi)} \qquad (4.6)$$

The singular parts come from $m = 0$ and when $x = \xi$ and by expanding $K_1\left[\frac{a}{2}|x - \xi|\right]$ for small a, one can see the singular portion has been subtracted off. With $m = 0$, the expansion of $K_o\left(\frac{a r_m}{2}\right)$ for small a reveals the weak logarithmic singularity referred to earlier. Since the $m = 0$ portions of the above series expressions for $K_{vrc}(x, \xi)$ had to be taken account of by hand calculation, for these terms an order $(a^2 \log^2 a)$ calculation was done. It was not possible to sum the infinite series in Eq. (4.6) exactly and a couple of approximations that help in the summation of this series are mentioned in Appendices 7 and 8.

Section 4: Discussion of Numerical Results for the Cascade of Airfoils in an Exponentially Converging Channel.

All the remarks mentioned in Section 3 of Chapter II regarding the two factors involved in the effect on the circulation, i.e., (a) the effect of freestream variation and (b) the altered behavior of the velocity fields of the sources and vortices (from the two-dimensional fields), apply to the cascade problem. The angle between the axis of convergence and the blade chord = λ and is positive for compressor cascades and so the freestream effect is also to decrease the circulation (unlike the case of the flat plate discussed in Section 4 of Chapter III where $\lambda = -\delta$). The reduction of circulation due to the altered behavior of the vortices is even stronger than that for a flat plate because we have an infinite set of vorticity distributions. By the use of the word "reduction" we have in mind the reduction from unity of the ratio of total circulation for a quasi-two-dimensional calculation as compared to a two-dimensional calculation for the same airfoil section. It is this quantity that is plotted as ordinate in the graphs in Figs. 8, 9 and 10 which present the results of the numerical work pertaining to this section.

There are quite large reductions of the order of 50 percent at unit solidity for axial velocity ratios of 1.15 or so. The reduction is less for lower solidities. It is also less for a cascade of thick, cambered airfoils as compared to a cascade of flat plates. The dependence on stagger is not very clear but it seems the strongest reduction of circulation is around $\lambda = 30^\circ$.

Only a few representative calculations have been performed for the cascade in an exponentially converging channel. The reason for this is contained in Fig. 10. For unit solidity and $\lambda = 45^\circ$, and a cascade of flat plates, it was decided to study the dependence of the reduction ratio on the axial velocity ratio (or on the contraction parameter a). Since we expect (from the study of the isolated flat plate) the reduction ratio to depend on a most strongly as $(a \ln a)$ and also because for small a, it would be difficult to exhibit clearly the reduction ratio "r" as a function of $(a \ln a)$ owing to crowding near the origin on the x-axis, it was decided to plot "r" against $(1/a \ln a)$. As $a \longrightarrow 0$, $(1/a \ln a) \longrightarrow \infty$ and hence on such a graph r should tend to unity as $(1/a \ln a) \longrightarrow \infty$ since $a = 0$ corresponds to the two-dimensional case. Unfortunately such a plot, shown in Fig. 10, showed a very slow approach of r to unity as $(1/a \ln a) \longrightarrow \infty$. The reason for this is presumed to be the fact that the exponentially converging channel is physically unrealistic for large x since it flares to an infinite width on the far upstream side and contracts to zero width on the far downstream side. (Recall $h = h_o \exp(-ax)$.)

Thus it was decided to study channels whose departure from constancy of channel height was over a finite extent only. Such channels will be referred to as finite channels. The fundamental singular solutions in such channels are studied in the next chapter and a detailed set of numerical experiments was also reserved for such finite channels.

CHAPTER V

CASE OF FINITE CHANNELS

Section 1: Introduction.

The calculations for fully exponential channels reveal a sharp reduction in total circulation for the cascade problem. Of greater concern was the fact that the rate of approach of the ratio $\Gamma_{Q.T.D.} \div \Gamma_{T.D.}$ to unity was very slow as $a \rightarrow 0$. With a view to clarifying the effects of contraction for more realistic channels, efforts were made to find the solutions for fundamental sources and vortices for channels where $\left(\frac{h'}{h}\right)$ differs from zero only over a finite extent of x. These solutions were later applied for the solution of the boundary value problems of isolated airfoils and airfoils in cascade.

Section 2: Assumption of $\left(\frac{h'}{h}\right)$ and Procedure of Solution.

The calculation procedures for general $\left(\frac{h'}{h}\right)$ were largely based on Ref. 22. The procedure involves the use of Fourier exponential transforms. The use of Fourier exponential transforms to reduce a partial differential equation to an ordinary differential equation necessitates the assumption that the dependent variable go to zero as the independent variable which is being eliminated goes to $\pm\infty$. Since the potentials and the stream functions do not possess this property it is more convenient to formulate the problem for the velocities themselves. Also generalized functions are introduced to represent the singularities. Before carrying out the calculations, however, the meaning of the generalized functions in terms of jump conditions is written out so that the final formulation is within the realm of ordinary analysis.

Consider as the first example the $\bar{v}$ component of velocity for a vortex of unit strength per unit length located at the origin. Since the field is completely free of sources the continuity equation is:

$$\frac{\partial}{\partial x}(h\bar{u}) + \frac{\partial}{\partial y}(h\bar{v}) = 0 \tag{5.1}$$

The z component of vorticity equation from Eq. (1.23) can be written:

$$\frac{\partial}{\partial x}(h\bar{v}) - \frac{\partial}{\partial y}(h\bar{u}) - h'\bar{v} = h_o\delta(x)\delta(y) \tag{5.2}$$

Differentiating Eq. (5.2) with respect to x and letting

$$\Delta = \frac{\partial^2}{\partial x^2} + \frac{\partial^2}{\partial y^2}$$

$$\Delta\bar{v} + \left(\frac{h'}{h}\right)\bar{v}_x = \frac{h_o}{h(x)}\,\delta'(x)\,\delta(y) \tag{5.3}$$

Let

$$\bar{v} = h_o^{\frac{1}{2}}\,h^{-\frac{1}{2}}(x)\,v_o \tag{5.4}$$

Then

$$\Delta v_o - \left[\frac{1}{4} \left(\frac{h'}{h} \right)^2 + \frac{1}{2} \left(\frac{h'}{h} \right)' \right] v_o = h_o^{\frac{1}{2}} h^{-\frac{1}{2}} \delta'(x)\, \delta(y) \qquad (5.5)$$

Let

$$u = \frac{1}{2\pi} \int_{-\infty}^{\infty} e^{jky}\, v_o(x, y)\, dy$$

so

$$v_o = \int_{-\infty}^{\infty} e^{-jky}\, u(x, k)\, dk$$

and if $u(x, k) = u(x, -k)$, then

$$v_o = 2 \int_0^{\infty} u(x, k) \cos(ky)\, dk$$

and if $u(x, +k) = -u(x, -k)$ then

$$v_o = -2j \int_0^{\infty} u(x, k) \sin(ky)\, dk \, .$$

Of course

$$\bar{v} = h_o^{\frac{1}{2}} h(x)^{-\frac{1}{2}} v_o \, .$$

Now consider a special channel that is sectionally continuous with

$$\frac{h'}{h} = -a \left[H_o(x + b) - H_o(x - a) \right]$$

where $H_o(x + b)$ is a unit step function, i.e., equal to unity if the argument $\geqslant 0$ and equal to zero otherwise. The shape of the channel is indicated in Fig. 11.

$$\left(\frac{h'}{h}\right)' = -\alpha \left[\delta(x+b) - \delta(x-a)\right] \tag{5.7}$$

where δ is the Dirac delta function.

Applying the integral operator $\frac{1}{2\pi} \int_{-\infty}^{\infty} e^{jky} (\ldots.) \, dy$ *

where $(\ldots.)$ denotes the quantity (a function of x and y) on which the operator operates and assuming $v_o(x, \pm\infty) = 0$ and also

$$\frac{\partial v_o}{\partial y}(x, \pm\infty) = 0$$

(which is quite reasonable since v_o is related to the velocity $\bar{v}$) the partial differential equation (5.5) reduces to an ordinary differential equation:

$$u'' - u\left[k^2 + \frac{\alpha^2}{4}\left[H_o(x+b) - H_o(x-a)\right] - \frac{\alpha}{2}\left[\delta(x+b) - \delta(x-a)\right]\right] = \frac{1}{2\pi}\left[\delta'(x) + \frac{h'(0)}{2h(0)}\delta(x)\right] \tag{5.8}$$

where we make use of the fact that

$$f(y)\,\delta'(y) = f(0)\,\delta'(y) - f'(0)\,\delta(y) \tag{5.9}$$

and primes in Eq. (5.8) denote differentiation with respect to x.

* In this thesis, j will be used to denote $\sqrt{-1}$.

Therefore we have to solve for

$$u'' - \left[k^2 + \frac{\alpha^2}{4}\left[H_o(x+b) - H_o(x-a)\right] - \frac{\alpha}{2}\left[\delta(x+b) - \delta(x-a)\right]\right] u = 0 \qquad \text{for } x \neq 0 \tag{5.10}$$

subject to the two jump conditions:

$$u\Big|_{0-}^{0+} = \frac{1}{2\pi} \quad \text{and} \quad u'\Big|_{0-}^{0+} = -\frac{\alpha}{4\pi} = -\frac{\alpha}{2}\left(\frac{1}{2\pi}\right) \tag{5.11}$$

For $x \neq 0$ write Eq. (5.10) as:

$$u'' = \left[k^2 + \frac{\alpha^2}{4}\left[H_o(x+b) - H_o(x-a)\right] - \frac{\alpha}{2}\left[\delta(x+b) - \delta(x-a)\right]\right] u \tag{5.12}$$

This shows u is continuous at $x = -b$ and $x = a$ but u' jumps at $x = -b$ and $x = a$ in the following manner:

$$u'\Big|_{x=-b^-}^{x=-b+} = -\frac{\alpha}{2} u(-b) \qquad \text{and}$$

$$u'\Big|_{x=a-}^{x=a+} = \frac{\alpha}{2} u(a) \quad . \tag{5.13}$$

The jump conditions (5.13) and (5.11) along with a statement that we seek a solution, subject to Eqs. (5.13) and (5.11), to the differential equation:

$$u'' - k^2 u = 0 \quad \text{for } x < -b \text{ and } x > a$$

and

$$u'' - (k^2 + \frac{a^2}{4})u = 0 \text{ for } -b < x < a$$

constitute a formulation of the problem for u in terms free of generalized functions.

Letting $k_1 = \sqrt{k^2 + \frac{a^2}{4}}$ and using the following solutions for regions $x < -b$, $-b < x < a$, and $x > a$

(a) for $x \leqslant -b$: $u(k,x) = D(k)e^{kx}$

(b) for $-b \leqslant x < 0$:

$$u(k,x) = B_o(k)e^{k_1 x} + A_R(k)e^{k_1(x-a)} + B_R(k)e^{-k_1(x+b)}$$

(c) for $0 < x \leqslant a$:

$$u(k,x) = A_o(k)e^{-k_1 x} + A_R(k)e^{k_1(x-a)} + B_R(x)e^{-k_1(x+b)}$$

(d) for $x \geqslant a$: $x = C(k)e^{-kx}$

$$\text{with } A_o(k) = \frac{1}{4\pi}(1 + \frac{a}{2k_1})$$

$$\text{and } B_o(k) = -\frac{1}{4\pi}(1 - \frac{a}{2k_1}) \tag{5.14}$$

a system of four simultaneous equations for A_R, B_R, D and C as functions of k can be set up to satisfy the two continuity conditions at $x = -b$ and $x = a$ on u, and the two jump conditions on u' at $x = -b$ and $x = a$. It should be noted the $A_o(k)$ and the $B_o(k)$ have been chosen to satisfy the jump conditions at the origin. A solution for $u(x, k)$ can indeed be found by solving the set of simultaneous equations. However, the problem of inverting the extremely complicated function of k that u turns out to be, proved impossible to solve and an alternative approach was used. The alternative approach is to solve the problem for u approximately, i.e., in powers of α. Also the way the alternative approach proceeds, the jump conditions at $x = -b$ and $x = a$ are satisfied automatically.

Section 3: The Approximate Calculation.

Let

$$g(x) = \frac{\alpha^2}{4} \cdot \left[H_o(x + b) - H_o(x - a)\right] - \frac{\alpha}{2}\left[\delta(x + b) - \delta(x - a)\right]$$

The solution to the problem for u is taken to be $A(k)u_1(x, k)$ for $x > 0$ and $B(k)u_2(x, k)$ for $x < 0$. $u_1(x, k)$ is taken to be the solution asymptotic to $\exp(-kx)$ as $x \to \infty$ and $u_2(x, k)$ is taken as the solution asymptotic to $\exp(kx)$ as $x \to -\infty$. Then u_1 satisfies the integral equation:

$$u_1(x, k) = e^{-kx}\left[1 + \int_x^{\infty}\left[\frac{1 - e^{-2k(q-x)}}{2k}\right] g(q)u_1(q, k)e^{kq}\, dq\right] \tag{5.15}$$

Incidentally the k used above is really $|k|$. The solutions for u turn out to be even functions of k and so we need to use the cosine transforms to obtain the velocities.

The above integral equation is got by the method of variation of parameters; i.e., we write $\left[u'' - k^2 u = g(x)u\right]$ and regard "$g(x)u$" as an inhomogenous term. Similarly for $u_2(x,k)$ we take the solution asymptotic to $\exp(kx)$ as $x \rightarrow -\infty$ and write it as the solution of the integral equation:

$$u_2 = e^{kx}\left[1 + \int_{-\infty}^{x} \left(\frac{1 - e^{2k(q-x)}}{2k}\right) g(q) e^{-kq} u_2(k,q)\, dq\right] \tag{5.16}$$

Now consider a calculation to $0(a)$:

$$\begin{aligned} u_1(x,k) &= e^{-kx}\left[1 + \frac{a}{4k}\left(1 - e^{-2k(a-x)}\right)\right] \\ u_2(x,k) &= e^{kx}\left[1 - \frac{a}{4k}\left(1 - e^{-2k(x+b)}\right)\right] \end{aligned} \tag{5.17}$$

The jump conditions at the origin are:

$$\begin{aligned} A(k)u_1(0,k) - B(k)u_2(0,k) &= \frac{1}{2\pi} \\ A(k)u_1'(0,k) - B(k)u_2'(0,k) &= -\frac{a}{2}\left(\frac{1}{2\pi}\right) \end{aligned} \tag{5.18}$$

where the primes denote differentiation w r t x. Incidentally the values given by Eq. (5.17) are only for $-b \leqslant x \leqslant a$ and the values of $u(x,k)$ outside this range of x are:

$$\begin{aligned} u_1(x,k) &= e^{-kx} \text{ for } x \geqslant a \qquad \text{and} \\ u_2(x,k) &= e^{kx} \text{ for } x \leqslant -b\,. \end{aligned} \tag{5.19}$$

We solve for the $A(k)$ and $B(k)$ and find them to $0(\alpha)$:

$$A(k) = \frac{1}{4\pi k}\left[u_2'(0,k) + \frac{\alpha}{2}u_2(0,k)\right]$$
$$B(k) = \frac{1}{4\pi k}\left[u_1'(0,k) + \frac{\alpha}{2}u_1(0,k)\right] \quad . \tag{5.20}$$

In general if we denote by W the Wronskian:

$$\left[u_1(0,k)\,u_2'(0,k) - u_1'(0,k)\,u_2(0,k)\right]$$

the solution for $A(k)$ and $B(k)$ can be written as

$$A(k) = \frac{1}{2\pi W}\left[u_2'(0,k) + \frac{\alpha}{2}u_2(0,k)\right]$$
$$B(k) = \frac{1}{2\pi W}\left[u_1'(0,k) + \frac{\alpha}{2}u_1(0,k)\right] \quad .$$

Calculation of the Wronskian to $0(\alpha^2)$ gives

$$2k\left[1 + \frac{\alpha^2}{8k}\left[(a+b) - \frac{1}{2k}\left(1 - e^{-2k(a+b)}\right)\right]\right] \quad .$$

This shows for all k the error involved in approximating the W by $2k$ is only of $0(\alpha^2)$. Inclusion of terms of $0(\alpha^2)$ in the transform give rise to the same problem as in an exact solution (using the set of simultaneous equations), i.e., it becomes extremely hard to invert the transforms. The calculation was therefore restricted to terms of $0(\alpha)$. Further the problem in the transform plane (x, k) was solved exactly and for selected values of a, b, x and k the exact solution and the solution to $0(\alpha)$ (for $\alpha = 0.1$) were compared numerically as functions of k. For $a = b = x = 1$, very good agreement was obtained (the differences were less than 0.4 percent). As a function of k, the $0(\alpha)$ calculation was systematically greater than the exact calculation for $|k| < 1$. The error is greatest for $k = 0$ (about 0.4 percent) and from then on decreases with increase of $|k|$. For $|k| > 1$, there is practically no difference between the two calculations.

Using the values of $A(k)\,u_1(x, k)$ and $B(k)\,u_2(x, k)$ and a table of Fourier cosine transforms one writes down the value of v for a vortex (to $0(\alpha)$) as:

$$\bar{v}_v = \frac{1}{2\pi}\left[\frac{x}{x^2 + y^2} + \frac{\alpha x^2}{2(x^2 + y^2)} + \frac{\alpha}{8}\,\ell n\left[\frac{\left[(x + 2b)^2 + y^2\right]\left[(2a - x)^2 + y^2\right]}{(x^2 + y^2)^2}\right]\right] \tag{5.21}$$

Again the above is for the region $-b \leqslant x \leqslant a$.

Consider now the $\bar{u}$ component of velocity for a unit source located at the origin. We now start with the pair:

$$\frac{\partial}{\partial x}(h\,\bar{u}) + \frac{\partial}{\partial y}(h\,\bar{v}) = h_o\,\delta(x)\,\delta(y)$$

$$\frac{\partial}{\partial x}(h\,\bar{v}) - \frac{\partial}{\partial y}(h\,\bar{u}) - h'\bar{v} = 0\ . \tag{5.22}$$

Elimination of $\bar{v}$ leads to:

$$\Delta\bar{u} + \frac{h'}{h}\,\bar{u}_x + \left(\frac{h'}{h}\right)'\bar{u} = \delta'(x)\,\delta(y)\ . \tag{5.23}$$

As before let

$$\bar{u} = h_o^{\frac{1}{2}} h^{-\frac{1}{2}}(x) \int_{-\infty}^{\infty} w(x,k)\, e^{-jky} dk \tag{5.24}$$

where

$$w(x,k) = \frac{h_o^{-\frac{1}{2}} h^{\frac{1}{2}}(x)}{2\pi} \int_{-\infty}^{\infty} e^{jky}\, \bar{v}(x,y)\, dy$$

we have

$$w'' - \left[k^2 + \frac{1}{4}\left(\frac{h'}{h}\right)^2 - \frac{1}{2}\left(\frac{h'}{h}\right)'\right] w = \frac{1}{2\pi}\left[\delta'(x) - \frac{h'(0)\,\delta(x)}{2h(0)}\right] \tag{5.25}$$

Again we need to solve for $x \neq 0$:

$$w'' - w\left[k^2 + \frac{a^2}{4} \cdot \left[H_o(x+b) - H_o(x-a)\right] + \frac{a}{2}\left[\delta(x+b) - \delta(x-a)\right]\right] = 0 \tag{5.26}$$

subject to

$$w'\Big|_{0^-}^{0^+} = \frac{a}{4\pi} = \left(\frac{a}{2}\right)\left(\frac{1}{2\pi}\right)$$

and

$$w\Big|_{0^-}^{0^+} = \frac{1}{2\pi} \quad .$$

Exactly the same approximate procedure of calculation as for $\bar{v}_v$ was adopted and to $0(\alpha)$:

$$\bar{u}_s = \frac{1}{2\pi}\left[\frac{x}{x^2+y^2} + \frac{\alpha x^2}{2(x^2+y^2)} - \frac{\alpha}{8}\,\ell n\left[\frac{\left[(2a-x)^2+y^2\right]\left[(x+2b)^2+y^2\right]}{(x^2+y^2)^2}\right]\right] .$$

As a check on the above, at this point, some alternative procedures of viewing $\bar{u}_s$ were considered and are described below.

Section 4: Some Checks on $\bar{u}_s$.

Before describing these checks, consider first the case where the contraction occurs fully upstream of the location of the singularity (see Fig. 12). The only changes from the calculation of $\bar{u}_s$ before are that:

$$\frac{h'}{h} = -\alpha\left[H_o(x+b) - H_o(x+a)\right] \qquad \text{and}$$

$$\frac{h''}{h} = -\alpha\left[\delta(x+b) - \delta(x+a)\right] . \tag{5.27}$$

The derivative of the transform with respect to x is continuous at the origin and the transform itself jumps by $\frac{1}{2\pi}$. The $\bar{u}$ component of velocity for a source turns out to be (to $0(\alpha)$) :

$$\bar{u}_s = \frac{1}{2\pi}\left[\frac{x}{x^2+y^2} - \frac{\alpha}{8}\,\ell n\left[\frac{(x+2b)^2+y^2}{(x+2a)^2+y^2}\right]\right] \tag{5.28}$$

For convenience, consider velocities for points on the x-axis, i.e., with $y = 0$:

$$\bar{u}_s = \frac{1}{2\pi}\left[\frac{1}{x} - \frac{\alpha}{4}\ln\left[\frac{|x+2b|}{|x+2a)}\right]\right] \tag{5.29}$$

Consider further the special case as a, b recede from the origin, i.e., let $(b - a) \ll (x + a + b)$. Expanding the logarithm as a power series the effect of the faraway contraction is seen to be an additional term of value approximately equal to

$$-\frac{1}{2\pi}\frac{\alpha}{2}\frac{(b-a)}{(x+a+b)} \quad .$$

As the contraction recedes further and further away from the location of the source one may reasonably expect that the exact details of the contraction should be less and less important for the calculation of the effect of it on the velocity near the source. Consider, e.g., a stepwise two-dimensional channel, as shown in Fig. 13. Assume a two-dimensional line source spans the channel at the origin 0. We need to calculate the effect of the step at $x = -\frac{1}{2}(a + b)$ where the height increases to $\exp\left[(b - a)\alpha\right]$ of its value ahead. The computation may be done by the method of images as follows: The flow in the region $x \leqslant -\left|\frac{a+b}{2}\right|$ is regarded as due to a transmitted source of strength m_t located at the origin and the flow for $x \geqslant -\left|\frac{a+b}{2}\right|$ as due to the source of strength unity at the origin and an image source of strength m_i located at the image point of the origin in the plane $x = -\left|\frac{a+b}{2}\right|$, i.e., at $x = -(a + b)$. The strengths m_i and m_t are obtained by considerations of continuity and that the y-component of velocity be continuous across $x = -\left(\frac{a+b}{2}\right)$. The absence of any solid boundaries normal to the y-axis precludes the transmission of any impulse parallel to the y-axis which alone can effect discontinuities in the velocity parallel to the y-axis. The above two conditions yield:

$$m_t = \exp\left[(a - b)\alpha\right] \quad (1 - m_i)$$

and $m_t = 1 + m_i$.

These lead to $$m_i = \frac{\exp\left[(b - a)\alpha\right] - 1}{1 + \exp\left[(b - a)\alpha\right]}$$, which is approximately equal to:

$$-\frac{(b - a)\alpha}{2} \quad \text{to} \quad 0(\alpha) .$$

The velocity field associated with m_i, in the region $x < -\left(\frac{a+b}{2}\right)$, for $y = 0$, is:

$$-\frac{\alpha(b - a)}{2(x + a + b)2\pi}$$

It is clear that a term equivalent to the one for the sectionally continuous channel is obtained for the stepwise discontinuity insofar as the alteration of the velocity field goes. The "method of images" used here is analogous to one discussed in Ref. 23.

It is appropriate to mention here an alternative derivation of Eq. (1.4). We consider a channel with discrete two-dimensional sections (i.e., sections of constant height) of incremental width ϵ.

In each section we use solutions to the two-dimensional potential equation to represent ϕ . The ϕ's in two adjacent sections are related by a continuity condition on (hu) and the requirement that v be continuous. Finally we let $\epsilon \rightarrow 0$ and it can be shown that ϕ satisfies Eq. (1.4). The details are given in Appendix 9. Again this approach is largely modelled on a similar derivation for the equation governing the perturbation velocities in a parallel, density stratified shear flow given in Ref. 24.

As a second check we note that if we were to solve for the velocity field by a perturbation technique we would assume for

$$\phi = \phi_o + a\phi_1 + a^2\phi_2 + \cdots .$$

Taking $\phi_o = \frac{1}{2\pi} \ell n(r)$ where $r = \sqrt{x^2 + y^2}$, for ϕ_1 one has a Poisson equation:

$$a\Delta^2\phi_1 = -\frac{h'}{h}\frac{x}{2\pi r^2} .$$

(Recall ϕ satisfies $\Delta\phi = -\frac{h'}{h}\phi_x$.)

Using the usual integral representation for ϕ_1 it was found that the first addition to the velocity field is indeed that as obtained by the technique of Fourier transforms. In retrospect it may be remarked that the main advantage in using transforms appears to be that in the transform plane (x, k) the problem can be formulated and solved exactly so that it becomes possible to make numerical evaluations of how accurate the $0(a)$ solution is. It is obvious that for fixed a, as a, b become very large the order α calculation will be increasingly inaccurate. Estimation of the inaccuracy in quantitative terms becomes possible if one uses the Fourier transform method. Neither the iterative procedure of solving the ordinary differential equation (5.10) based on the integral equations (5.15) and (5.16) nor the obtaining of successive approximations by evaluating a series of Poisson integrals can be expected to yield the fully exponential channel velocity fields (involving $K_o\left[\frac{\alpha r}{2}\right]$ and $K_1\left[\frac{\alpha r}{2}\right]$) in the limit as $a, b \rightarrow \infty$. Indeed, in case of either approach, the relevant integrals will diverge as $a, b \rightarrow \infty$. This is easily understandable since we cannot hope to solve by a perturbation technique the flow in a channel such as a fully exponential channel which is not just a perturbation from a basically two-dimensional channel. The exact formulation and solution of the problem for the transform is subject to no such limitation and in the limit as $a, b \rightarrow \infty$, one is left with the solutions for $x > 0$ and $x < 0$, in the notation of Eq. (5.14):

(a) for $x > 0$: $u(x, k) = A_o(k) \exp(-k, x)$

(b) for $x < 0$: $u(x, k) = B_o(k) \exp(k, x)$.

The inversion of the above and the resulting velocity fields got after incorporating the multiplicative factors $h_o^{\frac{1}{2}} h^{-\frac{1}{2}}(x)$ of Eq. (5.4), do indeed yield the velocity fields got in Chapter I by solution of the original partial differential equation by separation of variables.

Section 5: Calculation of $\bar{u}$ for a Vortex and $\bar{v}$ for a Source.

The only difference in what follows is that the transforms are now odd in k thus necessitating the use of sine transforms in inverting to get the velocity fields. Starting again with the pair Eqs. (5.1) and (5.2) and eliminating the $\bar{v}$ component, one arrives at (for $\bar{u}$) the following equation:

$$\Delta\bar{u} + \left(\frac{h'}{h}\right) \bar{u}_x + \left(\frac{h'}{h}\right)' \bar{u} = - \frac{h_o}{h(x)} \delta(x)\, \delta'(y) \quad . \tag{5.31}$$

Let

$$\bar{u} = u_o h_o^{\frac{1}{2}} h(x)^{-\frac{1}{2}} : \qquad \text{then}$$

$$\Delta u_o + \left[\frac{1}{2}\left(\frac{h'}{h}\right)' - \frac{1}{4}\left(\frac{h'}{h}\right)^2\right] u_o = - h_o^{\frac{1}{2}} h^{-\frac{1}{2}} \delta(x)\, \delta'(y)$$

Let

$$v = \frac{1}{2\pi} \int_{-\infty}^{\infty} e^{jky}\, u_o(x, y)\, dy$$

so that

$$u_o = \int_{-\infty}^{\infty} v(x, k)\, e^{-jky}\, dk$$

If $v(x, k) = - v(x, -k)$, then

$$\bar{u} = - h_o^{\frac{1}{2}} h^{-\frac{1}{2}}(x)\, 2j \int_{-\infty}^{\infty} v(x, k) \sin(ky)\, dk$$

The problem for v is:

$$v'' + \left[\frac{1}{2}\left(\frac{h'}{h}\right)' - k^2 - \frac{1}{4}\left(\frac{h'}{h}\right)^2\right] v = \frac{jk\delta(x)}{2\pi}$$

once again letting:

$$\frac{h'}{h} = -\alpha\left[H_o(x+b) - H_o(x-a)\right] ,$$

one carries out computations similar to that described before to finally arrive at:

$$\bar{u}_v = -\frac{1}{2\pi}\left[\frac{y}{x^2+y^2} + \frac{\alpha}{4}\left[\tan^{-1}\left(\frac{x+2b}{y}\right) - \tan^{-1}\left(\frac{2a-x}{y}\right)\right]\right.$$

$$\left. + \frac{\alpha xy}{2(x^2+y^2)}\right] \quad \text{to } 0(\alpha) . \qquad (5.32)$$

The $\bar{v}$ component of velocity for a source by a similar analysis works out to be

$$\bar{v}_s = \frac{1}{2\pi}\left[\frac{y}{y^2+x^2} + \frac{\alpha xy}{2(x^2+y^2)}\right.$$

$$\left. + \frac{\alpha}{4}\left[\tan^{-1}\left(\frac{2a-x}{y}\right) - \tan^{-1}\left(\frac{x+2b}{y}\right)\right]\right] \qquad (5.33)$$

<u>Section 6</u>: Case of Fully Upstream Contractions.

$$\frac{h'}{h} = -\alpha\left[H_o(x+b) - H_o(x+a)\right]$$

The four components $\bar{u}_s$, $\bar{v}$, $\bar{u}_v$ and $\bar{v}_s$ are listed below:

$$\bar{v}_v = \frac{1}{2\pi}\left[\frac{x}{x^2+y^2} + \frac{a}{8}\,\ell n\left[\frac{(x+2b)^2+y^2}{(x+2a)^2+y^2}\right]\right]$$

$$\bar{u}_s = \frac{1}{2\pi}\left[\frac{x}{x^2+y^2} - \frac{a}{8}\,\ell n\left[\frac{(x+2b)^2+y^2}{(x+2a)^2+y^2}\right]\right]$$

$$(5.34)$$

$$\bar{u}_v = \frac{1}{2\pi}\left[\frac{y}{x^2+y^2} + \frac{a}{4}\left[\tan^{-1}\left(\frac{y}{x+2a}\right) - \tan^{-1}\left(\frac{y}{x+2b}\right)\right]\right]$$

$$\bar{v}_s = \frac{1}{2\pi}\left[\frac{y}{x^2+y^2} - \frac{a}{4}\left[\tan^{-1}\left(\frac{y}{x+2a}\right) - \tan^{-1}\left(\frac{y}{x+2b}\right)\right]\right]$$

Section 7: Case of Fully Downstream Contraction.

Again the details are omitted and we reproduce below results analogous to Eq. (5.34). The notation is as in Fig. 14:

$$\bar{v}_v = \frac{1}{2\pi}\left[\frac{x}{x^2+y^2} - \frac{a}{8}\,\ell n\left[\frac{(2b-x)^2+y^2}{(2a-x)^2+y^2}\right]\right]$$

$$\bar{u}_s = \frac{1}{2\pi}\left[\frac{x}{x^2+y^2} + \frac{a}{8}\,\ell n\left[\frac{(2b-x)^2+y^2}{(2a-x)^2+y^2}\right]\right]$$

$$(5.35)$$

$$\bar{u}_v = -\frac{1}{2\pi}\left[\frac{y}{x^2+y^2} + \frac{a}{4}\left[\tan^{-1}\left(\frac{y}{2a-x}\right) - \tan^{-1}\left(\frac{y}{2b-x}\right)\right]\right]$$

$$\bar{v}_s = +\frac{1}{2\pi}\left[\frac{y}{x^2 + y^2} - \frac{a}{4}\left[\tan^{-1}\left(\frac{y}{2a - x}\right) - \tan^{-1}\left(\frac{y}{2b - x}\right)\right]\right]$$

Section 8: Solution of the Integral Equation.

The solution procedure is entirely analogous to that discussed in Chapter IV. The kernels $k_{vrc}(x, \xi)$ etc. are derived from the solutions discussed above.

Section 9: Estimation of Flow Inlet and Outlet Angles (Relative to Cascade Axis).

By considering the line integral of the velocity around ABCD in Fig. 15a which represents one spatial period of the flow, since the line integrals along AB and CD cancel out by periodicity, clearly,

$$\Delta V_t = (V_{it} - V_{ot}) = \frac{\Gamma_t}{s}$$

where "i" stands for inlet, "o" for outlet, "t" for tangential to cascade, "Γ_t" for the total circulation, and "s" for spacing of the cascade. The mean flow indicated by OV_m is assumed to be of unit magnitude and inclined at δ to the blade chord and hence at $(\lambda + \delta)$ to the cascade axis. The inlet and outlet angles relative to the cascade axis have been shown by I. A. and O. A.. Clearly then to $0(a)$:

$$\tan(\text{I.A.}) = \frac{\sin(\lambda + \delta) + \frac{\Delta V_t}{2}}{(1 - a\cos\lambda)\cos(\lambda + \delta)}$$

and

$$\tan(\text{O. A.}) = \frac{\sin(\lambda + \delta) - \frac{\Delta V_t}{2}}{(1 + \alpha\cos\lambda)\cos(\lambda + \delta)}$$

since the chord is taken 2 units long and the axis of convergence same as cascade axis. The Γ_t depends on airfoil shape and δ .

CHAPTER VI

RESULTS OF NUMERICAL WORK ON THE FINITE CHANNELS

The results for isolated airfoils were qualitatively similar to those for a cascade and hence the work on contractions fully upstream and fully downstream was restricted to isolated airfoil calculations only. In case of contractions fully covering the airfoil both cascade and isolated cases were treated.

The factor varied in cases where the contraction fully covered the airfoils was the extent of the contraction. There was no point in varying a since the results are linear in a. The contraction in these cases was assumed located symmetrically with respect to the chord. In cases of upstream and downstream contraction the spacing between the centerline of the contraction and that of the chord was also varied. The dependent quantity plotted and studied on the y-axis was the ratio "r" of total circulation for a quasi-two-dimensional calculation for the same airfoil section and angle of attack. The results of the work are presented in Figs. 16-23.

The effect of fully upstream and downstream contractions is in general not very much, insofar as reduction of circulation goes. This is true even when the contractions are just ahead or just behind the airfoil.

In case of cascade calculations the known parameters are taken as the stagger angle, the spacing, the airfoil section, the angle the mean vector velocity makes with the chord at mid-chord point, and the extent of the contraction.

Figure 19 shows the reduction of circulation is less for cambered airfoils than for flat plates. Thickness increases the reduction. The order of magnitude of the reduction ratio is pretty close to the ratio of inlet channel height (at the leading edge) to the channel height at exit. The reduction is also less with decreasing solidity (solidity $= \frac{c}{s}$). Figure 20 shows the effects of varying the extent. Two deductions may be made from Fig. 20. The cascade reductions are somewhat greater than those for an isolated airfoil and secondly the dependence of the reduction ratio on the extent of contraction is much weaker for isolated airfoils than it is for a cascade. Figure 21 simply confirms the qualitative similarity of the results for isolated airfoils and airfoils in cascade.

Figure 22 is undoubtedly the most interesting plot. There is a lively dependence on the stagger angle of the reduction ratio. This is due to the interplay of the freestream effect (which diminishes circulation for $\lambda > 0$ and increases it for $\lambda < 0$) and the effect due to altered behavior of vortices (which always diminishes the circulation provided $|\lambda| < \pi/2$). There is a pronounced minimum of circulation at $\lambda = 30^{\circ}$ and it takes a negative stagger of about $\lambda = -30^{\circ}$ for the abovementioned two effects to cancel out exactly.

Figure 23 is an attempt to give some idea of the effect of quasi-two-dimensionality on the actual distribution of vorticity and as may be seen the distribution near the leading edge is the most affected.

The effect on the inlet and outlet angles as compared to a two-dimensional calculation is slight. This is because the contraction by increasing the axial velocity tends to increase the turning of the flow. However the quasi-two-dimensional calculations show the contraction diminishes the circulation and this in itself tends to decrease the turning of the flow. There is a balance between these two factors because, as mentioned earlier, the reduction of circulation is pretty close to the ratio of inlet to exit height. Thus the inlet and exit angles are affected from the two-dimensional values only by a degree or so for the cases treated. The inlet and exit angles for the cascade have been presented in tabular form in Table I.

We make one remark here regarding a problem that may come up in case of cascade design. Usually it is the incidence angle (I. A.) that is known and not the angle that the mean flow makes with the chord. For a given cascade geometry, airfoil section and contraction parameters one would proceed as follows:

1. Obtain Γ_t first for $\delta = 0$ and then for some non-zero but small δ. Now express Γ_t as :

$$\Gamma_t = A_o + A_1 \delta \quad \text{(a linear relation).} \tag{6.1}$$

2. Expand the right hand side of the equation for tan (I.A.) in powers of δ restricting oneself to first order in δ, using Eq. (6.1). Now for given I.A. solve for δ and thus compute the outlet angle.

We wish to reiterate, at this point, that all comparisons in Table I and indeed throughout this work have been done on the assumption that the angle of attack for the two-dimensional and the quasi-two-dimensional cases is the same. (In what follows it will be convenient to use the abbreviations T.D. for "two-dimensional" and Q.T.D. for "quasi-two-dimensional.") It is undoubtedly true that a comparison for fixed angle of incidence would be more meaningful for design purposes. It is an unfortunate limitation of all singularity methods (Refs. 2, 4 and 25) that one is forced to use the angle of attack of the mean velocity as a reference quantity. As pointed out earlier, by doing two calculations, one with zero angle of attack and the other with a non-zero angle of attack, the problem of given incidence can indeed be solved in a specific instance. The graphs in Figs. 16-23 representing the effects of quasi-two-dimensionality are all complicated functions of α, the stagger angle, the solidity and the extent of contraction E. We would like to be able to give a simple deviation rule as, e.g., Constant's rule for circular arc airfoils (mentioned in Ref. 26) incorporating the effects of contractions. Owing to the abovementioned limitation that the Q.T.D. effect depends on too many factors, it was decided to merely indicate how one would solve a specific design problem for given incidence.

α and E will have to be estimated perhaps experimentally. It appears a vast amount of numerical experimentation will need to be done to be able to state a reasonably well-verified empirical rule. Since a rather specific channel shape (sectionally exponentially converging type) has been assumed, such a great deal of numerical work is of dubious value.

There are however some important conclusions to be drawn from Table I regarding the flow turning angle or deflection for fixed incidence. The deductions for fixed incidence from the data of Table I (which is for fixed mean angle of attack) were done on the following basis: We roughly correct the results of Table I to compare the deflection angles for given incidence on the basis of Fig. 3 of Ref. 26. This figure is a plot of deflection angle against incidence angle for a "typical cascade test". It indicates that over the compressor working range an increase or decrease of incidence by a degree produces a corresponding increase or decrease of about a degree in the deflection. All the deflection angles for the Q.T.D. flow were adjusted to what they might have been if the incidence angle for the Q.T.D. flow has been the same as for the T.D. flow. To be sure, Fig. 3 of Ref. 26 refers to a specific cascade geometry. But because the results of Fig. 3 are for a "typical cascade test" and also because as Table I shows the differences in the incidence angles for the Q.T.D. and the T.D. flow are only about a degree in most instances, no great error can result from this adjustment. Papers on cascade design (e.g., Ref. 26) usually give plots of deflection angles against incidence angle . We give below the chief conclusions principally for three kinds of variation: first, variation with extent of contraction E with all other factors held fixed; second, variation with solidity, again with other factors fixed; and thirdly, variation with stagger.

1. For given contraction ratio across the chord (equal to $\exp(-2a \cos\lambda)$ since the chord is two units long), given stagger and solidity the relevant data is in Table I(a). $\lambda = 45^{\circ}$ and $s/c = 1.00$ are about the most typical values for a compressor cascade. For this set of λ and (s/c) at $(E \div 2 \cos\lambda) = 1.061$, the flow turning for the T.D. and Q.T.D. cases is just about equal. For lesser $(E \div 2 \cos\lambda)$ than 1.061 the flow turning for the Q.T.D. flow is greater than the T.D. value, and for $(E \div 2 \cos\lambda)$ greater than 1.061 the T.D. flow deflection is greater. This is clearly because the effect of axial acceleration, which increases the deflection, is independent of E so long as the contraction fully covers the airfoils, i.e., so long as $(E \div 2 \cos\lambda)$ is greater than 1.00. The reduction of circulation, which decreases the deflection, increases with E. There is a balance of the two effects at $(E \div 2 \cos\lambda)$ equal to 1.061 while the former prevails for $(E \div 2 \cos\lambda)$ less than 1.061 and the latter for $(E \div 2 \cos(\lambda))$ greater than 1.061. The lower limit of $(E \div 2 \cos\lambda)$ is unity since we have assumed in all cascade calculations that the contraction fully covers the airfoils. All the tables can be explained by a study of this balance and we will, in what follows, merely state the conclusions. We note that the differences

in flow turning for the T.D. and Q.T.D. cases are quite small, i.e., of the order of a degree or so.

2. The deflection of the Q.T.D. flow gradually exceeds that of the T.D. flow with decreasing solidity. The two deflections are equal at about $c/s = 1.00$ for flat plate airfoils, at $c/s = 0.666$ for circular arc airfoils. The results in this regard for circular arc airfoils with zero thickness and circular arc airfoils that are 10 percent thick are practically the same. Other parameters are assumed equal in this study of the variation with solidity. For higher than the abovementioned solidities, the two-dimensional flow has the greater deflection. Again we emphasize that though there are differences between the two cases, they are quite small for contractions that may be regarded as physically reasonable (about 10-20 percent contraction).

3. For all staggers from about -30° to 60° the two-dimensional flow has the greater deflection. The difference is greatest (about 2 degrees) at a stagger of -30°. In the compressor range of staggers from 0° - 60° it is always less than a degree. The variation with stagger is studied with other factors held fixed.

Roughly speaking then, we have repeatedly emphasized the prediction that for fixed incidence the deflection angles for the two-dimensional and quasi-two-dimensional flow should not differ much - perhaps by a degree or so in the compressor range of parameters. Of course we restrict ourselves to physically reasonable contractions of around 10-20 percent. The velocity diagram in Fig. 15a shows however that the effect of the contraction on the magnitude of the inlet and outlet velocities is by no means inconsiderable. The effect of quasi-two-dimensionality is to increase the magnitude of the outlet velocity relative to the inlet velocity (as compared to its two-dimensional value), due to two causes. Firstly the axial component of the outlet velocity exceeds that of the inlet velocity due to the contraction. Secondly since the quasi-two-dimensionality reduces the circulation the reduction of tangential component of the outlet velocity from that of the inlet velocity (compared to its two-dimensional value) is also reduced. From Bernoulli's theorem, we expect the pressure rise for a quasi-two-dimensional flow through a compressor cascade to be noticeably lesser than for a two-dimensional flow even though the deflection angles would be in close agreement.

An explicit statement pertinent to the conclusions of this thesis appears on p. 4 of Ref. 26. This statement, which we reproduce below, is based on a survey of experimental data and supports the predictions of this thesis:

> The few tests available indicate that small amounts of contraction have little effect on the measurement of deflection and loss even though the effect on the pressure rise across the cascade may be relatively large so that some wind tunnel tests with contraction have been used in the test analysis of this report.

Since the present thesis is restricted to an inviscid flow without separation no losses can be accounted for by our calculations.

REFERENCES

1. "Aerodynamics of Turbines and Compressors," Vol. X of the High Speed Aerodynamics and Jet Propulsion Series published by the Princeton University Press, Section C, 1964.

2. Mellor, G. L., "An Analysis of Axial Compressor Aerodynamics," Trans. ASME, September 1959.

3. Schlichting, H., "Berechnung der reibungslosen inkompressiblem Stromung für ein Vorgegebenen ebenes Schaufelgitter," VDI Forschungsheft 447, 1955.

4. Martensen, E., "Calculation of the Pressure Distribution on a Cascade of Thick Airfoils Using Fredholm Integral Equations of the Second Kind," Communications from the Max Planck Institute for Fluid Mechanics and the Aerodynamic Experimental Station, No. 23, 1959.

5. Katzoff, S., Bogdonoff, H. E., and Boyet, H., "Comparisons of Theoretical and Experimental Lift and Pressure Distributions on Airfoils in Cascade," NACA TN 1376, July 1947.

6. Erwin, J.R. and Emery, J.C., "Effect of Tunnel Configuration and Testing Technique on Cascade Performance," NACA TN 2028, February 1950.

7. Hawthorne, W.R., "Induced Deflection Angle in Cascades," J. of the Aeronautical Sciences, Vol. 16, No. 4, 1949, p. 252.

8. Scholz, N., "Two-Dimensional Correction of the Outlet Angle in Cascade Flow," J. of the Aeronautical Sciences, Vol. 20, No. 11, 1953, p. 786.

9. Hausmann, F., "The Theoretical Induced Deflection Angle in Cascades Having Wall Boundary Layers," J. of the Aeronautical Sciences, Vol. 15, No. 11, 1948, p. 686.

10. Kubota, S., "Cascade Performance with Accelerated or Decelerated Axial Velocity," Bulletin of the Japan Society of Mechanical Engineers, Vol. 5, No. 19, 1962, p. 450.

11. Pollard, D., and Horlock, J.H., "A Theoretical Investigation of the Effect of Change in Axial Velocity on the Potential Flow Through a Cascade of Airfoils," ARC CP No. 619, 1963.

12. "Aerodynamics of Turbines and Compressors," Vol. X of the High Speed Aerodynamics and Jet Propulsion Series published by

the Princeton University Press, Section B, 1964.

13. International Association of Hydraulic Research, Tenth Congress, London, Vol. 4, 1963, pp. 223-226.

14. Van Dyke, M., "Perturbation Methods in Fluid Mechanics," Academic Press, 1964.

15. Muskhelishvili, N.I., "Singular Integral Equations," P. Noordhoff N.V., Groningen, Holland, 1953.

16. Tricomi, F.G., "Integral Equations," Interscience Publishers, 1957.

17. Glauert, H., "Elements of Airfoil and Airscrew Theory," Cambridge University Press, 1947.

18. Ryshik, I.M. and Gradstein, I.S., "Tables of Series, Products and Integrals," VEB Deutscher Verlag der Wissenschaften, Berlin, 1963.

19. Handbook of Mathematical Functions with Formulas, Graphs, and Mathematical Tables, edited by M. Abramowitz and I. A. Stegun, National Bureau of Standards, 1964.

20. Van Dyke, M. D., "Second Order Subsonic Airfoil Theory Including Edge Effects," NACA Rep. No. 1274, 1956.

21. Tables of Integral Tranforms, Bateman Manuscript Project, Vol. 1, McGraw-Hill, 1954.

22. Lighthill, M. J., "The Fundamental Solution for Small Steady Three-Dimensional Disturbances of a Two-Dimensional Parallel Shear Flow," J. of Fluid Mechanics, Vol. 3, 1957, p. 113.

23. Glauert, M. B., "The Method of Images in Shear Flow," J. of Fluid Mechanics, Vol. 9, 1960, p. 561.

24. Scorer, R. S., "On the Stability of Stably Stratified Shearing Layers," Quarterly J. of the Royal Meteorological Society, Vol. 77, 1951, p. 76.

25. Pollard, D. and Wordsworth, J., "A Comparison of Two Methods for Predicting the Potential Flow Around Arbitrary Airfoils in Cascade," ARC CP No. 618, 1963.

26. Howell, A.R., "The Present Basis of Axial Flow Compressor Design: Part I, Cascade Theory and Performance," ARC R&M 2095, 1942.

NOTATION

α	contraction parameter: channels are specified as $h_o \exp(-\alpha x)$
$\gamma(x)$	density at x of the vorticity distribution
Γ	total (integrated) circulation
δ	angle freestream velocity makes with blade chord at mid-point of blade chord: also used to denote the Kronecker delta and the Dirac delta function
ϕ	velocity potential: also used to denote angle used to parameterize chordwise length
ξ	running coordinate along chord
λ	stagger angle of cascade: also angle between axis of convergence and blade chord
η	running coordinate along chord
ψ	stream function: also angle used to parameterize chordwise length
θ	plane polar angle coordinate: also angle used to parameterize chordwise length
c	chord length
f_n $(n = 0, 1, 2 \ldots)$	series of functions of x and y used to study the potential ϕ
h	channel height

$k(x, \xi)$ or $K(x, \xi)$	in general denotes a kernel appearing in the integral equations: usually subscripted
$m(x)$	density at x of source distribution
r	plane polar radial coordinate
s	spacing between adjacent chords in a cascade
t	thickness of airfoil
u	x-component of velocity
v	y-component of velocity
w	z-component of velocity
x, y, z	Cartesian coordinates

C_L	lift coefficient
E	extent of contraction
K_n	Modified Bessel Function of second kind of order n
$K(x, \xi)$ or $k(x, \xi)$	in general, denotes a kernel appearing in the integral equations: usually subscripted
$S(x)$	strength of elementary source located between x and $(x+dx)$
U, V	used interchangeably to denote the freestream velocity

<u>Subscripts</u>

c	camber: also "cascade"
f	freestream
ℓ	used as integer: also "lower"
m	used as integer

n	used as integer: also "normal to chord"
o	used to indicate quantities in the centerspan x-y plane
r	portion of kernel left after most singular portion has been subtracted off
s	source term
t	thickness: also "tangential to blade chord" and in sense of "total"
u	upper
v	vortex term

APPENDIX I

$$\phi_{xx} + \phi_{yy} + \phi_{zz} = 0 \tag{A1.1}$$

Now

$$\int_0^{h(x)} \phi_x dz = \frac{\partial}{\partial x}(h\bar{\Phi}) - h'\phi(x, y, h) \tag{A1.1a}$$

Therefore

$$\int_0^{h(x)} \phi_{xx} dz = \frac{\partial^2}{\partial x^2}(h\bar{\Phi}) - 2u(x, y, h)\, h'$$

$$- \phi(x, y, h)\, h'' - w(x, y, h)\, h'^2$$

and

$$\int_0^{h(x)} \phi_{yy} dz = h\bar{\Phi}_{yy}$$

and

$$\int_0^{h} \phi_{zz} dz = w(x, y, h)$$

since by symmetry: $w(x, y, 0) = 0$.

Recalling the boundary condition at $z = h$ that

$$w(x, y, h) = h' u(x, y, h) ,$$

the result of integrating every term of (A1.1) is:

$$\left[h\bar{\phi}_{xx} + h\bar{\phi}_{yy} + h'\bar{\phi}_x\right] + h''\left[\bar{\phi} - \phi(x, y, h)\right]$$

$$+ h'\left[\bar{\phi}_x - u(x, y, h)(1 + h'^2)\right] = 0 \qquad (A1.2)$$

Equation (A1.1a) can be rewritten as:

$$h\bar{u} = h\bar{\phi}_x + \left[\bar{\phi} - \phi(x, y, h)\right] h'$$

$$\bar{u} = \bar{\phi}_x + \left[\bar{\phi} - \phi(x, y, h)\right]\left(\frac{h'}{h}\right) \qquad (A1.3)$$

Equation (A1.3) is of interest in its own right because it is physically clear that the difference between $\bar{\phi}$ and $\phi(x, y, h)$ is of order of the slope $h'(x)$ of the wall height and hence by equating $\bar{u}$ and $\bar{\phi}_x$ we commit an error of order $(\text{slope})^2$. Clearly,

$$\bar{v} = \bar{\phi}_y \quad . \qquad (A1.4)$$

Using Eq. (A1.3) in Eq. (A1.2) and dividing out by h,

$$\bar{\phi}_{xx} + \bar{\phi}_{yy} + \left(\frac{h'}{h}\right)\bar{\phi}_x + \left(\frac{h'}{h}\right)'\left[\bar{\phi} - \phi(x, y, h)\right]$$

$$+ \left(\frac{h'}{h}\right)\left[\bar{u} - u(x, y, h)(1 + h'^2)\right] = 0 \ .$$

APPENDIX 2

$$\phi = f_o + \sum_{n=1}^{\infty} \frac{z^{2n} f_n}{2n(2n-1)} \tag{A2.1}$$

$$\nabla^2\phi = \Delta f_o + \sum_{1}^{\infty} \frac{z^{2n} \Delta f_n}{2n(2n-1)} + \sum_{1}^{\infty} z^{2(n-1)} f_n \tag{A2.2}$$

or

$$\Delta f_o + f_1 + \sum_{1}^{\infty} z^{2n} \left[f_{n+1} + \frac{\Delta f_n}{2n(2n-1)} \right] = 0$$

therefore

$$f_1 = -\Delta f_o \quad \text{and} \quad f_n = \frac{(-)^{n-1} \Delta^{n-1} f_1}{(2n-2)!} \tag{A2.3}$$

therefore

$$\phi = \sum_{0}^{\infty} \left[\frac{(-)^n \Delta^n f_o}{(2n)!} \right] \tag{A2.4}$$

APPENDIX 3

$$\Phi_{xx} + \Phi_{yy} = \alpha\Phi_x \qquad \text{(A3.1)}$$

Let

$$\Phi = \exp\left(\frac{\alpha x}{2}\right) F(x, y) \qquad \text{(A3.2)}$$

Then

$$\Delta F = \frac{\alpha^2}{4} \cdot F . \qquad \text{(A3.3)}$$

or

$$\frac{1}{r}\frac{\partial}{\partial r}\left(r\frac{\partial F}{\partial r}\right) + \frac{1}{r^2}\frac{\partial^2 F}{\partial \theta^2} = \frac{\alpha^2}{4} \cdot F .$$

If $F = R(r)\ \Theta(\theta)$ then

$$\frac{r}{R} \cdot \frac{d}{dr}\left(r\frac{dR}{dr}\right) - \left(\frac{\alpha r}{2}\right)^2 = -\frac{d^2\Theta}{d\theta^2} = n^2 \qquad \text{(A3.5)}$$

(n has to be an integer for single valuedness.)

$$r^2 R'' + rR' - \left[n^2 + \left(\frac{\alpha r}{2}\right)^2\right] R = 0 .$$

The solution to above that's bounded at infinity is: $R = K_n\left(\frac{\alpha r}{2}\right)$

so that

$$\bar{\Phi} = \exp \left(\frac{\alpha r}{2}\right) \begin{cases} \sin (n\theta) \\ \cos (n\theta) \end{cases} K_n\left(\frac{\alpha r}{2}\right) \tag{A3.7}$$

APPENDIX 4

For very large r, both $K_1\left(\frac{\alpha r}{2}\right)$ and $K_o\left(\frac{\alpha r}{2}\right)$ are like $\exp\left(-\frac{\alpha r}{2}\right)\sqrt{\frac{\pi}{\alpha r}}$. The height of the channel at (r, θ) is $\ell_o \exp(-\alpha r \cos\theta)$. This means the total outward flux out of a circle of radius R is

$$I = \frac{\alpha \ell_o R}{4\pi} \int_0^{2\pi} \exp\left(-\frac{\alpha R \cos\theta}{2}\right) \left[K_1\left(\frac{\alpha R}{2}\right) - \cos(\theta) K_o\left(\frac{\alpha R}{2}\right)\right] d\theta$$

$$= \frac{\alpha \ell_o R}{2\pi} \int_0^{\pi} \exp\left(-\frac{\alpha R}{2}\cos\theta\right) \left[K_1\left(\frac{\alpha R}{2}\right) - \cos(\theta) K_o\left(\frac{\alpha R}{2}\right)\right] d\theta.$$

$$I \cong \frac{\alpha \ell_o R}{2\pi} e^{-\frac{\alpha R}{2}} \sqrt{\frac{\pi}{\alpha R}} \int_{-1}^{1} \exp\left(-\frac{\alpha R x}{2}\right) \sqrt{\frac{1-x}{1+x}}\, dx$$

$$\cong \frac{\alpha \ell_o R}{2\pi} \sqrt{\frac{\pi}{\alpha R}} \int_0^{2} \exp\left(-\frac{\alpha R x}{2}\right) \sqrt{\frac{2-x}{x}}\, dx$$

$$\cong \frac{\alpha \ell_o R}{2\pi} \sqrt{\frac{2\pi}{\alpha R}} \int_0^{\infty} \exp\left(-\frac{\alpha R x}{2}\right) \sqrt{\frac{1}{x}}\, dx = \ell_o.$$

The notation "$\cong$" in the above indicates the other terms left out can be shown to go to zero as $R \rightarrow \infty$.

A numerical integration of I with $\alpha = 0.1$, $R = 2$, also gave $(359.27 \div 360.00)\, \ell_o$. The expression for $\bar{u}_r$ is therefore well checked.

APPENDIX 5

Consider:

$$I = \frac{1}{\pi}\sqrt{\frac{1-y}{1+y}} \int_{-1}^{1} \sqrt{\frac{1+x}{1-x}} \frac{f(x)\, dz}{(x-y)}$$

where $y \in [-1, 1]$.

Let $f(x) = C_o + \sum_{1}^{\infty\,'} C_n \cos(n\theta)$ where $x = \cos\theta$,

$\theta \in [0, \pi]$ and let $y = \cos(\phi)$ with $\phi \in [0, \pi]$.

Therefore

$$I = \frac{1}{\pi}\tan\left(\frac{\phi}{2}\right) \int_{0}^{\pi} \cot\left(\frac{\theta}{2}\right) \frac{\sin(\theta)\left[C_o + \sum_{1}^{\infty} C_n \cos(n\theta)\right]}{\left[\cos(\theta) - \cos(\phi)\right]} d\theta$$

$$= \frac{1}{\pi}\tan\frac{\phi}{2} \int_{0}^{\pi} \frac{\left[1+\cos(\theta)\right]\left[C_o + \sum_{1}^{\infty} C_n \cos(n\theta)\right]}{\left[\cos(\theta) - \cos(\phi)\right]} d\theta$$

The integrand $= \Bigg[\left(C_o + \frac{C_1}{2}\right) + C_o\cos(\theta) + \frac{C_1}{2}\cos(2\theta)$

$$+ \; C_1 \cos(\theta) + \sum_{2}^{\infty} \left[C_n \cos(n\theta) + \frac{C_n}{2} \left[\cos \left[(n+1)\theta \right] \right. \right.$$

$$\left. \left. + \cos \left[(n-1)\theta \right] \right] \right] \div \left[\cos(\theta) - \cos(\phi) \right] \; .$$

$$I = \tan\left|\frac{\phi}{2}\right| \left[(C_o + C_1) + C_1 \cos(\phi) + \sum_{2}^{\infty} C_n \sin(n\phi) \cot\left|\frac{\phi}{2}\right| \right]$$

$$= C_o \tan\left|\frac{\phi}{2}\right| + \sum_{1}^{\infty} C_n \sin(n\phi) \; .$$

APPENDIX 6

Let $x = \cos(\theta)$ and $\xi = \cos(\phi)$: then

$$\ell n \left[|x - \xi| \right] = \ell n \left[|\cos(\theta) - \cos(\phi)| \right]$$

$$\begin{aligned} &= \ell n \; |\cos(\phi) - \cos(\theta)| \quad \text{when } \phi < \theta \text{ and} \\ &= \ell n \; |\cos(\theta) - \cos(\phi)| \quad \text{when } \phi > \theta . \end{aligned} \qquad (A6.1)$$

Let

$$\ell n \left[|\cos(\theta) - \cos(\phi)| \right] = \sum_{0}^{\infty} a_n(\theta) \cos(n\phi) \qquad (A6.2)$$

$$a_n(\theta) \; (n \quad 0) = \frac{2}{\pi} \int_0^{\pi} \ell n \left[|\cos(\theta) - \cos(\phi)| \right] \cos(n\phi)\, d\phi \qquad (A6.3)$$

$$= \frac{2}{\pi} \left[\int_0^{\theta} \ell n \left[\cos(\phi) - \cos(\theta) \right] \cos(n\phi)\, d\phi \right.$$

$$\left. + \int_{\theta}^{\pi} \ell n \left(\cos\theta - \cos\phi \right) \cos(n\phi)\, d\phi \right]$$

$$= \frac{2}{\pi n} \sin(n\phi)\, \ell n \left[\cos(\phi) - \cos(\theta) \right] \Big|_0^{\theta}$$

$$+ \frac{2}{\pi n} \sin(n\phi)\ \ell n\ (\cos\theta - \cos\phi) \Big|_{\theta}^{\pi} + \frac{2}{\pi n} \int_{0}^{\pi} \frac{\sin(n\phi)\sin(\phi)\,d\varphi}{[\cos(\phi) - \cos(\theta)]}$$

$$= \frac{2}{\pi n} \int_{0}^{\pi} \frac{\sin(n\phi)\sin(\phi)\,d\phi}{\cos(\phi) - \cos\theta} = -\frac{2}{n}\cos(n\theta) \qquad \text{(A6.4)}$$

Since

$$- \frac{2}{\pi n} \sin(n\phi)\ \ell n\ \left|\cos(\theta) - \cos(\phi)\right| \Big|_{\phi \to \theta^{+}}$$

and

$$\frac{2}{\pi n} \sin(n\phi)\ \ell n\ \left|\cos(\phi) - \cos(\theta)\right| \Big|_{\phi \to \theta^{-}}$$

cancel out provided $\phi \longrightarrow \theta^{+}$ at the same rate in the first expression above, as it tends to θ^{-} in the second.

Case of $a_o(\theta)$:

$$a_o = \frac{1}{\pi} \int_{0}^{\pi} \ell n \left[\left| \cos(\theta) - \cos(\phi) \right| \right] d\phi$$

$$= \frac{1}{\pi} \phi \log \left(\cos(\phi) - \cos(\theta) \right) \Big|_{0}^{\theta} + \frac{1}{\pi} \phi \log \left(\cos(\theta) - \cos(\phi) \right) \Big|_{\theta}^{\pi}$$

$$+ \frac{1}{\pi} \int_{0}^{\pi} \frac{\phi \sin(\phi)\,d\phi}{\cos(\phi) - \cos(\theta)}$$

once again $\frac{\phi}{\pi}$ log $\left|\cos(\phi) - \cos(\theta)\right| \Big|_{\phi \to \theta^-}$ and

$$- \frac{\phi}{\pi} \log \left|\cos(\theta) - \cos(\phi)\right| \Big|_{\phi \to \theta^+}$$

cancel out if $\phi \to \theta^-$ and $\phi \to \theta^+$ at the same rate. The integral

$$\frac{1}{\pi} \int_0^\pi \frac{\phi \sin(\phi)\, d\phi}{\cos(\phi) - \cos(\theta)} = - \ell n\left[2(1 + \cos\theta)\right]$$

according to p. 166 of Ref. 18. Therefore $a_o = - \ell n(2)$.

Hence

$$\ell n \left[\left|\cos(\theta) - \cos(\phi)\right| \right] = - \ell n(2) - 2 \sum_1^\infty \frac{\cos(n\theta)\cos(n\phi)}{n} \tag{A6.5}$$

A check:

Let $\theta = \left(\frac{\pi}{4}\right)$, $\phi = \left(\frac{\pi}{2}\right)$

$$\ell n \left[\left|\cos(\theta) - \cos(\phi)\right| \right] = - \frac{1}{2} \ell n(2) \quad .$$

The series (A6.5) gives

$$- \ell n(2) - 2 \sum_1^\infty \frac{\cos\left(\frac{n\pi}{4}\right) \cos\left(\frac{n\pi}{2}\right)}{n}$$

$$= - \ell n(2) - 2 \sum_{1}^{\infty} \frac{(-)^n}{4n} = - \frac{1}{2} \ell n(2)$$

since

$$\ell n(2) = \sum_{1}^{\infty} \frac{(-)^{n+1}}{n} .$$

APPENDIX 7

This appendix is concerned with the summation of the following type of series: Let

$$r_n = \sqrt{n^2 s^2 - 2ns(x - \xi)\sin(\lambda) + n^2 s^2}$$

where $r_n > 0$.

To sum (typically),

$$S = \sum_{n=-\infty}^{\infty}{}^{*} K_o\left(\frac{a r_n}{2}\right) .$$

where the (*) on the summation sign indicates the summation excludes $n = 0$. We take the sum from $n = -4$ to $n = 4$ exactly, i.e., let

$$S = F + G \quad \text{where}$$

$$F = \sum_{-4}^{4}{}^{*} K_o\left(\frac{r_n a}{2}\right) \quad \text{and}$$

$$G = \sum_{-\infty}^{-5} K_o\left(\frac{a r_n}{2}\right) + \sum_{5}^{\infty} K_o\left(\frac{a r_n}{2}\right) .$$

For $|n| \gg 5$ we use the following Taylor series representation for K_o:

$$K_o\left(\frac{a r_n}{2}\right) \cong K_o\left[\frac{a s\, |n|}{2}\right] \quad \pm \frac{a}{2}(x - y)\sin(\lambda) \;.$$

$$K_1\left[\frac{a s}{2}|n|\right] + (x-y)^2\left[\frac{a^2 \sin^2\lambda}{8}\left[K_o\left[\frac{a s}{2}|n|\right]\right.\right.$$

$$\left.+ \frac{2}{a s\, |n|} K_1\left[\frac{a s}{2}|n|\right]\right] - \frac{a \cos^2(\lambda)}{4s} \cdot \frac{1}{|n|} \;.$$

$$\left. K_1\left[\frac{a s}{2}\;|n|\right]\right]$$

where the plus sign goes with $n > 0$ and the negative sign with $n < 0$. The above is only a two term series and essentially assumes that for large $|n|$, r_n is substantially $|n|\, s$. For higher solidities it may be necessary to sum a greater number of terms exactly (i.e., increase the limits for F) before using a Taylor series representation. The Taylor series uses:

$$K_o^{'}(x) = -K_1(x) \quad \text{and} \quad K_o^{''}(x) = K_o + \frac{1}{x} K_1 \;.$$

The advantage of the above is that if we denote as follows:

$$S_1 = 2\sum_{5}^{\infty} K_o\left[\frac{a n s}{2}\right] \;;\; S_2 = 2\sum_{5}^{\infty} \frac{1}{n} K_1\left[\frac{a n s}{2}\right]$$

then

$$G = S_1 + (x-y)^2\left[\frac{a^2 \sin^2(\lambda)}{8}\left(S_1 + \frac{2}{a s} S_2\right) - \frac{a \cos^2(\lambda)}{4s}\; S_2\right] \;.$$

Such a procedure does indeed effect a considerable saving in computing time.

APPENDIX 8

Consider $\sum_{5}^{\infty} K_o \left[\frac{\alpha n s}{2}\right]$.

Once again depending on s and α, we sum exactly in the above till some (N - 1) where (N - 1) > 5 and where $K_o \left(\frac{\alpha N s}{2}\right)$ has an argument large enough to be well approximated by

$$K_o \left(\frac{\alpha N s}{2}\right) = \frac{1.2533}{\sqrt{\frac{\alpha s}{2}}} \frac{\exp\left(-\frac{\alpha N s}{2}\right)}{\sqrt{N}}$$

which is the first term in the asymptotic expansion of $K_o(x)$ for large x. Let

$$\sum_{5}^{\infty} K_o \left(\frac{\alpha n s}{2}\right) = J + L \quad \text{where}$$

$$J = \sum_{5}^{N-1} K_o \left(\frac{\alpha n s}{2}\right) \quad \text{and} \quad L = \sum_{N}^{\infty} K_o \left(\frac{\alpha n s}{2}\right) .$$

$$L \cong \frac{1.2533}{\sqrt{\frac{\alpha s}{2}}} \sum_{N}^{\infty} \frac{e^{-\frac{\alpha n s}{2}}}{\sqrt{n}}$$

Now

$$\frac{\exp\left(-\frac{\alpha ns}{2}\right)}{\sqrt{n}} = \frac{1}{\pi} \int_{\frac{\alpha s}{2}}^{\infty} \frac{\exp(-nx)\,dx}{\sqrt{x}}$$

from a table of Laplace transforms (cf., Ref. 21).

$$\sum_{N}^{\infty} \frac{e^{-\frac{\alpha ns}{2}}}{\sqrt{n}} = \frac{1}{\pi} \sum_{N}^{\infty} \int_{\frac{\alpha s}{2}}^{\infty} \frac{\exp(-nx)\,dx}{\sqrt{x}}$$

$$= \frac{1}{\pi} \int_{\frac{\alpha s}{2}}^{\infty} \frac{\exp(-Nx)\,dx}{\sqrt{x}\left[1 - e^{-x}\right]}$$

interchanging the order of integration and summation, using

$$\sum_{N}^{\infty} e^{-nx} = \exp(-Nx) \,/\, \left[1 - e^{-x}\right] \quad .$$

The last integral is evaluated by the methods of asymptotic expansions for large N to yield (approximately for large N):

$$\frac{\exp\left(-\frac{\alpha Ns}{2}\right)}{\sqrt{N}\left[1 - \exp\left(-\frac{\alpha s}{2}\right)\right]} \left[1 - \frac{\exp\left(-\frac{\alpha s}{2}\right)}{2N\left[1 - \exp\left(-\frac{\alpha s}{2}\right)\right]}\right]$$

APPENDIX 9

Consider the stepwise discontinuous channel shown in Fig. 16. Let the potential for $x_{n-1} \leqslant x \leqslant x_n$ be ϕ_n and that for $x_n \leqslant x \leqslant x_{n+1}$ be ϕ_{n+1} . Further let

$$\phi_n = \left[A_n e^{-kx} + B_n e^{kx}\right] \cos (ky)$$

and

$$\phi_{n+1} = \left[A_{n+1} e^{-kx} + B_{n+1} e^{-kx}\right] \cos (ky) \ .$$

The boundary conditions at $x = x_n$ are $h_n \phi_{n,x} = \phi_{n+1,x} \cdot h_{n+1}$ and $\phi_{n,y} = \phi_{n+1,y}$. It is easily observed the second condition implies the continuity of ϕ_n itself (i.e., $\phi_n = \phi_{n+1}$). These two conditions yield for A_{n+1} and B_{n+1} in terms of A_n and B_n:

$$A_{n+1} = \frac{1}{2}\left[1 + \frac{h_n}{h_{n+1}}\right] A_n + \frac{1}{2} B_n e^{2kx_n} \left[1 - \frac{h_n}{h_{n+1}}\right]$$

and

$$B_{n+1} = \frac{1}{2}\left[1 - \frac{h_n}{h_{n+1}}\right] A_n e^{-2kx_n} + \frac{B_n}{2}\left[1 + \frac{h_n}{h_{n+1}}\right] \ .$$

Now use the continuity of ϕ at the jumps to write:

$$\phi(x_{n+1,y}) = \cos(ky)\left[A_n e^{-kx_n}\left[\cosh(k\epsilon) - \frac{h_n}{h_{n+1}}\sinh(k\epsilon)\right]\right.$$

$$\left. + B_n e^{kx_n}\left[\cosh(k\epsilon) + \sinh(k\epsilon)\frac{h_n}{h_{n+1}}\right]\right]$$

$$\phi(x_{n,y}) = \left[A_n e^{-kx_n} + B_n e^{kx_n}\right] \cos(ky)$$

$$\phi(x_{n-1,y}) = \left[A_n e^{-kx_n} e^{k\epsilon} + B_n e^{kx_n} e^{-k\epsilon}\right] \cos(ky)$$

We calculate $\phi_{,x}(x_{n,y}) = \left[\phi\left[x_{n+1,y}\right] - \phi\left[x_{n-1,y}\right]\right] \div 2\epsilon$

taking the limit as $\epsilon \rightarrow 0$. Similarly $\phi_{xx}(x_{n,y})$ is found as the limit as $\epsilon \rightarrow 0$ of

$$\left[\phi(x_{n+1,y}) + \phi(x_{n-1,y}) - 2\phi(x_{n,y})\right] \div \epsilon^2 .$$

The results are:

$$\phi_{,xx} = -k^2\phi - \frac{h'}{h}\phi_{,x} .$$

Since $-k^2\phi$ is equivalent to $\phi_{,yy}$ considering the form of the solution assumed:

$$\Delta\phi + \left(\frac{h'}{h}\right)\phi_x = 0 .$$

TABLE I

INCIDENCE, DEVIATION AND FLOW TURNING ANGLES

Explanation of the notation used in Table I:

α is the contraction parameter. In the contracting portion, the channel height is given by $h(x) = h_o \exp(-\alpha x)$, where x is the distance from mid-chord point along the axis of convergence.

δ is the angle the freestream flow velocity vector makes with the blade chord at mid-chord point.

λ is the stagger angle of the cascade.

s and c are respectively the spacing between adjacent blades and the length of the blade chord. Thus c/s is the solidity of the cascade.

E is the extent of the contraction indicated, e.g., in Fig. 19. $E \div 2\cos(\lambda)$ indicates the fraction of the airfoils covered by the chord because (a) the chord is taken 2 units long and (b) the axis of convergence and cascade axis are taken coincident.

Incidence, deviation and flow turning angles are used in the sense of usual cascade terminology. Incidence angle is the angle between the inlet velocity vector and the tangent to the blade camber line at the leading edge. Deviation angle is the angle between the outlet flow velocity vector and tangent to the blade camber line at the trailing edge. Flow turning angle is the angle between inlet and outlet flow velocity vectors.

For the circular arc airfoils:

1. Cb is the theoretical lift coefficient at zero angle of attack for an isolated airfoil.

2. θ is the camber of the airfoil, i.e., the angle between the tangents to the camber line at the leading and trailing edges. Cb and θ are not independent and if θ is expressed in radians, for small θ, Cb is approximately,

$$Cb = \frac{\pi}{2}\theta(1 - 0.05\,\theta^2) \;.$$

3. t/c is the thickness ratio of the airfoil.

All cases: $a = 0.100$; $\delta = 15.00$ Degrees.

(a) Cascade of Flat Plates: $\lambda = 45^{o}$, Variation with $E \div 2 \cos \lambda$

$\frac{s}{c} = 1.00.$

All angles are in degrees.

$E \div 2 \cos (\lambda)$	Incidence	Deviation	Flow Turning
1.061	23.127	2.027	21.100
1.414	23.027	2.315	20.712
1.771	22.930	2.587	20.343
2.122	22.840	2.839	20.001
2.475	22.751	3.08	19.671
Two Dim. Case	22.301	2.028	20.273

(b) Cascade of Flat Plates, $\lambda = 45^{o}$, E = 1.500, Variation with c/s = solidity.

All angles are in degrees.

c/s or	Incidence		Deviation		Flow Turning	
Solidity	Q.T.D. Flow	T.D. Flow	Q.T.D. Flow	T.D. Flow	Q.T.D. Flow	T.D. Flow
1.25	23.425	22.743	1.134	0.586	22.292	22.156
1.00	23.127	22.301	2.027	2.028	21.100	20.273
0.80	22.578	21.659	3.540	3.910	19.038	17.749
0.666	21.997	20.957	4.981	5.719	17.016	15.238
0.500	21.017	19.855	7.097	8.138	13.920	11.717

(c) Cascade of Circular Arc Airfoils, $Cb = 1.0$, $\lambda = 45^{o}$, $E = 1.500$, $t/c = 0.00$,

$\theta = 25^{o}$ where θ denotes the camber of airfoil in degrees. Variation with solidity.

All angles are in degrees.

c/s or	Incidence		Deviation		Flow Turning	
Solidity	Q.T.D.Flow	T.D.Flow	Q.T.D.Flow	T.D.Flow	Q.T.D.Flow	T.D.Flow
1.25	13.405	12.749	3.564	1.678	34.840	36.071
1.00	12.963	12.253	5.786	4.479	32.177	32.775
0.80	12.3	11.509	8.731	8.123	28.569	28.386
0.666	11.618	10.744	11.341	11.282	25.278	24.461
0.500	10.424	9.406	15.105	15.713	20.319	18.692

(d) Cascade of Circular Arc Airfoils: Cb = 1.0, $\lambda = 45^{o}$, E = 1.500, t/c = 0.100

$\theta = 25^{o}$. Variation with solidity.

All angles are in degrees.

c/s or	Incidence		Deviation		Flow Turning	
Solidity	Q.T.D. Flow	T.D. Flow	Q.T.D. Flow	T.D. Flow	Q.T.D. Flow	T.D. Flow
1.25	12.845	12.202	6.344	4.753	31.501	32.448
1.00	12.450	11.748	8.101	7.02	29.349	29.728
0.80	11.875	11.084	10.402	9.942	26.473	26.142
0.666	11.265	10.390	12.551	12.574	23.713	22.817
0.500	10.171	9.152	15.795	16.429	19.376	17.723

(e) Cascade of Flat Plates: $\frac{s}{c} = 1.00$, E = 2.05. Variation with stagger.

All angles are in degrees.

λ	Incidence		Deviation		Flow Turning	
	Q.T.D. Flow	T.D. Flow	Q.T.D. Flow	T.D. Flow	Q.T.D. Flow	T.D. Flow
-30	30.839	30.799	3.183	1.196	27.656	29.604
0	28.606	27.210	2.347	1.245	26.26	25.965
10	27.767	26.204	2.033	1.344	25.734	24.861
20	26.712	25.222	1.845	1.436	24.867	23.786
30	25.421	24.23	1.845	1.463	23.577	22.767
40	23.886	22.992	2.094	1.809	21.792	21.182
45	23.107	22.301	2.342	2.028	20.676	20.273
60	19.884	19.701	3.857	2.982	16.028	16.719

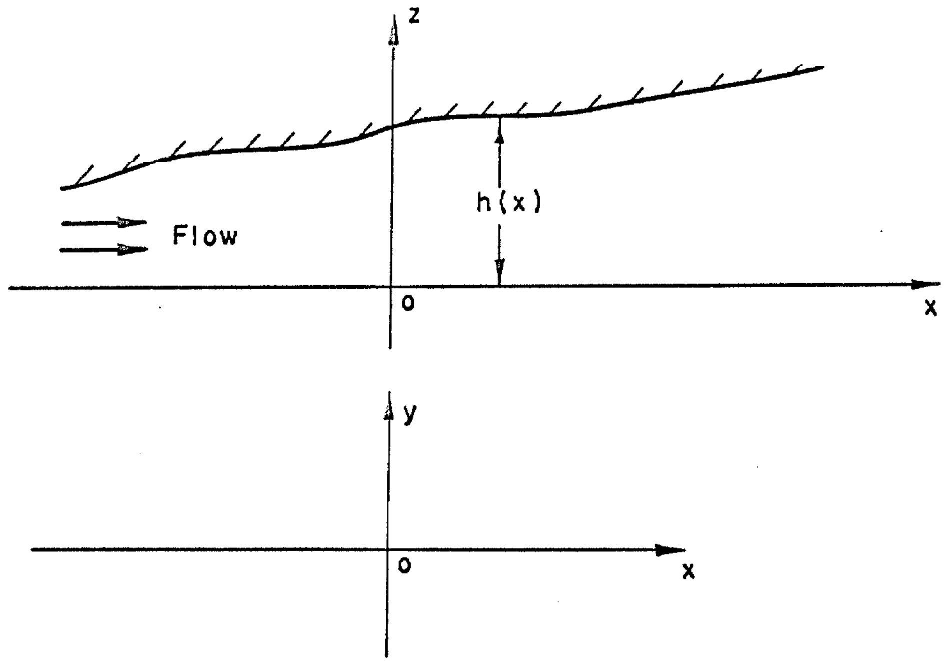
z
h(x)
Flow
o
x
y
o
x

Fig. 1

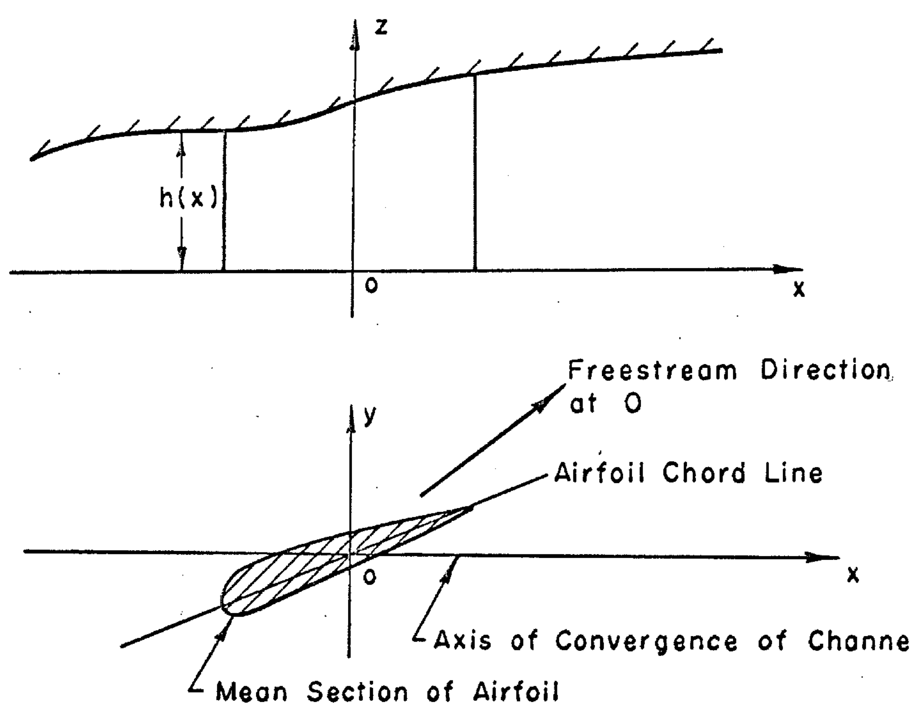
z
h(x)
o
x
Freestream Direction
at O
y
Airfoil Chord Line
o
x
Axis of Convergence of Channel
Mean Section of Airfoil

Fig. 2

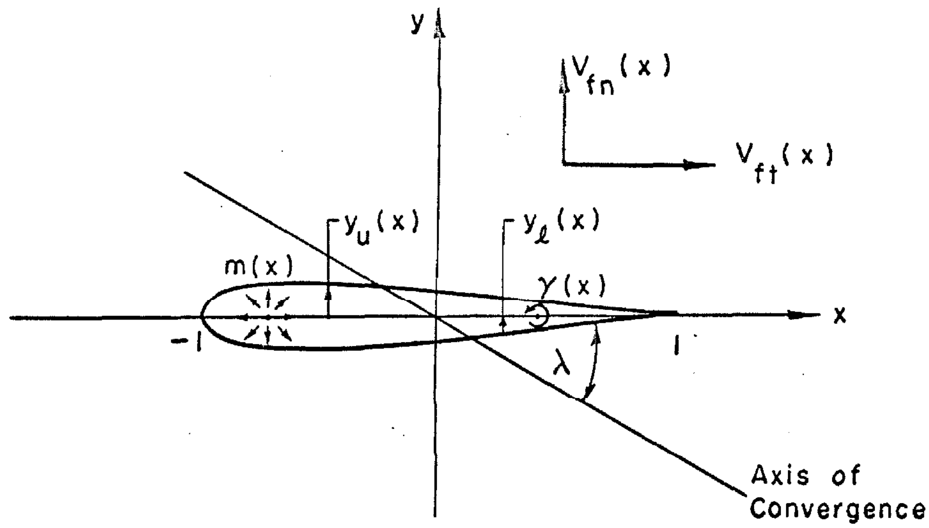
y
$V_{fn}(x)$
$V_{ft}(x)$
$y_u(x)$
$y_\ell(x)$
m(x)
γ(x)
x
-1
1
λ
Axis of
Convergence

Fig. 3

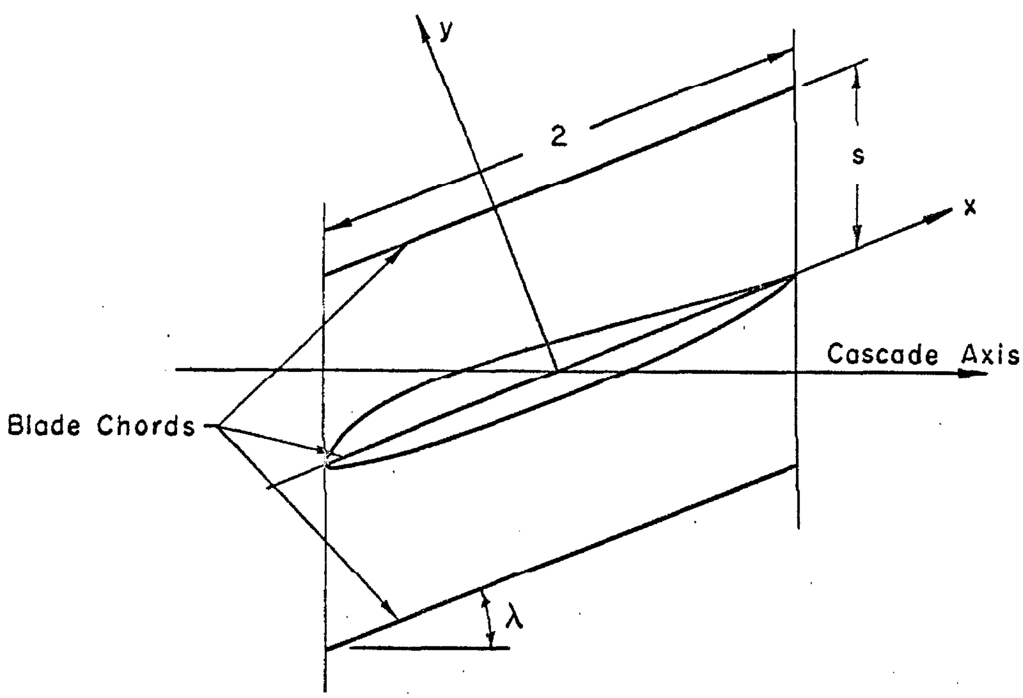
y
2
s
x
Cascade Axis
Blade Chords
λ

Fig. 4

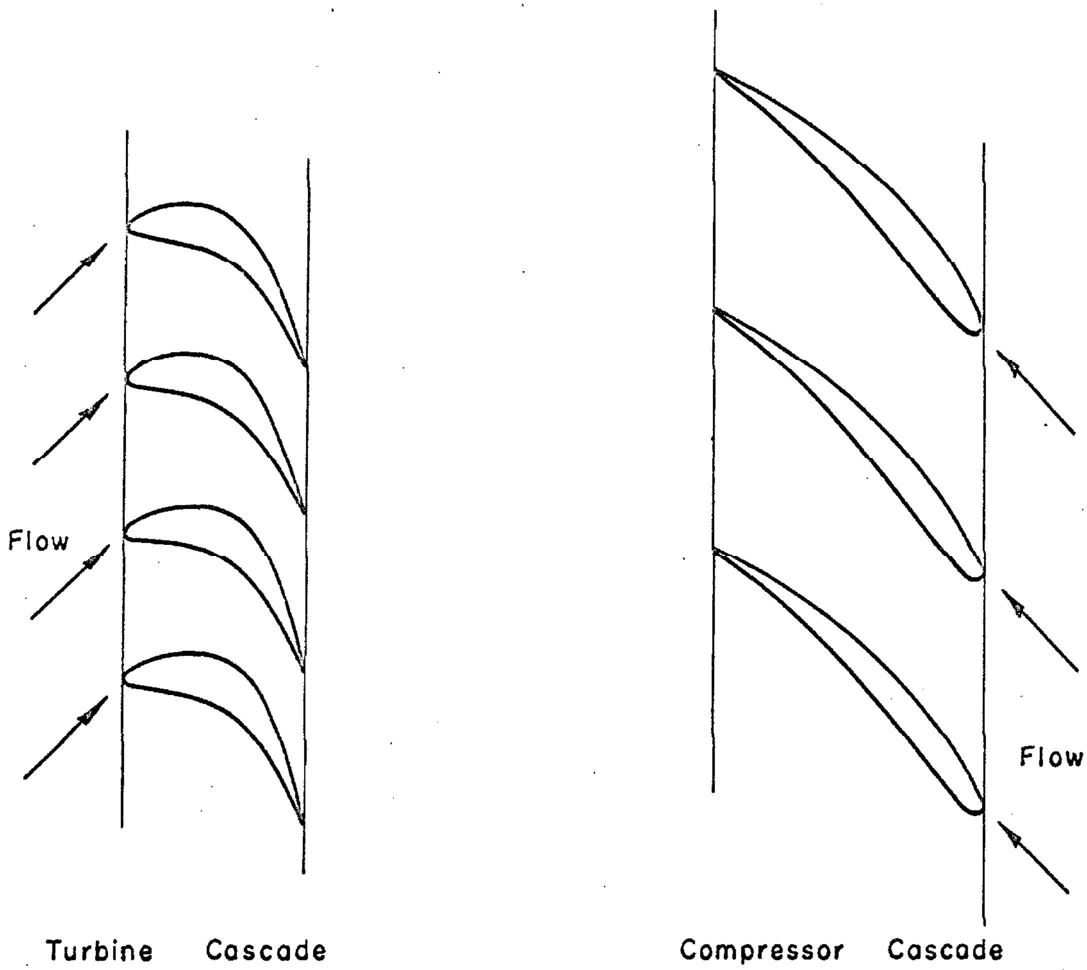
Flow
Turbine Cascade
Flow
Compressor Cascade

Fig. 5

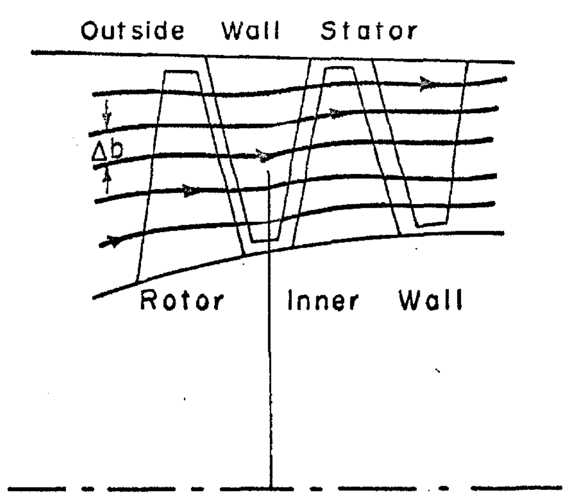
Outside Wall Stator
Δb
Rotor Inner Wall

Fig. 6

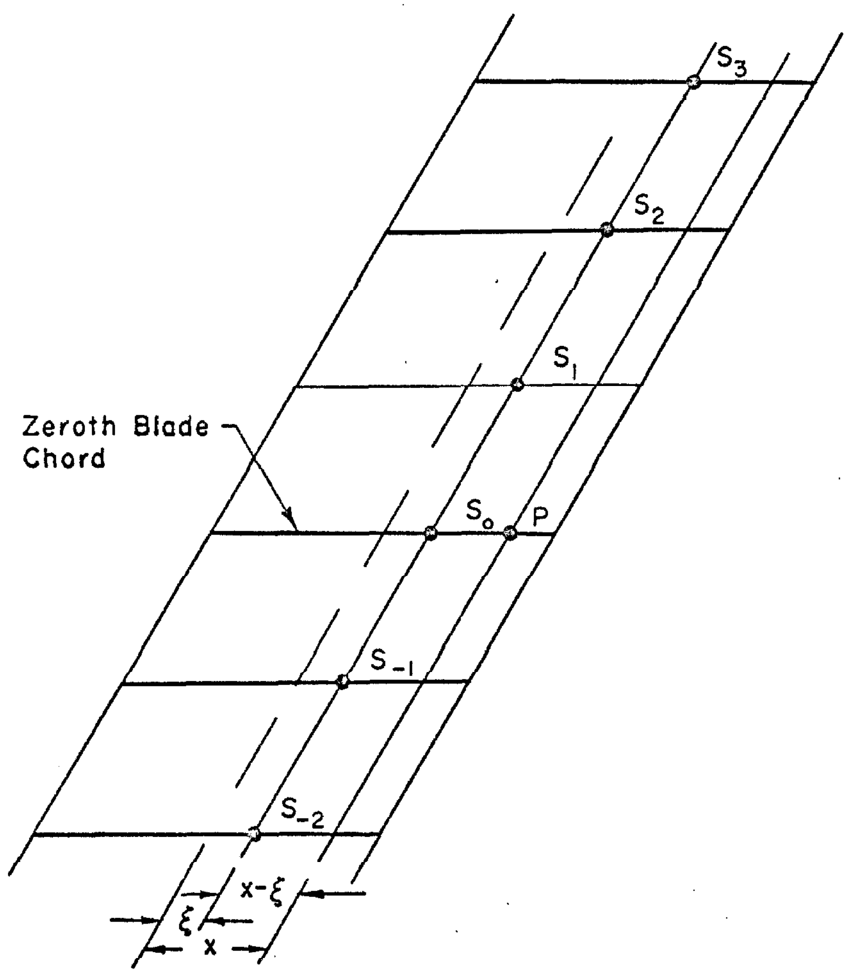

Fig. 7

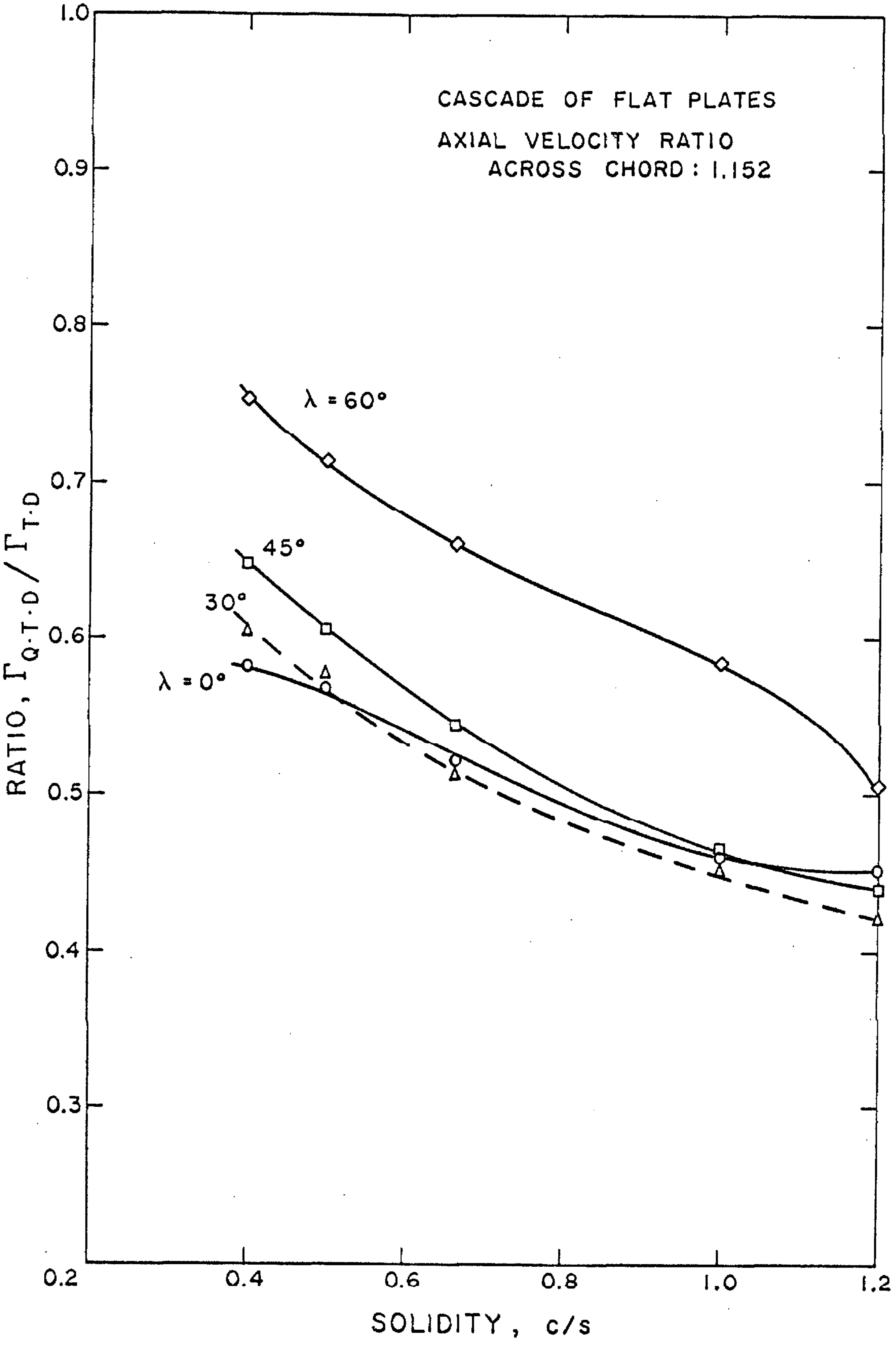
CASCADE OF FLAT PLATES
AXIAL VELOCITY RATIO ACROSS CHORD: 1.152
λ = 60°
45°
30°
λ = 0°
RATIO, $\Gamma_{Q\cdot T\cdot D}/\Gamma_{T\cdot D}$
SOLIDITY, c/s
1.0
0.9
0.8
0.7
0.6
0.5
0.4
0.3
0.2
0.4
0.6
0.8
1.0
1.2

Fig. 8

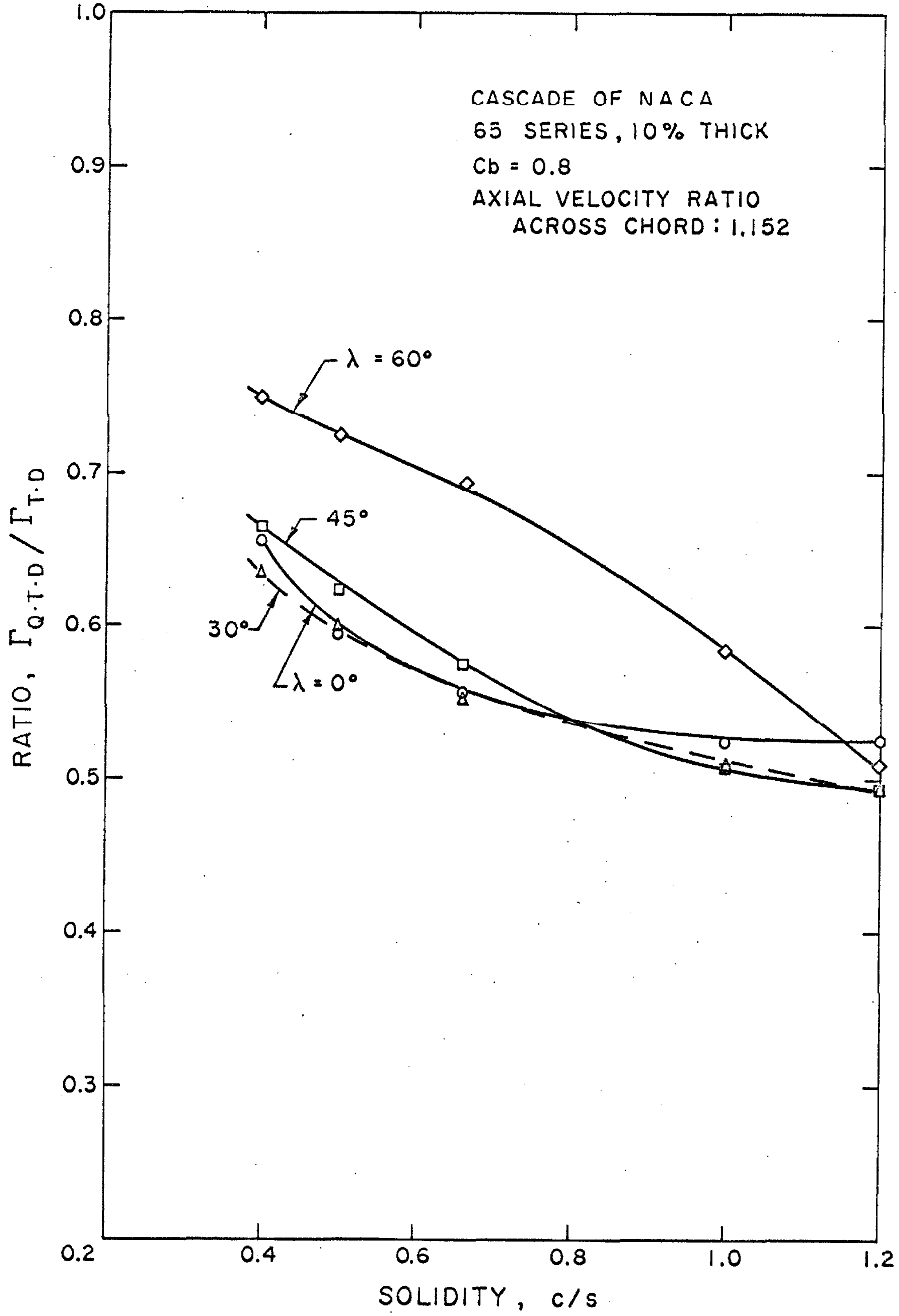
CASCADE OF NACA
65 SERIES, 10% THICK
Cb = 0.8
AXIAL VELOCITY RATIO
ACROSS CHORD: 1.152
λ = 60°
45°
30°
λ = 0°
RATIO, $\Gamma_{Q \cdot T \cdot D} / \Gamma_{T \cdot D}$
SOLIDITY, c/s
1.0
0.9
0.8
0.7
0.6
0.5
0.4
0.3
0.2
0.4
0.6
0.8
1.0
1.2

Fig. 9

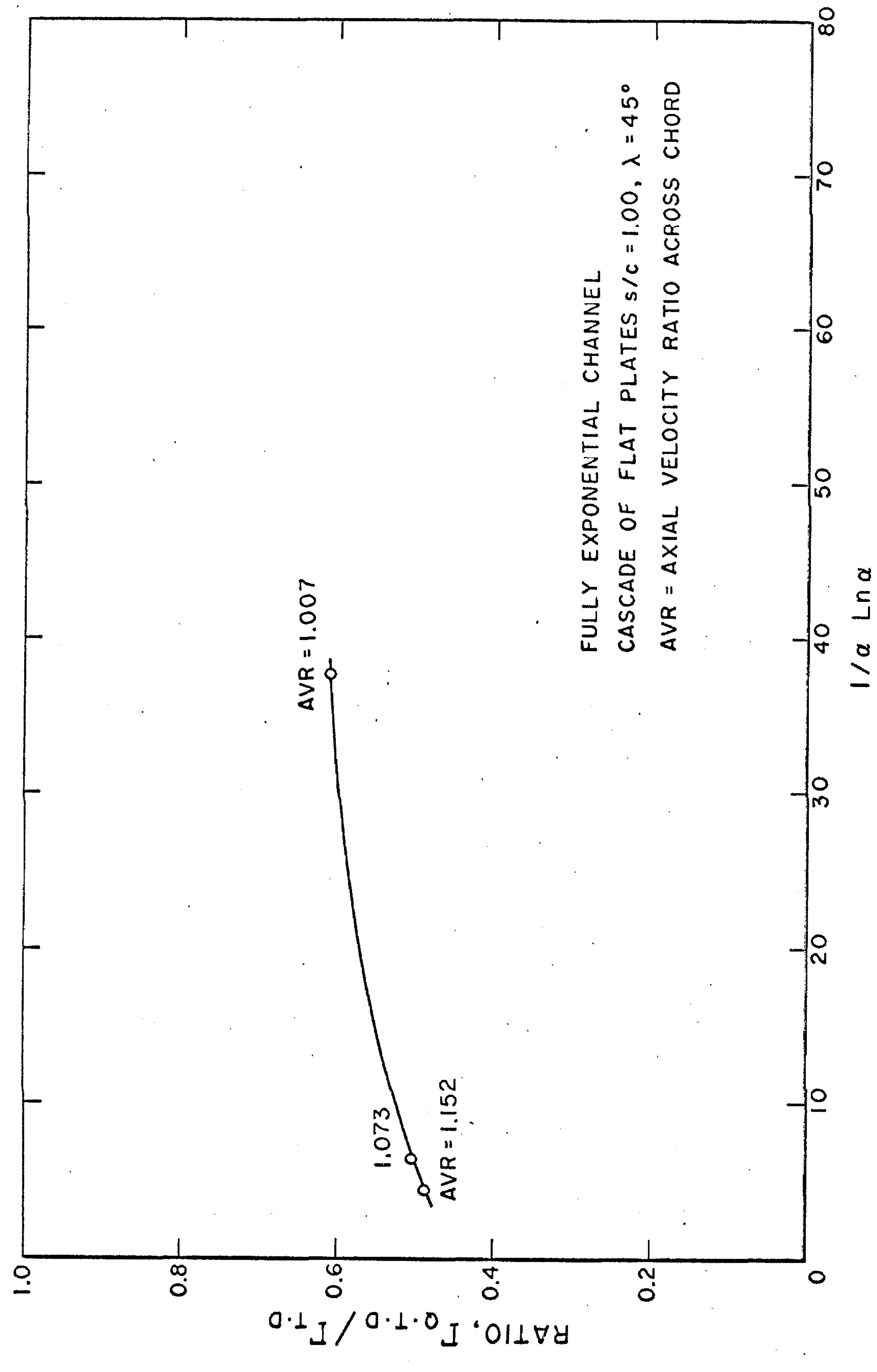
FULLY EXPONENTIAL CHANNEL
CASCADE OF FLAT PLATES s/c = 1.00, λ = 45°
AVR = AXIAL VELOCITY RATIO ACROSS CHORD
AVR = 1.007
1.073
AVR = 1.152
RATIO, Γ Q.T.D / Γ T.D
1/a Ln a
1.0
0.8
0.6
0.4
0.2
0
10
20
30
40
50
60
70
80

Fig. 10

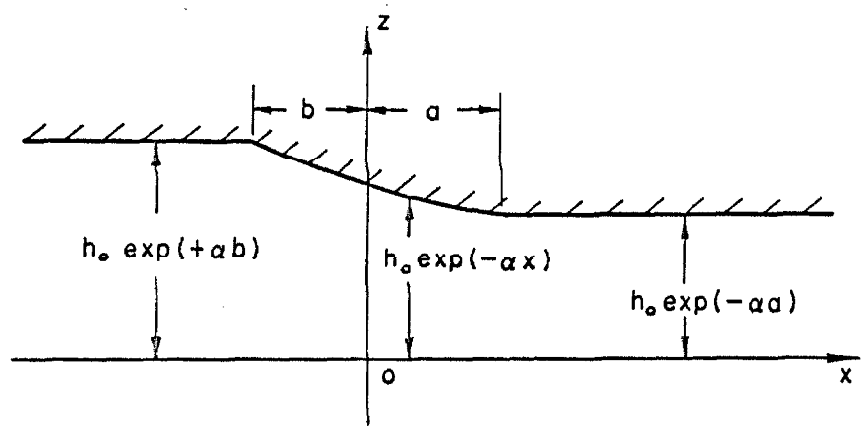

Fig. 11

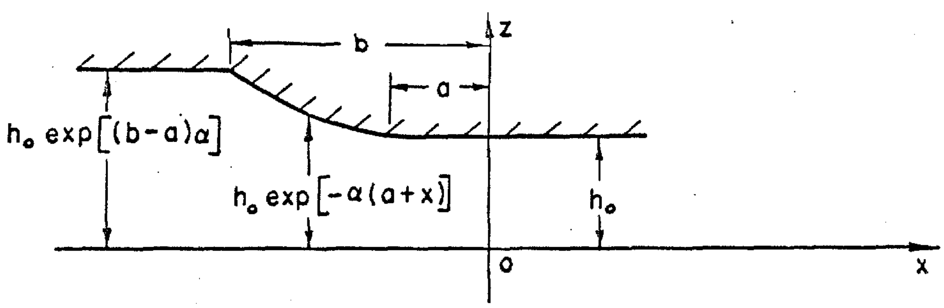

Fig. 12

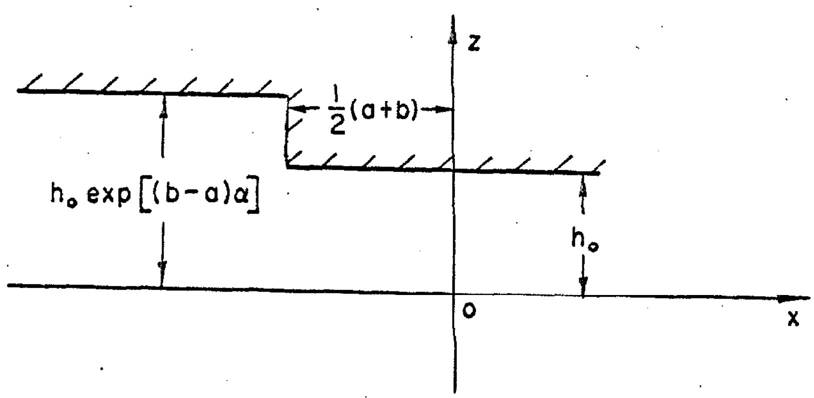

Fig. 13

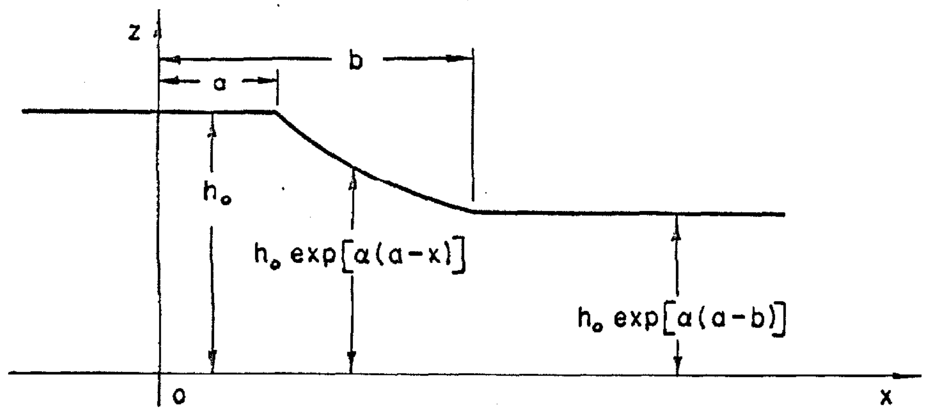

Fig. 14

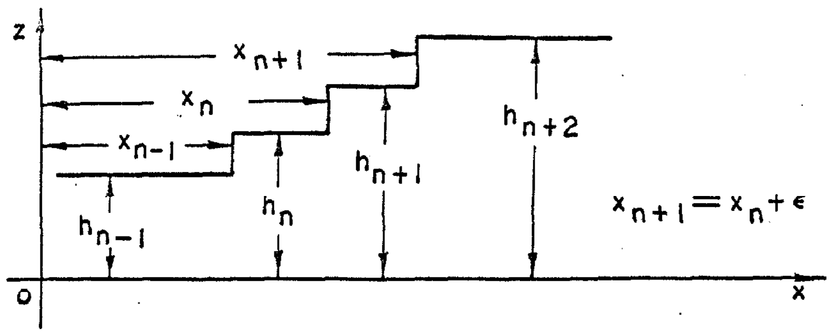

Fig. 15

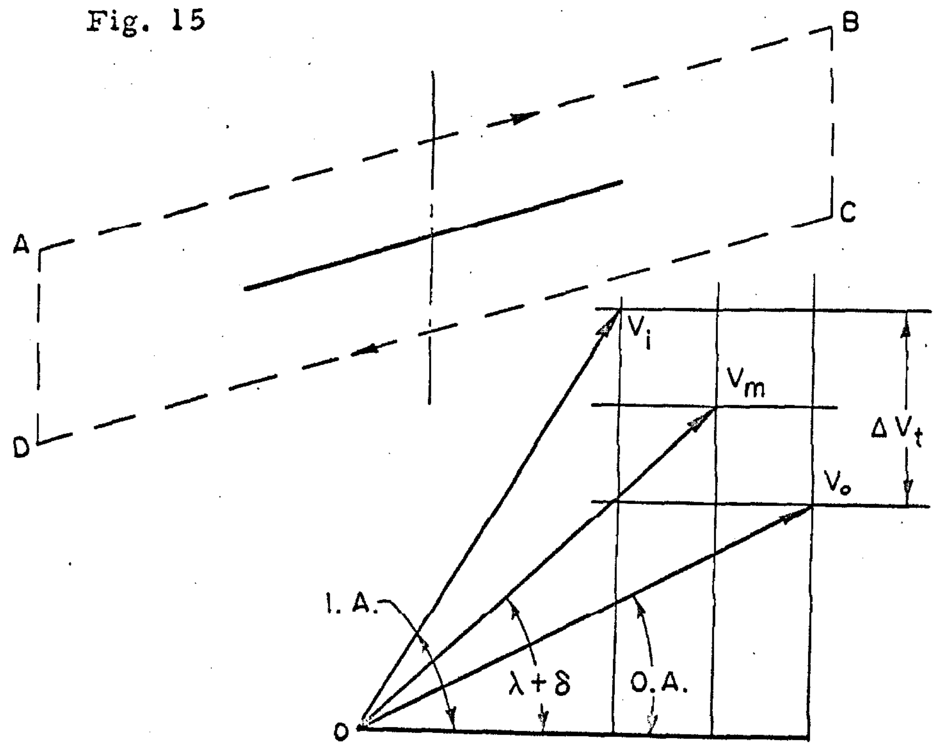

Fig. 15a

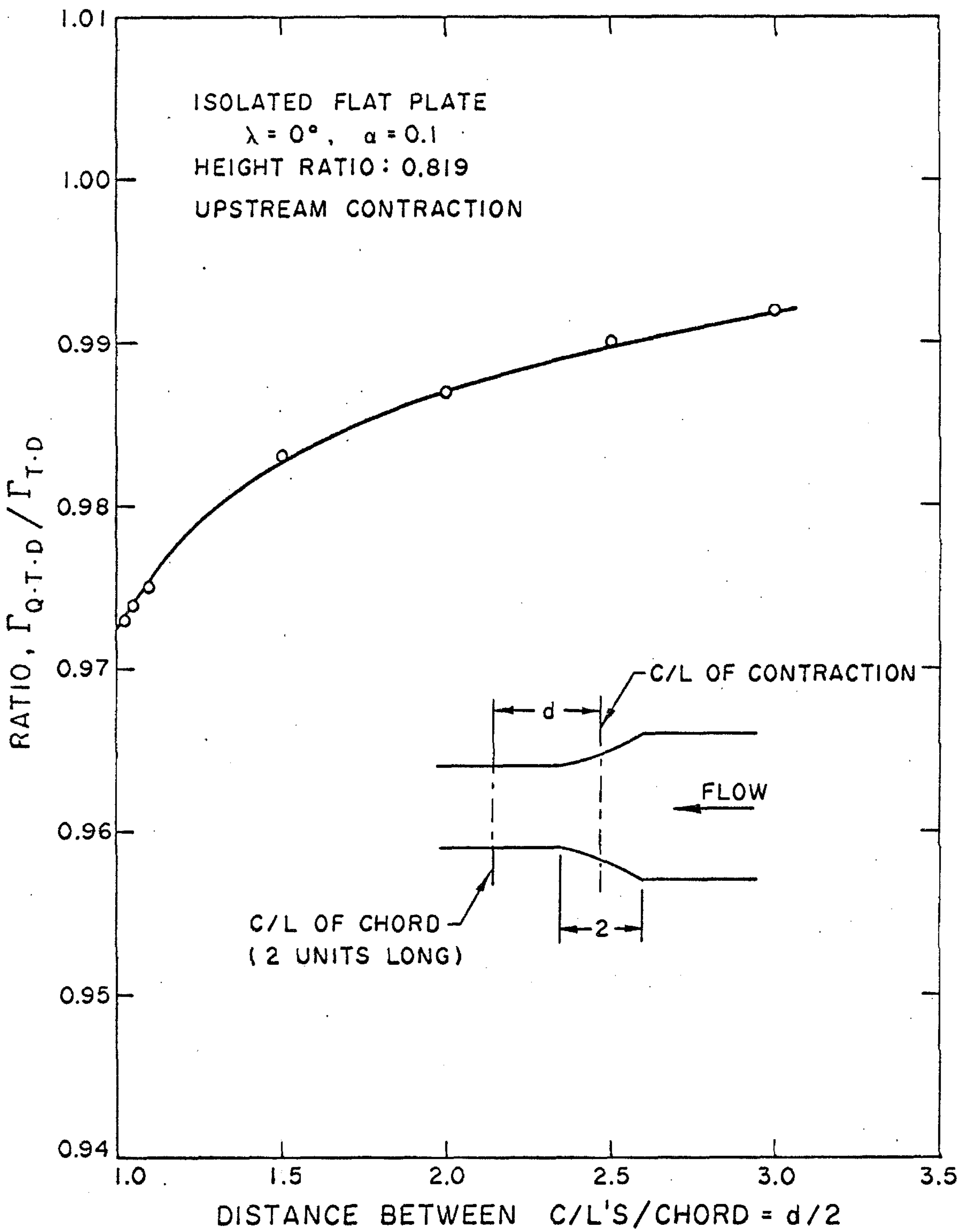
ISOLATED FLAT PLATE
λ = 0°, α = 0.1
HEIGHT RATIO: 0.819
UPSTREAM CONTRACTION
C/L OF CONTRACTION
d
FLOW
2
C/L OF CHORD
(2 UNITS LONG)
RATIO, Γ Q·T·D / Γ T·D
DISTANCE BETWEEN C/L'S/CHORD = d/2
1.01
1.00
0.99
0.98
0.97
0.96
0.95
0.94
1.0
1.5
2.0
2.5
3.0
3.5

Fig. 16

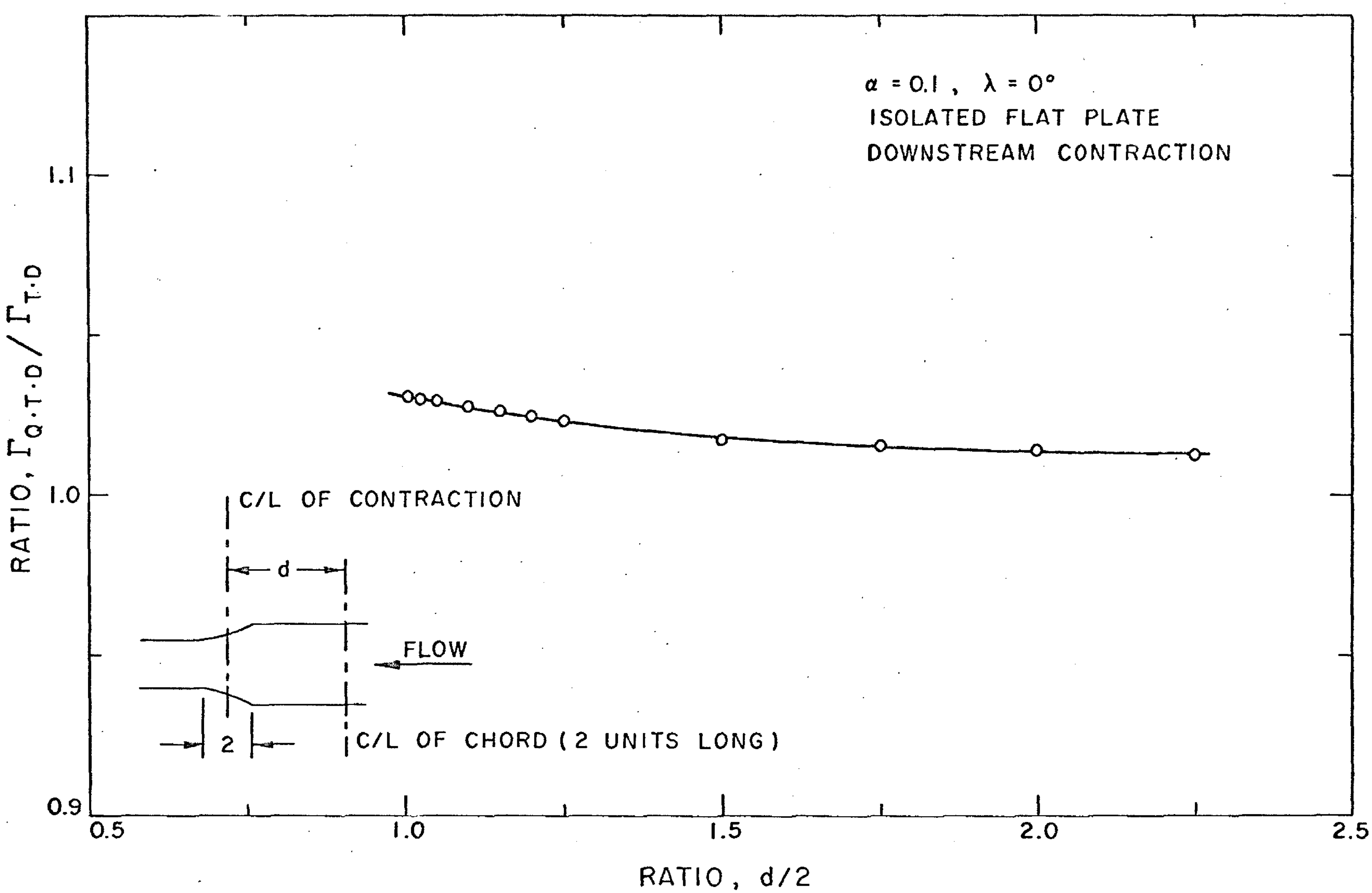
α = 0.1 , λ = 0°
ISOLATED FLAT PLATE
DOWNSTREAM CONTRACTION
C/L OF CONTRACTION
d
FLOW
2
C/L OF CHORD (2 UNITS LONG)
RATIO, Γ Q·T·D / Γ T·D
1.1
1.0
0.9
0.5
1.0
1.5
2.0
2.5
RATIO, d/2

Fig. 17

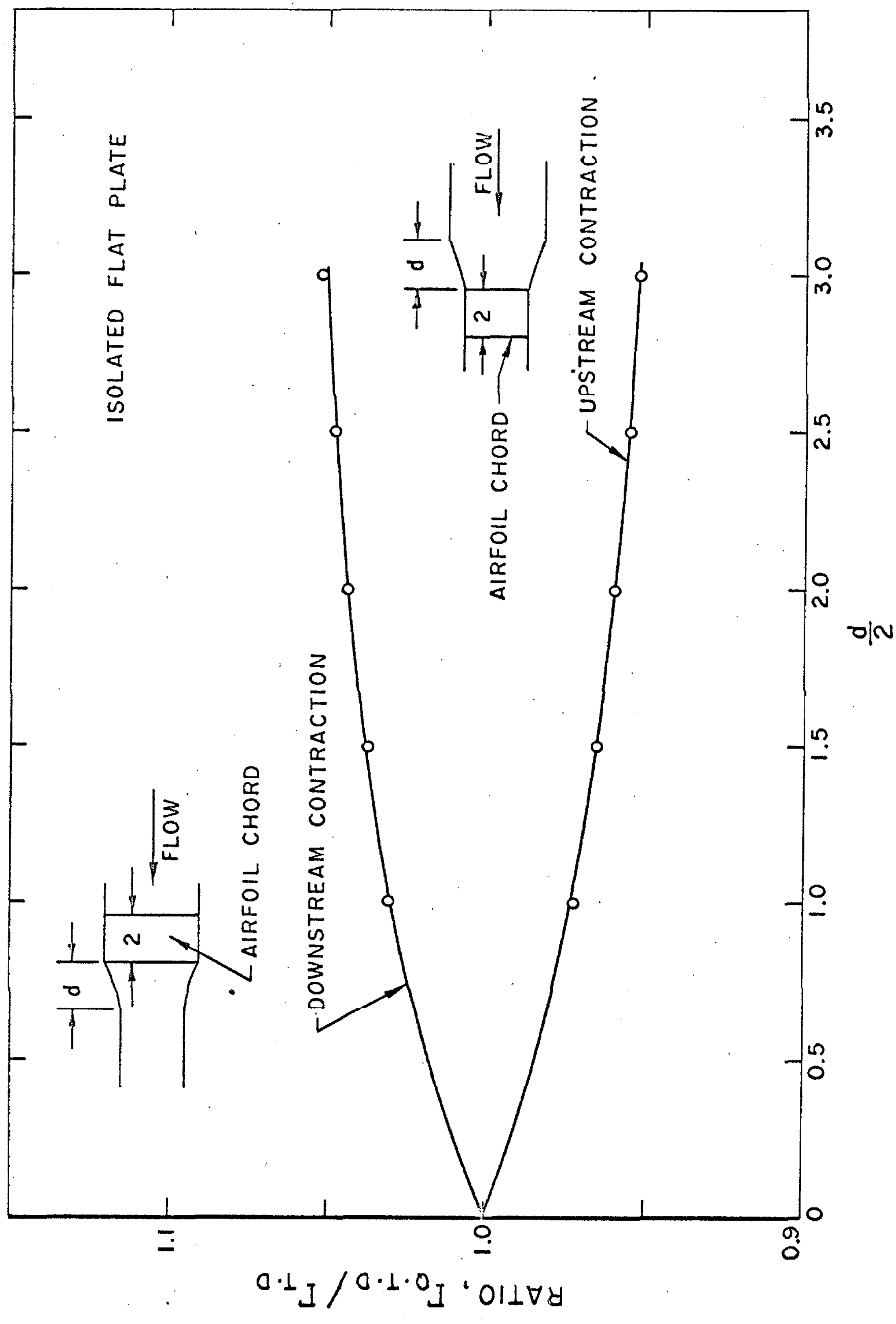
ISOLATED FLAT PLATE
DOWNSTREAM CONTRACTION
UPSTREAM CONTRACTION
AIRFOIL CHORD
FLOW
d
2
AIRFOIL CHORD
FLOW
d
2
RATIO, Γ O.T.D / Γ T.D
1.1
1.0
0.9
0
0.5
1.0
1.5
2.0
2.5
3.0
3.5
d/2

Fig. 18

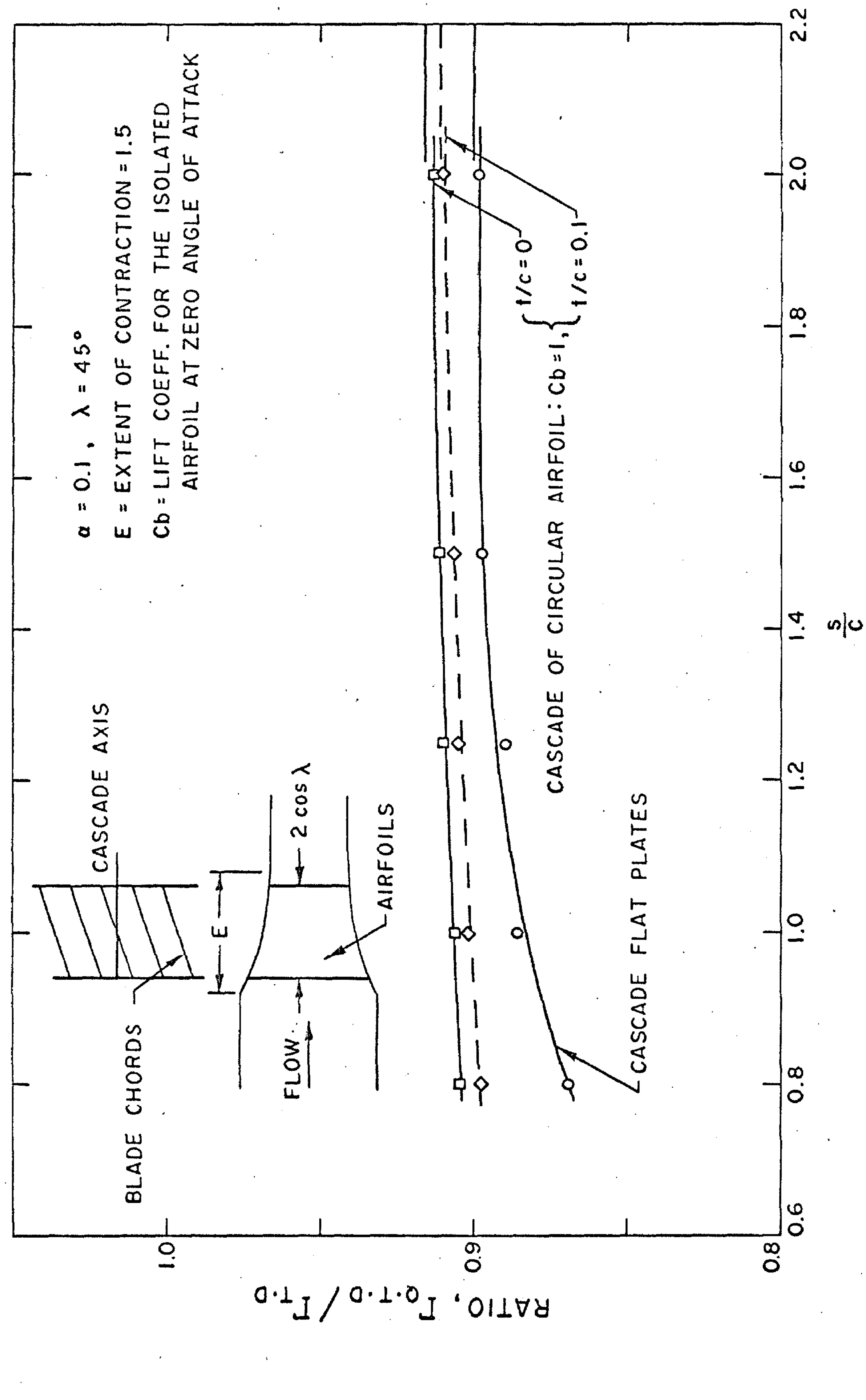
a = 0.1 , λ = 45°
E = EXTENT OF CONTRACTION = 1.5
Cb = LIFT COEFF. FOR THE ISOLATED AIRFOIL AT ZERO ANGLE OF ATTACK
CASCADE AXIS
BLADE CHORDS
E
2 cos λ
AIRFOILS
FLOW
CASCADE OF CIRCULAR AIRFOIL : Cb = 1, f/c = 0
f/c = 0.1
CASCADE FLAT PLATES
RATIO, Γ_{O.T.D} / Γ_{T.D}
1.0
0.9
0.8
0.6
0.8
1.0
1.2
1.4
1.6
1.8
2.0
2.2
s/c

Fig. 19

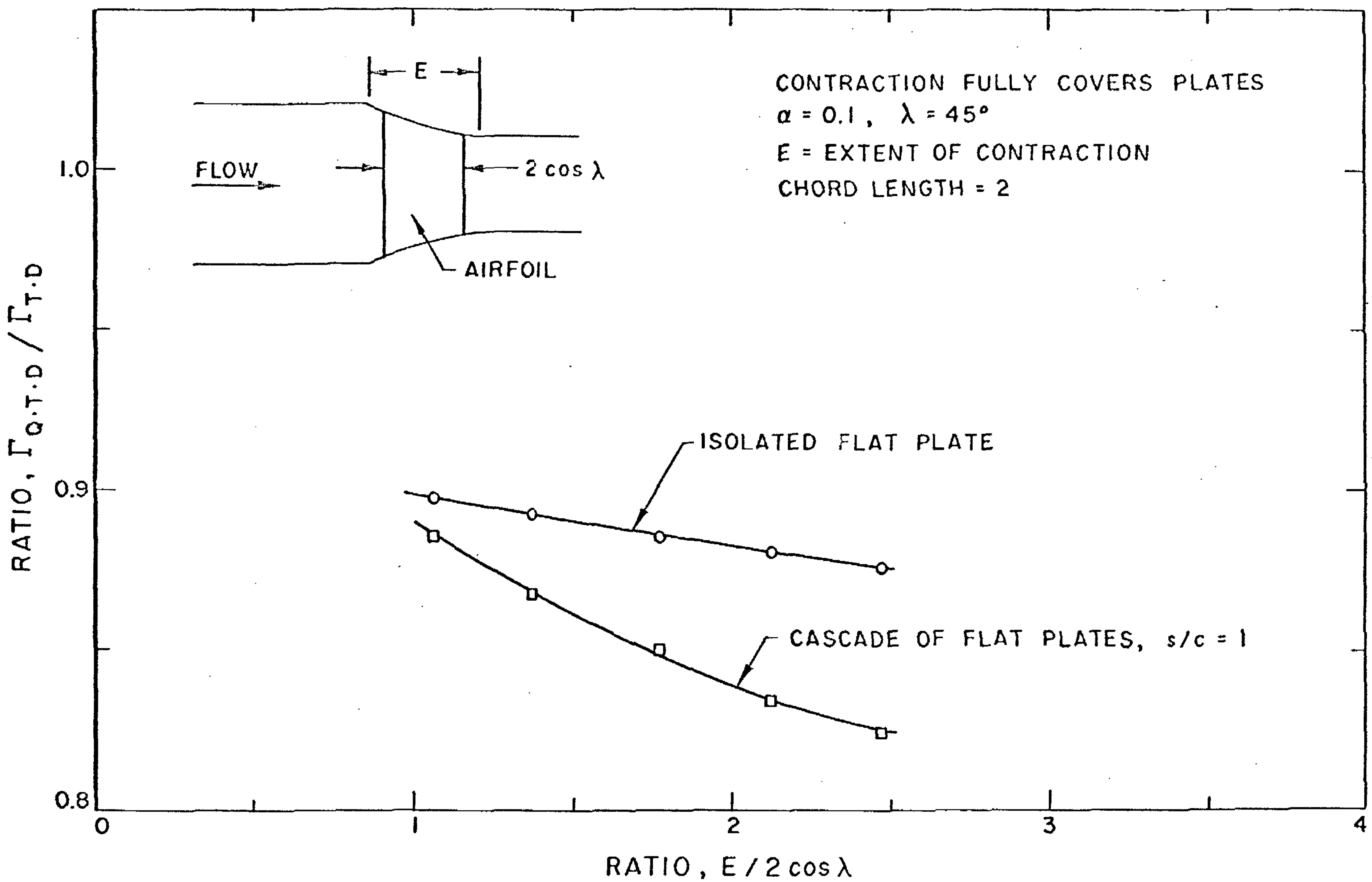

CONTRACTION FULLY COVERS PLATES
α = 0.1 , λ = 45°
E = EXTENT OF CONTRACTION
CHORD LENGTH = 2
E
FLOW
2 cos λ
AIRFOIL
ISOLATED FLAT PLATE
CASCADE OF FLAT PLATES, s/c = 1
1.0
0.9
0.8
0
1
2
3
4
RATIO, Γ Q·T·D / Γ T·D
RATIO, E / 2 cos λ

Fig. 20

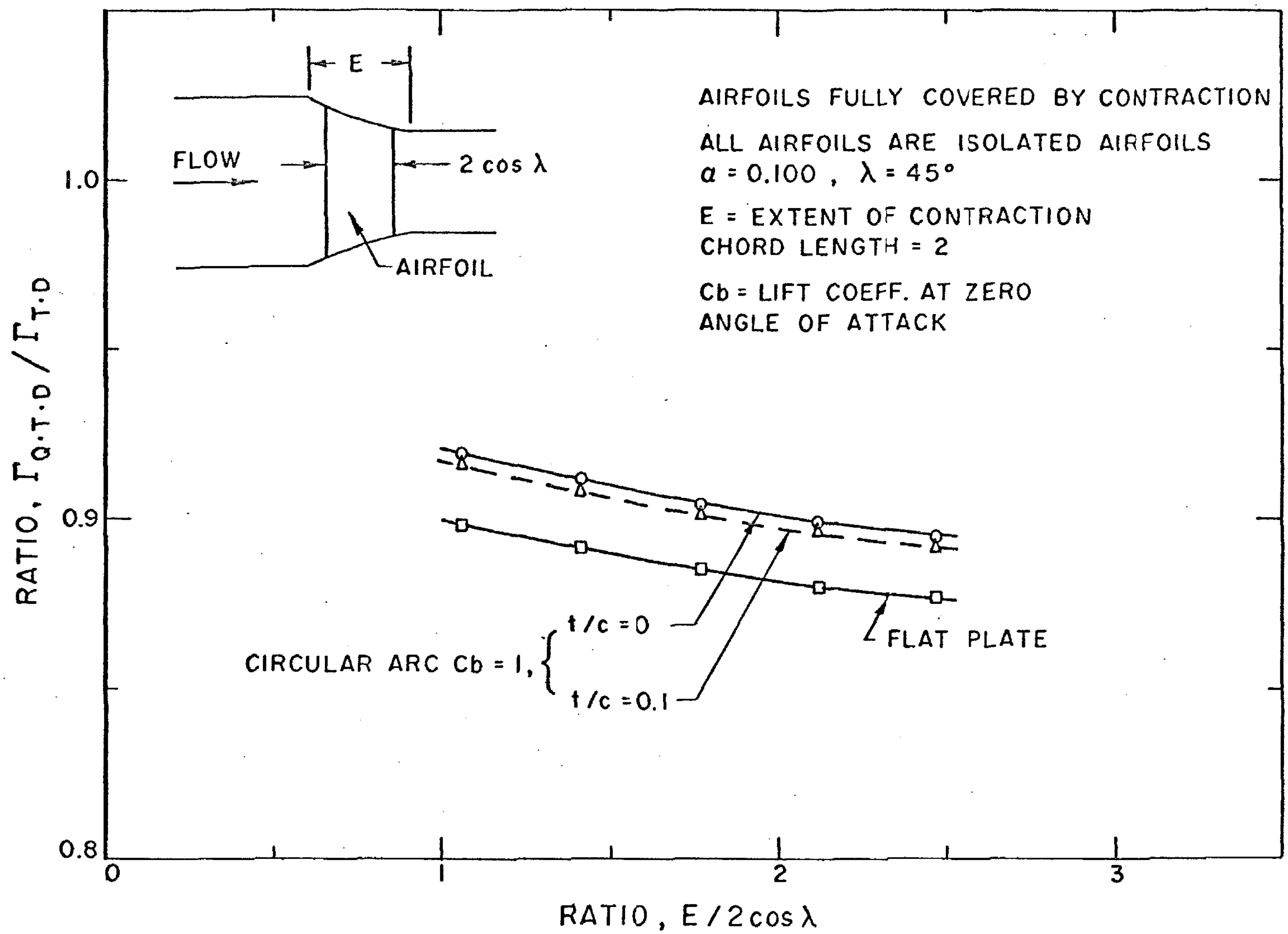
AIRFOILS FULLY COVERED BY CONTRACTION
ALL AIRFOILS ARE ISOLATED AIRFOILS
α = 0.100 , λ = 45°
E = EXTENT OF CONTRACTION
CHORD LENGTH = 2
Cb = LIFT COEFF. AT ZERO
ANGLE OF ATTACK
E
FLOW
2 cos λ
AIRFOIL
CIRCULAR ARC Cb = 1,
t/c = 0
t/c = 0.1
FLAT PLATE
RATIO, Γ Q·T·D / Γ T·D
1.0
0.9
0.8
0
1
2
3
RATIO, E/2 cos λ

Fig. 21

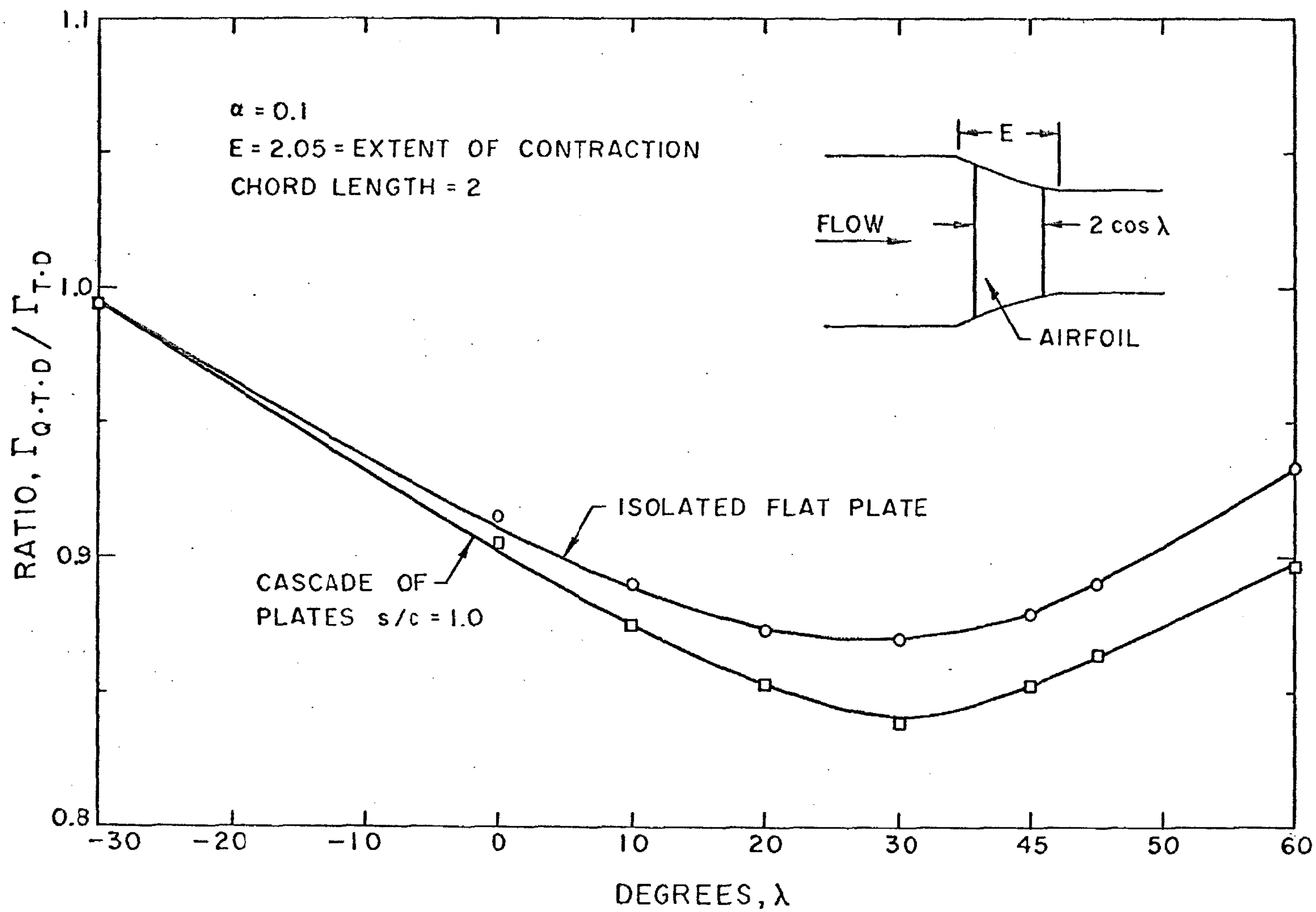
α = 0.1
E = 2.05 = EXTENT OF CONTRACTION
CHORD LENGTH = 2
E
FLOW
2 cos λ
AIRFOIL
ISOLATED FLAT PLATE
CASCADE OF
PLATES s/c = 1.0
1.1
1.0
0.9
0.8
RATIO, $\Gamma_{Q\cdot T\cdot D} / \Gamma_{T\cdot D}$
-30
-20
-10
0
10
20
30
45
50
60
DEGREES, λ

Fig. 22

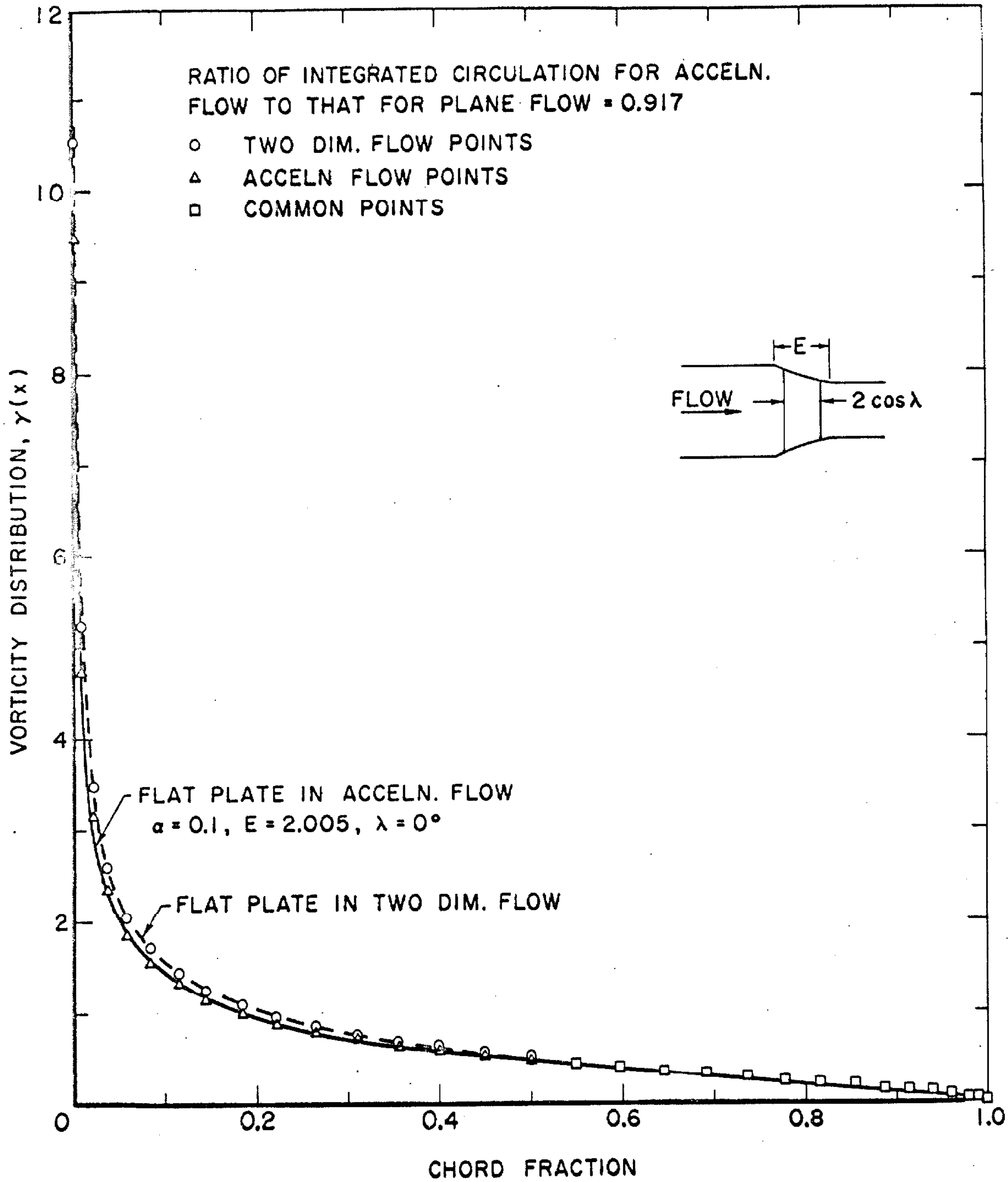
RATIO OF INTEGRATED CIRCULATION FOR ACCELN. FLOW TO THAT FOR PLANE FLOW = 0.917
○ TWO DIM. FLOW POINTS
△ ACCELN FLOW POINTS
□ COMMON POINTS
E
FLOW
2 cos λ
FLAT PLATE IN ACCELN. FLOW
α = 0.1, E = 2.005, λ = 0°
FLAT PLATE IN TWO DIM. FLOW
VORTICITY DISTRIBUTION, γ(x)
CHORD FRACTION
0
2
4
6
8
10
12
0.2
0.4
0.6
0.8
1.0

Fig. 23